



UNIVERSITAT  
POLITÈCNICA  
DE VALÈNCIA



ETS INGENIEROS DE CAMINOS,  
CANALES Y PUERTOS

# TRABAJO DE FIN DE MASTER

---

Static and dynamic analysis and design of frame bridge  
subjected to railways load: application to single-track  
structures under high-speed traffic

---

*Presentado por*

Cristian Ioan Timbolmas

---

*Para la obtención del*


Master en Ingeniería de Caminos, Canales y Puertos

*Curso: 2017/2018*

*Fecha: 18/07/2018*

*Tutor: Pedro Museros Romero*

*Cotutor: Carlos Lazaro Fernandez*



**MASTER THESIS**  
**TRABAJO FIN DE MASTER**

**Static and dynamic analysis and design of frame bridge  
subjected to railways load: application to single-track  
structures under high-speed traffic**

**Análisis estático y dinámico, y proyecto de puentes  
marco sometidos a cargas ferroviarias: aplicación a  
estructuras de vía única bajo tráfico de alta velocidad**

Student: CRISTIAN IOAN ȚIMBOLMAȘ

Supervisor: Associate Professor PEDRO MUSEROS ROMERO

Co-supervisor: Associate Professor CARLOS MANUEL LÁZARO FERNÁNDEZ

School of Civil Engineering, Polytechnic University of Valencia, Spain

External co-supervisor: Associate Professor TEFAN GUȚIU

Faculty of Civil Engineering, Technical University of Cluj-Napoca, Romania



## Preface

This thesis has been written as the concluding part of the M.Sc. program in Civil Engineering, during my Erasmus mobility at Polytechnic University of Valencia, Spain (Universitat Politècnica de València, UPV).

First and foremost, I would like to thank my supervisor Mr. Professor Museros Romero Pedro from *Department of Continuum Mechanics and Theory of Structures* for his great support and true enthusiasm for my work. The time he has spent answering questions and giving me advices has been valuable for me.

As well, I give my thanks to Mr. Professor Carlos M. Lázaro Fernández, also from *Department of Continuum Mechanics and Theory of Structures*, for his helpful advices and positive remarks during my work.

Also, I am grateful for the opportunity of carrying out my thesis at School of Civil Engineering (Escuela Técnica Superior de Ingeniería de Caminos, Canales y Puertos) from Polytechnic University of Valencia (Universitat Politècnica de València, UPV).

Valencia, July 2018

Cristian Ioan ȚIMBOLMA



## Abstract (English)

High-speed trains are getting more and more common around the whole world and high-speed lines offer a sustainable and comfortable way of travel. The high-speed trains are very efficient, with a low environmental impact and they promote economic growth by connecting different regions or different countries.

The interest in dynamic behavior of railway bridges has increased in recent years, due to high-speed trains. Under high-speed dynamic loads, the bridges are subjected to large dynamic effects. The dynamic aspects have often shown to be the most important factors in structural design. Generally, for all railway bridges induced by train speed over 200 km/h or for bridges with a fundamental frequency outside specified limits, dynamic analysis is required according to Eurocode 1 – Part 2, EN 1991-2. A Finite Element Analysis (FEA) is required to simulate in an accurate way the response and account for the dynamic effects of the bridge.

Correct understanding of railway bridge dynamic is essential, since a correct prediction of the structural response contributes to an economic design of new bridges.

When designing a railway bridge for high-speed traffic, it is important to understand how different parameters influence the dynamic response. Even if a bridge is satisfactory for static load effects, it may be inadequate for dynamic behavior.

Also, the design of reinforced concrete bridges is normally performed on the basis of a structural analysis. In the past, structural analysis were often performed with simplified models, for example two-dimensional (2D) equivalent beam or frame models. These types of models are not able to describe the distribution of forces in transversal directions, neither to take into account interaction with the soil.

Therefore, the 3D-Finite Element Model (FEM) is necessary in order to simulate a realistic behavior of the structure. In this thesis such a model is developed for a single-track frame bridge of 7 m span. The ANSYS Finite Element software is employed in order to compute the static and dynamic effects, which are required for a subsequent assessment of the Ultimate and Serviceability Limit States according to the Eurocodes. A further analysis of the behavior of 10 m and 13 m frame bridges is accomplished. Due to time restrictions, the dynamic analysis is carried in a simplified manner resorting to mode superposition, while in future developments such procedure should be improved in order to account for the time-domain interaction of soil and structure, and the wave transmission and energy dissipation through the boundaries of the numerical model.



## Resumen (Español)

Los trenes de alta velocidad son cada vez más habituales en todo el mundo, ya que las líneas de alta velocidad ofrecen una forma de viaje cómoda y sostenible. Los trenes de alta velocidad son muy eficientes, con un bajo impacto ambiental, y promueven el crecimiento económico conectando diferentes regiones o países.

El interés en el comportamiento dinámico de los puentes ferroviarios se ha incrementado en los últimos años a causa de los trenes de alta velocidad. Bajo cargas dinámicas de alta velocidad, los puentes sufren importantes efectos dinámicos. Los aspectos dinámicos a menudo han demostrado ser los factores más significativos en el diseño estructural. En general, para todos los puentes ferroviarios con velocidades de proyecto superior a 200 km/h, o para puentes con una frecuencia fundamental fuera de ciertos límites especificados, se requiere un análisis dinámico según el Eurocódigo 1 - Parte 2, EN 1991-2. Para simular de forma precisa la respuesta y tener en cuenta los efectos dinámicos del puente se necesita un análisis tridimensional por Elementos Finitos.

La comprensión correcta de la dinámica del puente ferroviario es esencial, ya que una predicción adecuada de la respuesta estructural contribuye al diseño económico de los nuevos puentes.

Al diseñar un puente ferroviario para el tráfico de alta velocidad, es importante entender cómo los diferentes parámetros influyen en la respuesta dinámica. Aunque un puente sea satisfactorio para los efectos de las cargas estáticas, puede ser inadecuado para el comportamiento dinámico.

En el pasado, el análisis dinámico de los puentes de hormigón armado a menudo se realizaba con modelos simplificados, por ejemplo, modelos bidimensionales (2D) de vigas o marcos equivalentes. Estos tipos de modelos no son capaces de describir la distribución de fuerzas en direcciones transversales, ni tampoco de tener en cuenta la interacción con el suelo.

Por lo tanto, se hace necesario el uso de un modelo de tridimensional de elementos finitos para simular un comportamiento realista de la estructura. En este trabajo, dicho modelo se desarrolla para un puente marco de vía única de 7 m de luz. El software ANSYS de elementos finitos se utiliza para determinar los efectos estáticos y dinámicos, que son necesarios para una evaluación posterior de los Estados Límite Último y de Servicio, de acuerdo con los Eurocódigos. Se lleva a cabo un análisis adicional del comportamiento de puentes de marco de 10 m y 13 m. Debido a restricciones de plazos, el análisis dinámico se lleva a cabo de manera simplificada recurriendo a la superposición modal mientras que, en desarrollos futuros, tal procedimiento debería mejorarse para tener en cuenta la interacción suelo-estructura en el dominio del tiempo, así como la transmisión de ondas y disipación de energía a través del contorno del modelo numérico.



# Contents

Preface.....	ii
Abstract (English) .....	iii
Resumen (Español) .....	iv
Contents .....	v
List of Figures .....	vii
List of Tables .....	ix
1. INTRODUCTION.....	1
1.1. Origin of the Thesis .....	1
1.2. Scope of the Thesis .....	2
1.3. Objectives of the Thesis.....	2
2. DYNAMIC ANALYSIS OF RAILWAY BRIDGES.....	4
2.1. Structural Dynamics of Railway Bridges .....	4
2.2. Dynamic effects according to EN 1991-2.....	5
2.3. Dynamic factor, Ultimate Limit States and Serviceability Limit States in EN 1991-2 and EN 1990 - Annex 2.....	7
3. STRUCTURAL MODEL OF FRAME BRIDGE FOR DYNAMIC ANALYSIS UNDER MOVING LOADS.....	10
3.1. Definition of a frame bridge for static and dynamic analysis.....	10
3.2. Finite Element Program .....	10
3.3. Geometry and characteristics of the 3D model.....	12
3.4. Boundary conditions and mesh.....	16
4. STATIC AND DYNAMIC ACTIONS CONSIDERED IN THE MODEL.....	19
4.1. Static loads .....	19
4.2. Permanent loads .....	21
4.3. Dynamic loads .....	22
4.4. Thermal loading and rheological effects .....	23
4.5. Loads not considered in the model .....	25
5. RESULTS OF THE ANALYSIS .....	26
5.1. Static analysis.....	26
5.2. Dynamic analysis .....	31
6. COMBINATION OF EFFECTS FOR ULS AND SLS ASSESSMENT.....	35
6.1. Combinations of actions .....	35
6.2. ULS assessment .....	35



6.3.	Computing of deck reinforcement .....	36
6.4.	SLS assessment .....	37
7.	SENSITIVITY ANALYSIS FOR DIFFERENT SPAN LENGTHS.....	40
7.1.	Static effects for 10 m and 13 m span lengths .....	40
7.2.	Dynamic effects for 10 m and 13 m span lengths.....	43
8.	CONCLUSIONS AND FUTURE DEVELOPMENT .....	49
8.1.	Conclusions.....	49
8.2.	Future development .....	50
BIBLIOGRAPHY .....		51
ANNEXES .....		52
Annex A1. Verification of bridge model in SAP 2000 software .....		52
Annex A2. Verification of settlement of the embankment's layer .....		55
Annex A3. Computation of the pressure below sleepers due to Load Model 71 (LM71). 58		
Annex A4. Thermal loading and rheological effects assessment .....		59
Annex A5. Computing the deck reinforcement .....		63
Annex A6. D-region verification .....		80
Annex A7. Bridge parameters .....		83
Annex A8. Vertical mode shapes and natural frequencies for 7 meters span length.....		85
Annex A9. Input parameters for ANSYS software.....		88
Annex A10. Determination of dynamic factor according to Annex C from EN 1991-2... 90		
Annex A11. Drawings of slab reinforcement details .....		94

## List of Figures

Figure 1.1 – Concrete frame bridge of the Spanish railway network .....	1
Figure 1.2 – Isometric view of the entire model (CAD model).....	3
Figure 1.3 – Isometric view of the concrete structure (CAD model) .....	3
Figure 2.1 - Flow chart in EN 1991 - Part 2, for determining whether a dynamic analysis is required .....	5
Figure 2.2 - The limits of bridge natural frequency $n_0$ (Hz) as a function of $L$ (m), EN 1991 - Part 2 .....	6
Figure 2.3 - Maximum permissible vertical deflection for railway bridges with 3 or more successive simply supported spans corresponding to a permissible vertical acceleration of $b_v = 1 \text{ m/s}^2$ in a coach for speed $V$ [km/h] .....	8
Figure 3.1 - Geometry and surrounding soil properties of model taken as an example [15] .....	10
Figure 3.2 - Cross-section at mid-span of the bridge.....	12
Figure 3.3 - Longitudinal section of studied model.....	13
Figure 3.4 - Plan view of bridge structure .....	13
Figure 3.5 - SOLID 187 used in ANSYS .....	14
Figure 3.6 - Volumes used for meshing the 3D-Finite Element Model (FEM) .....	16
Figure 3.7 - 3D-Finite Element Mesh .....	18
Figure 4.1 - Load Model 71 (LM71) .....	19
Figure 4.2 - Longitudinal distribution of a point force or wheel load by the rail .....	19
Figure 4.3 - The divided bridge deck and ballast layer .....	20
Figure 4.4 - The distribution of loads due to Load Model 71 considered in the 3D-FEM....	21
Figure 4.5 - Train configurations of High Speed Lane Model – HSLM-A.....	22
Figure 4.6 - Effect of thermal contraction of deck in frame bridge: a) deflected shape; b) distribution of bending moments .....	23
Figure 4.7 - Deformed shape due to: a) maximum negative temperature b) shrinkage .....	24
Figure 5.1 - Distribution of studied sections.....	26
Figure 5.2 - The normal stress $\sigma_x$ due to self-weight in section S1: a) distribution of normal stress in point S1-1; b) distribution of normal stress in deck's cross-section.....	26
Figure 5.3 - The tangential stress $\sigma_{xz}$ due to self-weight in section S1: a) distribution of tangential stress in point S1-2; b) distribution of tangential stress in deck's cross-section ..	27
Figure 5.4 - The normal stress $\sigma_x$ due to LM 71 in section S2: a) distribution of normal stress in point S2-1; b) distribution of normal stress in deck's cross-section.....	27
Figure 5.5 - The vertical displacements of the deck due to LM 71 .....	28
Figure 5.6 - The vertical displacements of the deck due to self-weight .....	28





Figure 5.7 - The total vertical displacements of 3D-FE Model due to self-weight and LM 17 .....	29
Figure 5.8 - Stage 1: a) the considered model; b) the normal stress ( $\sigma_x$ ) at mid-span .....	30
Figure 5.9 - Stage 2: a) the considered model; b) the normal stress ( $\sigma_x$ ) at mid-span .....	30
Figure 5.10 - Stage 3: a) the considered model; b) the normal stress ( $\sigma_x$ ) at mid-span .....	31
Figure 5.11 - The first natural bending frequency of the bridge deck .....	32
Figure 5.12 - The first vertical mode shape .....	33
Figure 5.13 - Vertical displacements at mid-span due to train model HSLM-A for 7 meters span length .....	34
Figure 6.1 - The 3D-bridge reinforcement.....	37
Figure 6.2 - Vertical acceleration of the bridge deck at mid-span due to HSLM-A .....	39
Figure 7.1 - Variation of normal stresses on the section due to permanent loads .....	41
Figure 7.2 - Variation of normal stresses on the section due to Load Model 71 .....	42
Figure 7.3 - The bending moment in deck slab .....	42
Figure 7.4 - The mode shapes of the bridge for a) 10 meters span length; b) 13 meters span length.....	44
Figure 7.5 - Vertical displacements at mid-span due to train model HSLM-A for 10 meters span length .....	46
Figure 7.6 - Vertical displacements at mid-span due to train model HSLM-A for 13 meters span length .....	46
Figure 7.7 - Vertical acceleration of the bridge deck at mid-span due to HSLM-A for 10 meters span length.....	47
Figure 7.8 - Vertical acceleration of the bridge deck at mid-span due to HSLM-A for 13 meters span length.....	48



## List of Tables

Table 3.1 - Geometrical characteristics of studied bridges.....	12
Table 3.2 - Characteristics of the materials .....	15
Table 3.3 – The size of meshes for the bridge with 7 m. span length .....	17
Table 4.1 - Characteristics values of High Speed Lane Model – HSLM-A.....	22
Table 4.2 - Results of internal forces due to thermal and shrinkage effect .....	24
Table 5.1 - The characteristics values of stresses from static analysis .....	29
Table 5.2 - The normal stress due to construction stages .....	31
Table 5.3 - The values of dynamic increment corresponding to the HSLM-A .....	33
Table 5.4 - The value of displacements due to static and dynamic analysis .....	34
Table 6.1 - The coefficients used in ULS and SLS combinations.....	35
Table 6.2 - The values of internal forces at ULS combination.....	36
Table 6.3 - The summary of the deck reinforcement.....	36
Table 6.4 - Deflections and their limits .....	38
Table 7.1 - The value of normal stresses and vertical deflection due to permanent loads ....	40
Table 7.2 - The value of normal stresses and vertical deflection due to Load Model 71 .....	41
Table 7.3 - Deflections and their limits .....	43
Table 7.4 - Bridge parameters for studied bridges.....	43
Table 7.5 - Natural frequencies from the FE-analysis.....	44
Table 7.6 - The values of dynamic increments corresponding to the HSLM-A trains.....	45



# 1. INTRODUCTION

## 1.1. Origin of the Thesis

This thesis was written during my Erasmus mobility at Polytechnic University of Valencia, Spain. I chose to finish my studies in this university because it is well known in this area as a top university. Having theoretical knowledge in composite bridges, initially, my idea was to study integral bridges for road traffic with steel-concrete structure. After my collaboration with Mr. Professor Pedro Museros started, we decided the topic of the future thesis. We agreed to study the bridges subjected to high-speed railway traffic, and more precisely about portal frame bridge. I welcomed this idea with enthusiasm because it represented a good way to gain sound technical knowledge in this field of high-speed railway traffic and it could be a new opportunity for my professional development. Also, I knew that Spain had one of the most modern railway networks in Europe and the world. As well, the complexity of problems encountered in these types of bridges have been a strong reason to choose this theme. These kind of bridges are well known in the Spanish railway network.



Figure 1.1 – Concrete frame bridge of the Spanish railway network



## 1.2. Scope of the Thesis

The purpose of this thesis is to analyze the static and dynamic effect of high-speed railway traffic on frame bridges according to the Eurocode, with particular application to a real example. This kind of structures are prone to vibration due to its relatively short span and require careful assessment in order to evaluate the effects of fast railway vehicles.

These bridges are the most common type of overpasses along modern railway lines. This type of structure is designed as a reinforced concrete rigid frame with integral wing walls and is surrounded by an embankment reasonably longer than its span length.

The action of the moving loads will be introduced in the models in an appropriate manner and the maximum forces and vibration levels will be obtained for Ultimate Limit State (ULS) and Serviceability Limit State (SLS) analysis.

A 3D Finite Element Model (FEM) has been built up, using the finite element program, ANSYS Mechanical APDL and for additional verifications of the model was used SAP2000 software together with simple hand calculations.

Another aim of thesis is represented by the 3D model of work, which is a parametric model. This means is easier to adjust the model to different geometrical dimensions of the bridge (e.g. span length, width, height, and so on) and also dimensions of the soil layers.

Finally, in this thesis, the bridge deck will be designed for a certain span length, while the internal forces (shear, bending moment, etc.) will be analyzed for different span lengths.

## 1.3. Objectives of the Thesis

Considering the time and material restraints, in this thesis the following aspects of the static and dynamic behavior of frame bridges under railway traffic will be taken into account for the global scope of the work:

- Analysis of the behavior of a single span, single track frame bridge;
- Analysis of the static effects under permanent loads, as well as traffic loads as defined in EN1991-2;
- Assessment of dynamic effects of traffic loads as defined in EN1991-2;
- Simultaneous inclusion of the static and dynamic influence of both structure and surrounding soil by means of a 3D Finite Element Model (FEM);
- Assessment of the sectional properties and reinforcement in order to fulfill the Ultimate Limit States (ULS) and Serviceability Limit States (SLS);
- Evaluation of the influence of the span length on the variation of the internal forces (e.g. bending moment), vertical deflection and the maximum acceleration of the deck;
- The behavior of the railway bridge is evaluated using the finite element program ANSYS;
- Thermal and rheological effects will be analyzed in a simple manner.

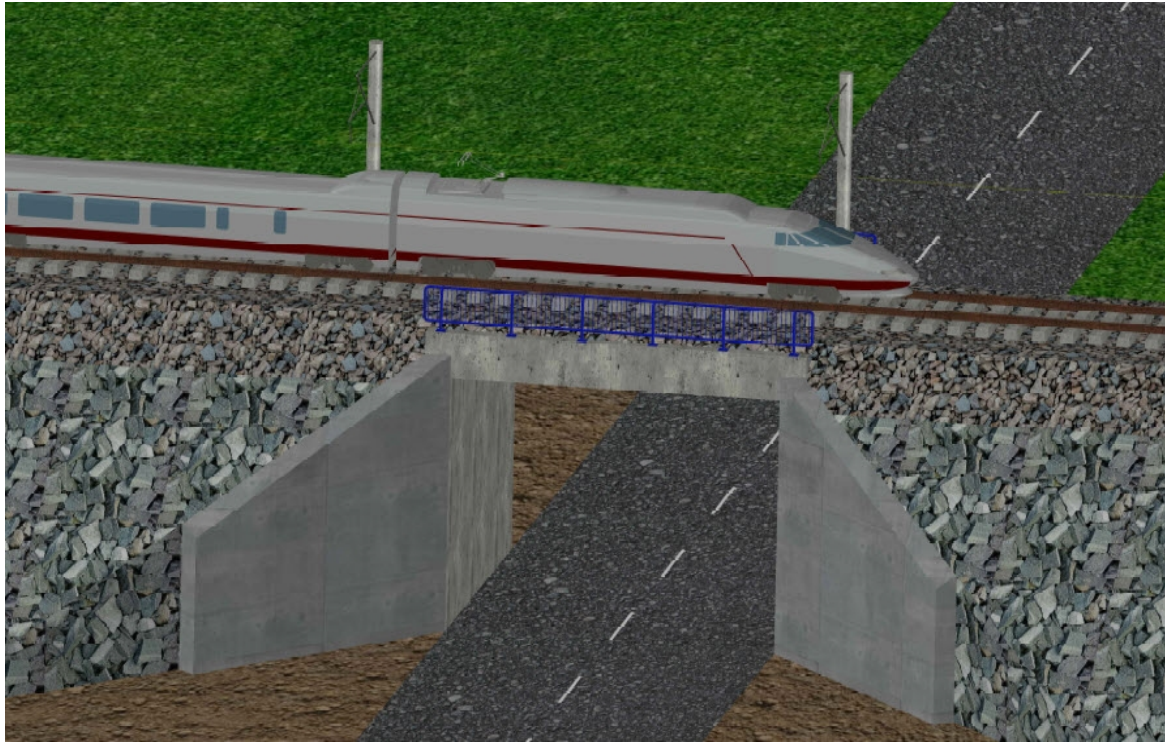


Figure 1.2 – Isometric view of the entire model (CAD model)

Due to time restrictions and being a complex and parametric 3D Finite Element Model (FEM), the following loads were not considered in the analysis for this thesis:

- Earthquake and wind loads;
- Derailment, centrifugal forces, noising force, traction and braking force;
- Fatigue assessment;
- The static effects of vertical loading due to heavy freight traffic (model SW/2);
- The effects of the Load Model “Unloaded train”;
- The effects of eccentricity of vertical loads;



Figure 1.3 – Isometric view of the concrete structure (CAD model)



## 2. DYNAMIC ANALYSIS OF RAILWAY BRIDGES

### 2.1. Structural Dynamics of Railway Bridges

In the following chapter a general introduction about the structural dynamics of railway bridges and the dynamic effects according to Eurocode is given.

The dynamics of railway bridges is a scientific discipline forming part of applied mechanics and its subdivision *dynamics of structures*. It is concerned with the study of deflections, vibration levels and stresses in railway bridges.

Dynamic considerations are often more complex and complicated than its static counterpart, mainly due to the time-varying nature of the dynamic problem. The parameters influencing the dynamic stresses in railway bridges are: the frequency characteristics of bridge structures, the damping in bridges and in vehicles, the speed of vehicles, and so on. In design practice, these effects are largely described by the dynamic coefficient or dynamic impact factor which, however, only states how many times the static effect must be multiplied in order to cover the dynamic loads effect.

*Fryba* affirmed that "the vertical acceleration is a decisive parameter to study the dynamic behavior, especially in high speed railway bridges. The conclusion was satisfactory supported with some in-situ measurements. In fact, to ensure the safety at bridges for high speed trains, the maximum bridge deck acceleration is limited up to  $3.5 \text{ m/s}^2$  in ballasted tracks. This comes from the risk of ballast instability".

Therefore, acceleration is a decisive part of the dynamic behavior of a bridge that is to be analyzed, particularly, when resonance phenomena occur.

Resonance is a potentially harmful phenomenon which occurs due to high-speeds and regularly distance axle groups of a train. In case of resonance and/or large track irregularities, excessive bridge deck vibration (vertical acceleration) may cause loss of wheel-rail contact, destabilization of the ballast prism, occurrence of cracks of concrete and exceeding the stress limits of the bridge structures. The resonance phenomenon always has to be taken into account when designing railway bridges subjected to high-speeds. However, if the traffic speeds remains under 200 km/h, this phenomenon is unlikely to occur and there is no need to take it into account. Risk of resonance arise when the excitation frequency of the loading, or a multiple of it, coincides with a natural frequency of the bridge structure. When resonance occurs, the dynamic response of the structure increase very fast.

The most important dynamic characteristics of railway bridges are their natural frequencies which actually characterize the extent to which the bridge is sensitive to dynamic loads. They are measured by the number of vibrations per unit time and the unit of the frequency is "Hertz" (Hz), which is the number of cycles executed per second. The resonance depends on the number of spaced loads, type of loading and the damping of the structure, for instance, a low value of the damping of the structure gives high resonance peaks.

## 2.2. Dynamic effects according to EN 1991-2

According to Eurocode 1, EN 1991-2, for some simple cases only static analysis is required. The static analysis must be carried out with the load models defined in “*Vertical loads – Characteristics values (static effects) and eccentricity and distribution of loading*” considering the model LM71, and also the load models SW/0 and SW/2 where it is required. The results of the static analysis must be multiplied by the dynamic factor and, if required, multiplied by factor. The requirements for determining whether a static or dynamic analysis is necessary are shown in Figure 2.1.

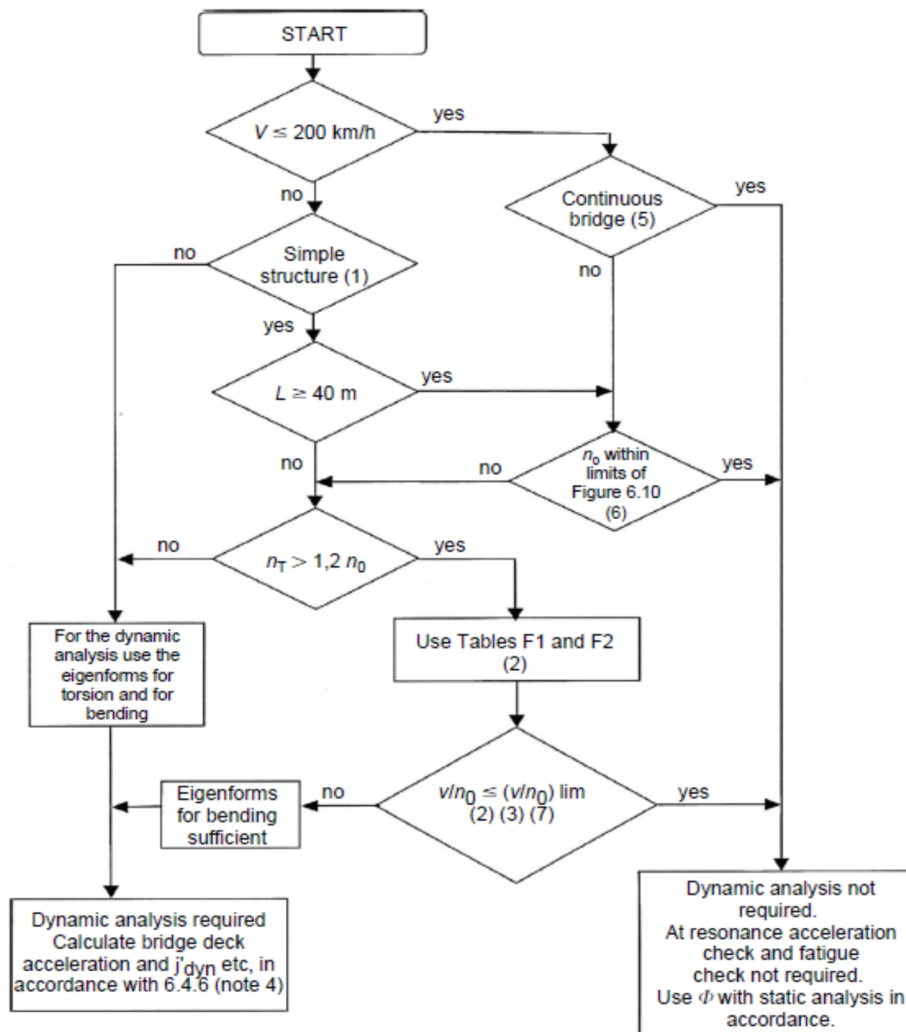


Figure 2.1 - Flow chart in EN 1991 - Part 2, for determining whether a dynamic analysis is required

The symbols in Figure 2.1 have the following meaning:

- V the maximum line speed at the site (km/h)
- L the span length (m)
- $n_0$  the first natural bending frequency of the bridge loaded by permanent actions (Hz)

$n_T$  the first natural torsional frequency of the bridge loaded by permanent actions (Hz)

$(\gamma/n_0)_{lim}$  is given as a function of  $f_{lim}/n_0$  in annex F, referred to Eurocode.

Figure 6.10 in EN 1991 - Part 2 is reproduced as Figure 2.2 below. For bridges with a first natural frequency within the limits given by Figure 2.2 and a maximum line speed at the site not exceeding 200 km/h, a dynamic analysis is not required. However, if the first natural frequency exceeds the upper limit, a dynamic analysis is required.

The upper limit of  $n_0$  is governed by dynamic increments due to track irregularities and is given by:

$$n_0 = 94.76L^{-0.748} \quad (2.1)$$

The lower limit of  $n_0$  is governed by dynamic impact criteria and is given by:

$$\begin{aligned} n_0 &= 80/L, \text{ for } 4\text{m} \leq L \leq 20\text{m} \\ n_0 &= 23.58L^{-0.592}, \text{ for } 20\text{m} \leq L \leq 100\text{m} \end{aligned} \quad (2.2)$$

where:

$n_0$  is the first natural frequency of the bridge taking into account the mass due to permanent actions.

$L$  is the span length for simply supported bridges and for other bridge types,  $L_{eff}$ .

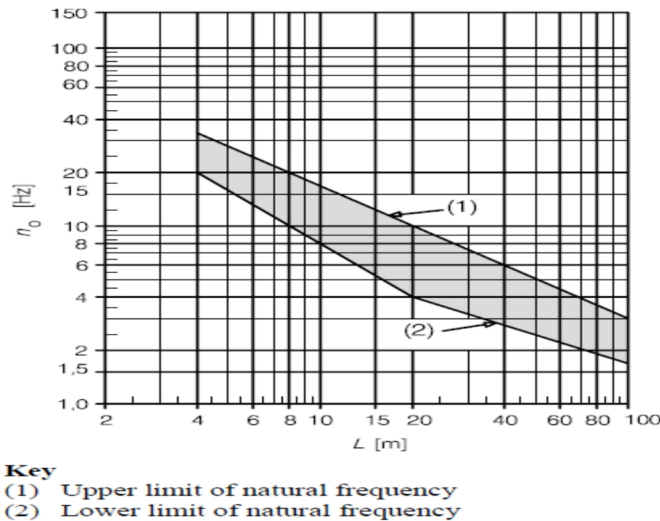


Figure 2.2 - The limits of bridge natural frequency  $n_0$  (Hz) as a function of  $L$  (m), EN 1991 - Part 2

The use of this chart is not so easy in the cases where a dynamic analysis is required, for instance: non simple structures such as bridges with continuous decks, skew decks, concrete frames, concrete portals. Another issue is that for small reinforced concrete bridges, the models for dynamic analysis are not described in European standards.



## 2.3. Dynamic factor, Ultimate Limit States and Serviceability Limit States in EN 1991-2 and EN 1990 - Annex 2

### 2.3.1. Dynamic amplification factor according to EN 1991-2

For bridges on conventional (non high-speed) railway lines, dynamic effects are most often taken into account by increasing the static response with a dynamic amplification factor.

The dynamic factor takes into account the magnification of stresses and vibration effects in the structure due to dynamic loading. However, the dynamic factor does not take into account resonance effects due to high-speed trains.

Where a dynamic analysis is required, in accordance with Figure 2.1 and Figure 2.2, there is a risk of resonance and excessive vibration of the bridge. For such cases, the dynamic analysis must be effectively carried out, instead of using dynamic amplification factor. The dynamic analysis takes into account the time dependent nature of the loading from the high speed train and predicts the effects of resonance.

There are two different definitions of the dynamic factor, according to the quality of the track maintenance. Generally, carefully maintained track gives a lower dynamic factor than track with standard maintenance, based on a determinant length which originally was derived from cases of simply supported beam.

In the design of a new bridge, EN 1991-2 state that Eq. (2.3) or Eq. (2.4) shall be used in combination with the design train load models: LM71, SW/0 and SW/2.

For carefully maintained track:

$$q_2 = \frac{1.4}{\sqrt{L} - 0.2} + 0.82 \quad (2.3)$$

With: 1.00  $q_2$  1.67

For standard maintained track:

$$q_3 = \frac{2.1}{\sqrt{L} - 0.2} + 0.73 \quad (2.4)$$

With: 1.00  $q_3$  2.00

Where:

L is determinant length defined in table 6.2 from EN 1991-2.

The dynamic factor, shall not be used with: the loading due to *Real Trains*, *Fatigue Trains*, *Load Model HSLM* and *Unloaded Train*.

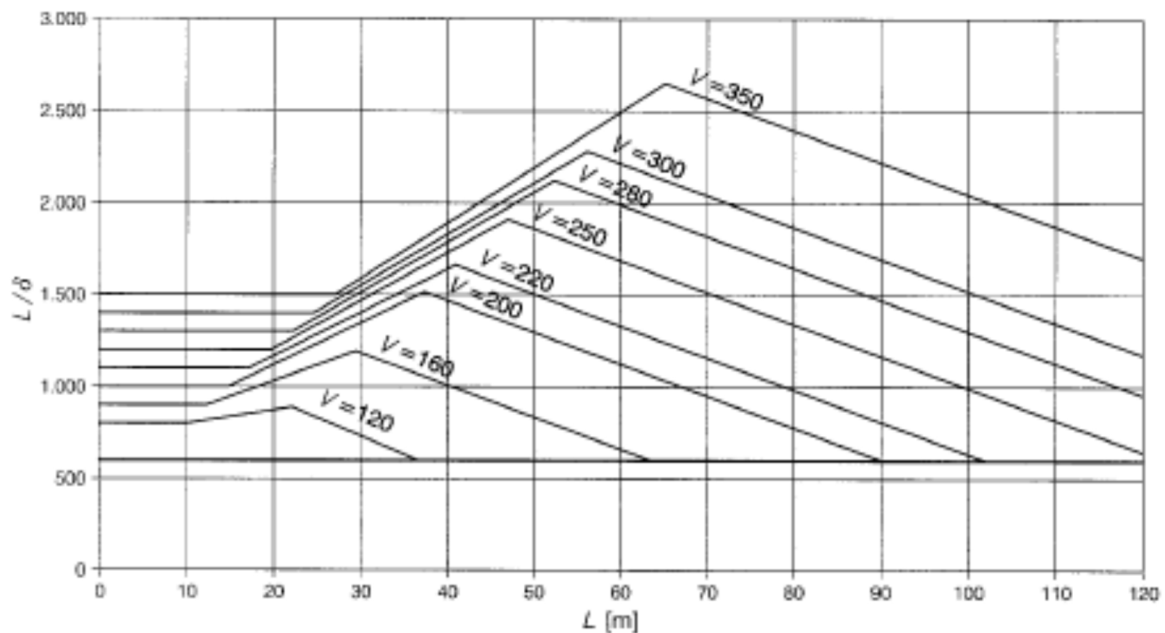


### 2.3.2. Ultimate Limit States and Serviceability Limit States according to EN 1991-2 and EN 1990 - Annex 2

All the limit state verifications are specified in Annex A2 from EN 1990. Particularly for short span bridges, the most important criterion that must be checked when a dynamic analysis is required is the vertical acceleration of the deck. For ballasted tracks, the peak value of vertical acceleration should not be greater than  $3,5 \text{ m/s}^2$ , considering the frequencies (including consideration of associated mode shape) up to the greater of:

- 30 Hz;
- 1,5 times the frequency of the first mode of vibration of the considered element, including at least the three first modes.

In principle, comfort criteria can be checked without dynamic analysis. Static deflections should be determined with Load Model 71 multiplied by the impact factor and with the value of  $\delta$  taken as unity and should be smaller than the value given in the chart below (Figure 2.3). However, the comparison of equations (2.6) and (2.7) below also applies, as specified in section 6.4.6.5(3) of EN 1991-2.



**$L/\delta = 600$  Limit :** The factors listed in A2.4.4.3.2.(5) should not be applied to this limit.

Figure 2.3 - Maximum permissible vertical deflection for railway bridges with 3 or more successive simply supported spans corresponding to a permissible vertical acceleration of  $b_v = 1 \text{ m/s}^2$  in a coach for speed  $V$  [km/h]

The dynamic analysis should be used to determine the following dynamic increment:

$$\varphi_d = \max |y_d / y_s| - 1 \tag{2.5}$$



Where:

$y_{dyn}$  is the maximum dynamic response and the  $y_{sta}$  the corresponding maximum static response at any particular point in the structural element due to Real Train or Load Model HSLM.

For the design of the bridge, taking into account all the effects of vertical traffic loads, the most unfavorable value of the next two equations should be used:

$$(1 + \varphi_d + \varphi/2)x(H_R) \quad (2.6)$$

$$\Phi (L_{71} + S/0) \quad (2.7)$$

Where:

**HSLM** - is the load for high speed lines defined in 6.4.6.1.1(2) from EN 1991 – Part 2;

**LM71+SW/0** - is Load Model 71 and is relevant Load Model SW/0 for continuous bridges;

**RT** - is the loading due to all Real trains defined in 6.4.6.1.1 from EN 1991 – Part 2;

$\varphi/2$  - is the increase in calculated dynamic load effects (stresses, deflections, bridge deck accelerations, etc.) resulting from track defects and vehicle imperfections in accordance with annex C for carefully maintained track;

$\varphi_d$  - is the dynamic factor in accordance with 6.4.4 from EN 1991 – Part 2;

### 3. STRUCTURAL MODEL OF FRAME BRIDGE FOR DYNAMIC ANALYSIS UNDER MOVING LOADS

#### 3.1. Definition of a frame bridge for static and dynamic analysis

As mentioned in the chapter 1, the bridge that was studied in this thesis is an integral reinforced concrete bridge, carrying a single ballasted track. These bridges are the most common type of overpasses along modern railway lines.

To create this model, there is needed to adopt a suitable geometry and appropriate material properties. The geometry is defined based on the following article: “*Identification of soil-structure interaction effect in a portal frame railway bridge through full-scale dynamic testing*” [15]. However, regarding the values for properties of the soil material have been chosen from different studies is this field.

The main characteristics of the model from the mentioned article are illustrated in the following figure (Figure 3.1).

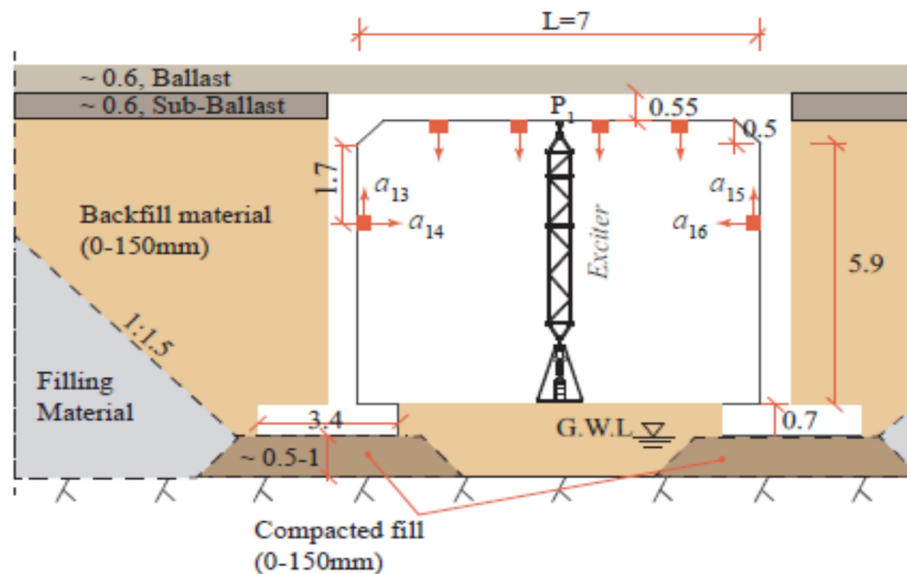


Figure 3.1 - Geometry and surrounding soil properties of model taken as an example [15]

#### 3.2. Finite Element Program

In engineering, physical phenomenon are mathematically described by differential equations. Usually, the equations are too complicated to be solved by classical analytical methods. The finite element method (FEM) is a mathematical technique for setting up and solving systems of partial differential or integral equations. In engineering, the FEM is used to divide a system whose behavior cannot be predicted using closed form equations into small pieces or elements whose solution is known or can be approximated. Finite element analysis is applicable to



tasks, involving for instance structural analysis with applications in strength analysis, vibration, thermal analysis, rigid body dynamics and so on.

As basic procedure for Finite Element Analysis (FEA), according to “ANSYS Mechanical APDL for Finite Element Analysis [1]”, ten steps can be considered in any FEA. First, the solid model geometry is created, the element type(s) and material properties are defined and the solid model geometry is meshed to create the finite element model. In ANSYS, these steps are performed in the Preprocessor (PREP7). Next, load and constraints are applied, solution options are defined and the problem is solved. These steps are performed in the Solution processor (SOL). After the solution is ready, the results are plotted, viewed and exported in one of the postprocessors (POST1 or POST26). Finally, the results are compared to first-order which estimates closed-form solutions, mathematical models or experimental results, to ensure that the output of the program is reasonable and as expected.

Therefore, the procedure for Finite Element Analysis (FEA) in ANSYS could be summarized as:

#### **/PREP7**

1. Define the Solid Model Geometry;
2. Select the Element Types;
3. Define the Material Properties;
4. Mesh;

#### **/SOLUTION**

5. Define the Boundary Conditions;
6. Define the Loads;
7. Set the Solution Options;
8. Solve;

#### **/POST1 or POST26**

9. Plot, View and Export the Results;
10. Compared and Verify the Results.

In order to have realistic and accurate results of the bridge, a finite element analysis should be carried out. The model has been created with ANSYS Mechanical APDL, which is a powerful finite element analysis software. APDL is an acronym for ANSYS Parametric Design Language, a powerful scripting language that allows you to parameterize your model and automate common tasks. Using APDL, you can:

- Input model dimensions, material properties and so on in terms of parameters rather than numbers;
- Retrieve information from the ANSYS database, such as a node location, maximum stress or displacement;
- Perform mathematical calculations among parameters;
- Define abbreviations for mostly used commands or macros;
- Create a macro to execute a sequence of tasks, do-loops and user prompts.

### 3.3. Geometry and characteristics of the 3D model

The characteristic dimensions for each element and every type of material, used in the model, are presented in the drawings below.

The main bridge of the study is the one with 7 meters span length and 0.55 meters thickness of deck. The dimensions of the others studied bridges were chosen keeping the slenderness ratio, between span length and thickness of slab, and are presented in following table:

Element of the bridge	Span Length 7m	Span Length 10m	Span Length 13m
Bridge deck thickness (m)	0.55	0.79	1.02
Wall thickness (m)	0.55	0.67	0.78
Bottom slab thickness (m)	0.55	0.67	0.78

Table 3.1 - Geometrical characteristics of studied bridges

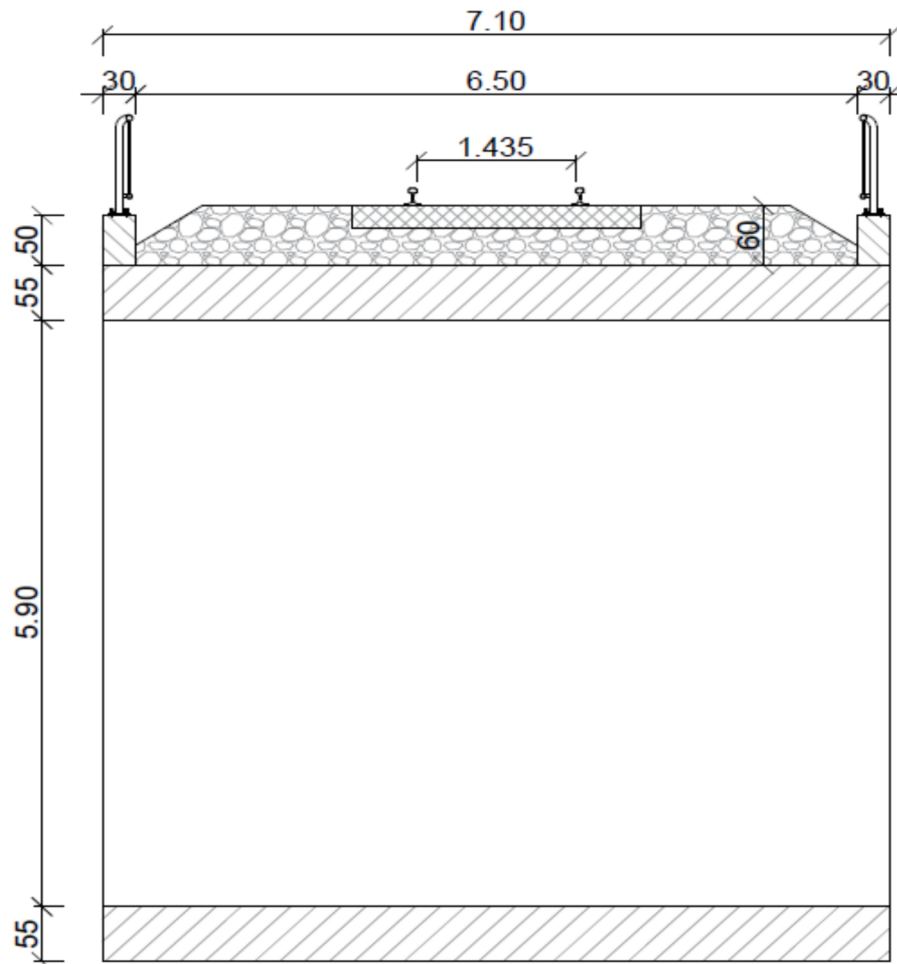


Figure 3.2 - Cross-section at mid-span of the bridge

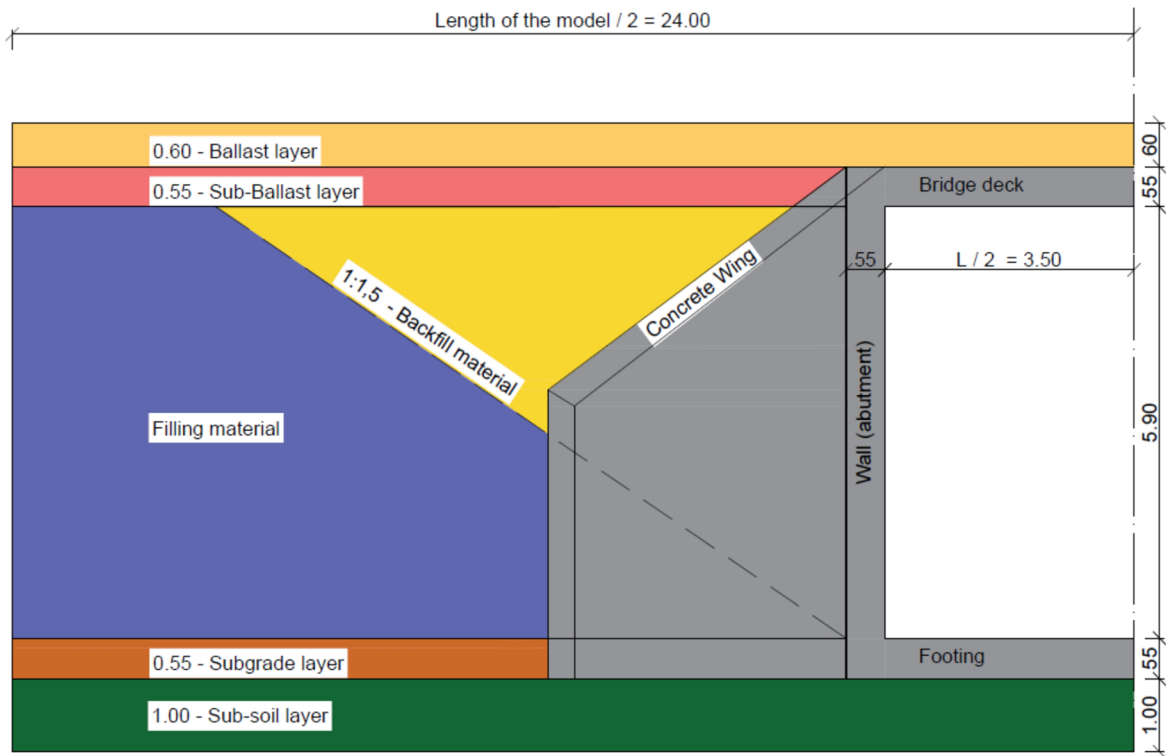


Figure 3.3 - Longitudinal section of studied model

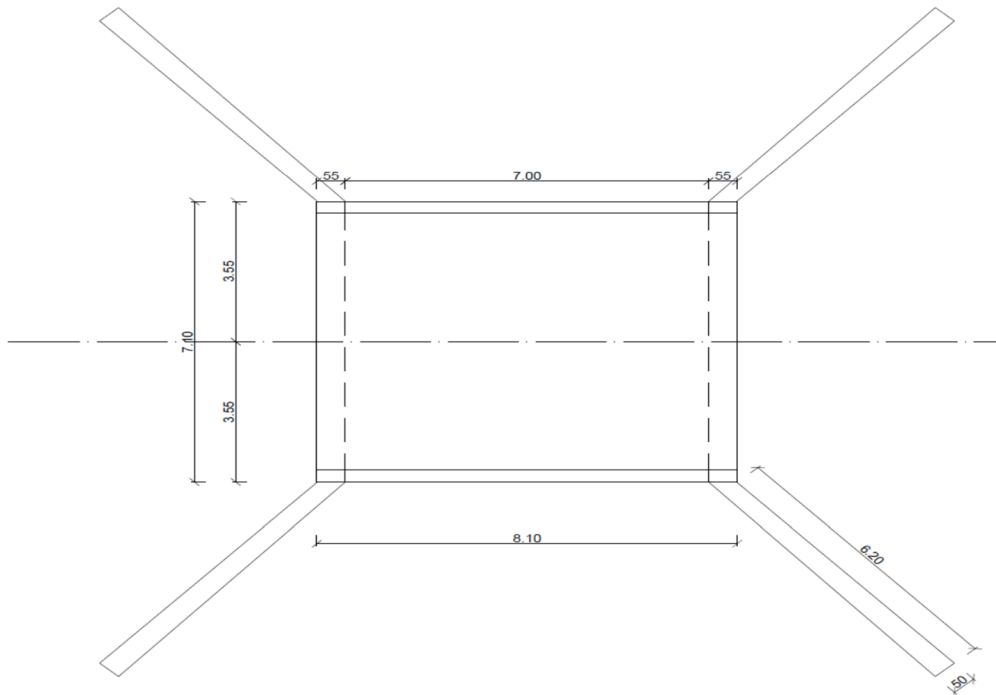


Figure 3.4 - Plan view of bridge structure

These kind of structures have a 3D action under the loads, so loads produce two directional bending, which can not be truly captured in 2D modeling. So a 3D modelling of the model has been performed.



The whole 3D-Finite Element Model (FEM) was created using just 3D solid elements such as prisms, tetrahedrons and pyramids, in order to create an accurate and detailed model. To create all these, “SOLID187” was used which is a higher order 3-D, 10 – node elements. It has a quadratic displacement behavior and is well suited to model irregular meshes. The geometry, node locations and the coordinate system for this type of solid is showed in next figure.

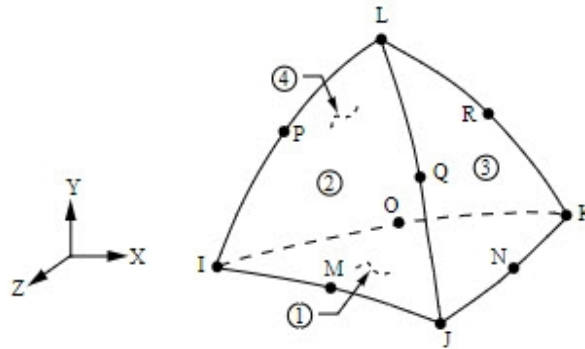


Figure 3.5 - SOLID 187 used in ANSYS

Most elements types require material properties and, depending on the application, these can be linear or nonlinear. In this thesis, all elements were defined as linear material: for isotropic material was defined only the X direction property and for the other directions a default value of X direction.

The geometry and characteristics of the elements are defined as inputs. Before defining, the type of elements used in the model should be chosen, for instance:

“*et,1,187*” - to define a type of element, in this case is Solid 187

Further, to define the characteristics of the materials has been used the “MP” command, which defines a linear material property as a constant, for instance:

- For concrete structure:

“*mp,ex,1,3.4e10 ! Young's modulus for concrete C35/45*”

“*mp,nuxy,1,0.3 ! Poisson ratio*”

“*mp,dens,1,2500 ! Density of material*”

- For ballast layer:

“*mp,ex,1,1.3e8 ! Young's modulus*”

“*mp,nuxy,1,0.2 ! Poisson ratio*”

“*mp,dens,1,1530 ! Density of material*”





The mechanical and physical properties of the materials considered in model are presented in the following table:

Materials	E (MPa)	(kg/m <sup>3</sup> )	(-)
Concrete structure – C35/45	34000	2500	0.20
Ballast layer	200	1800	0.20
Sub-Ballast layer	120	1935	0.25
Backfill material	130	2040	0.25
Filling material	170	1900	0.30
Subgrade	700	1900	0.40
Sub-soil	700	1900	0.40

Table 3.2 - Characteristics of the materials

The physical properties of the concrete are supposed to be elastic and un-cracked. The effect of cracking is not taken into account in this study. Thus, the standard static value of the modulus of elasticity is used in the further analysis. Generally, cracked concrete may provide a lower value of the modulus of elasticity and a higher value of the Poisson's ratio.

Generally, any solid model is defined in terms of keypoints, lines, area and volumes. The studied model in this thesis was created using keypoints, lines, volumes. Keypoints are the vertices, lines are the edges, areas are the faces and volumes are the interior of the object. Keypoints were defined within the currently active coordinate system, then lines connected these keypoints and finally the volumes that formed the model were created between these keypoints.

To create the keypoints, the command “K” was used to define the location in the active coordinate system. The volumes were created using the command “V” which defines volumes through keypoints, for instance:

“v,41,35,36,42,1041,1035,1036,1042” – to create a prism element;

“v,32,34,99,9938,37,89,89” – to create a tetrahedral element;

The command for lines, mentioned above, defines two volumes with different shapes, where the numbers from the inside of command are the keypoints which were defined in a parametric form, for example:

“k,35,0.,b,h1+l2; - to create a keypoint with coordinates  $x = 0$ ;  $y = 3.55$ ;  $z = 6.45$ ;

k,36,0.,b,h1+l2+h3; - to create a keypoint with coordinates  $x = 0$ ;  $y = 3.55$ ;  $z = 7.00$ ;

k,41,-h2,b,h1+l2, ” - to create a keypoint with coordinates  $x = -0.55$ ;  $y = 3.55$ ;  $z = 6.45$ ;

The whole 3D Finite Element Model is composed of 584 keypoints, that have been parametrically defined, 323 solid volumes and contains 261156 nodes. Because the number of elements which form the model is very big and the time was limited, it was created only half of the model.

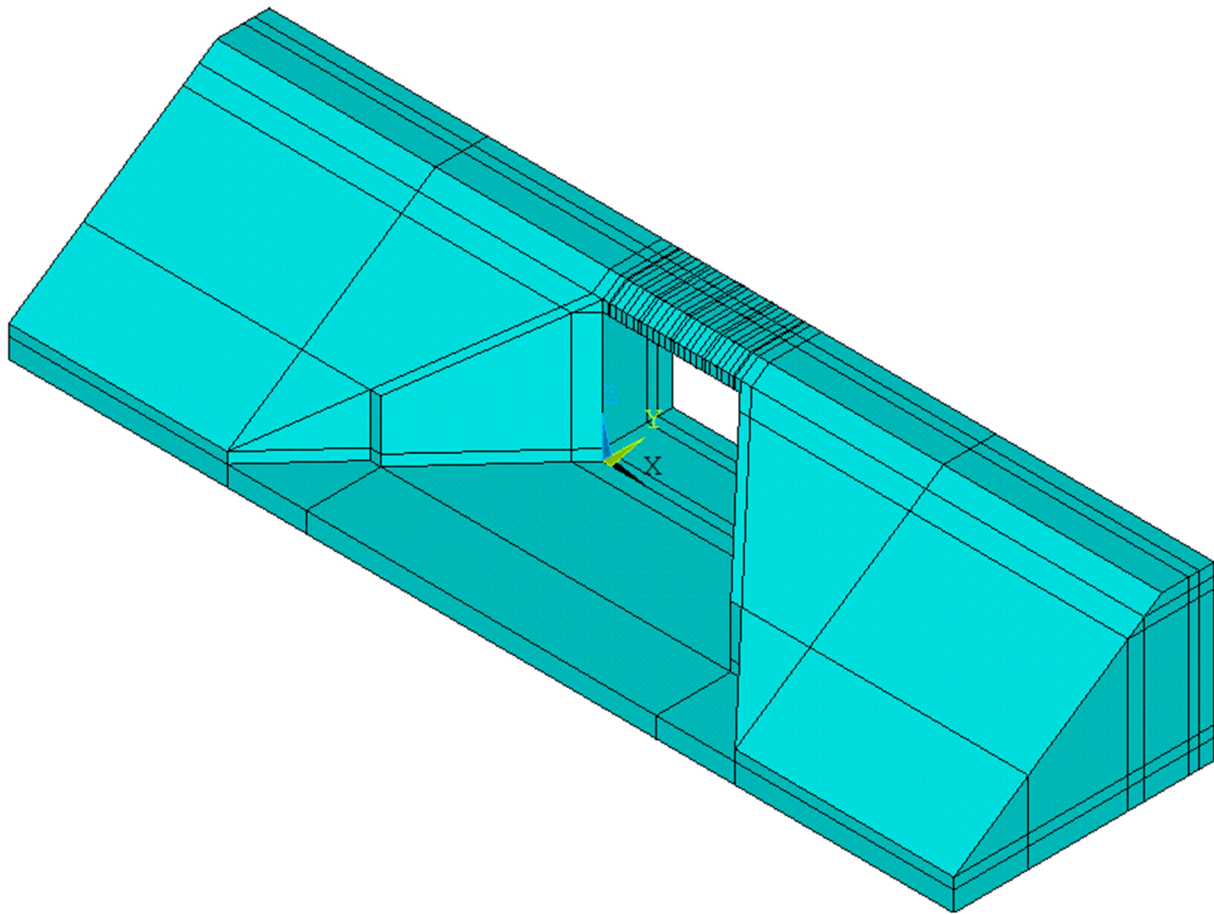


Figure 3.6 - Volumes used for meshing the 3D-Finite Element Model (FEM)

### 3.4. Boundary conditions and mesh

As it was mentioned before, the 3D Finite Element Model has a huge number of elements and also the computation time is an important factor, so these are the reasons why was defined a symmetry plan along the longitudinal axis of the track.

The boundary conditions were defined such that the bottom edge of the sub-soil layer to have fixed horizontal, vertical and rotational degrees of freedom and the symmetry plan to have fixed only the horizontal degree of freedom, in order to be considered as an entire model. The “D” command has been used to define degree of freedom constrains at nodes. For instance, in order to define the symmetry plan along the longitudinal axis of the track, the following sequence was typed:

“*n sel,s,loc,y,bhalf* “ – to select all the nodes from the longitudinal axis of the track;

“*d,all,UY,0*” - to define the constrains in Y directions for previous selected nodes;

The model of real bridges structures usually involves assumptions in modelling, such as boundary conditions, length of the model, mesh size and so on. Therefore, in case of complicated and sophisticated models, it is helpful to develop an appropriate model with realistic prediction and economical, together with a reasonable design. Mesh size and length of the model is a common problem in FEA for this field. But, there is a clear line about them:

bigger elements give bad results, but smaller elements make computing time much longer. Hence, in order to have a reasonable model and to consider the computer resources, a 3D Finite Element Model with the following dimensions was chosen: in longitudinal direction (O-X) 48.00 meters and in transvers direction (O-Y) 13.22 meters.

To mesh the model it has been used a free mesh, because has no restrictions in terms of element shapes and has no specified pattern applied to it. The finite element mesh needs to be sufficiently dense in order to capture all the aspects of the structure, especially in that zones which represent important points such: deck, walls and ballast layer above the deck. For these important parts of the structure has been used a fine mesh, with the size of element equal with 0.25 m, and for elements that form the rest of the model the size has varied between 0.40 - 1.40 m. in order to create a smooth transition between them.

<b>Materials/Elements of the 3D-FE Model</b>	<b>The size of mesh (m)</b>
Bridge structure	0.25
Ballast prism above the bridge deck	0.25
Ballast prism above the earthworks	0.40
First part of wings (connection with bridge)	0.25
Wing's elevation	0.40
Sub-ballast layer	0.40
Backfill material	0.40
Filling material	0.60
Slopes of embankments	0.95
Sub-grade layer	1.20
Subsoil layer	1.40

Table 3.3 – The size of meshes for the bridge with 7 m. span length

Obviously, a reduction of finite element size gives more elements, but in turn leads to more nodes in the model, so for each model it is advisable to compare computing time and the desired accuracy.

The command used to mesh the model was “VMESH” which generates nodes and volume elements within volumes. The syntax of command is “VMESH, NV1, NV2, NINC” which means that it meshes volumes from “NV1” to “NV2” in steps of “NINC”, for instance:

- Bridge deck: “ *size1=0.25*”

*Esize,size1*

*Mat,1*

*Vmesh,1,62”*

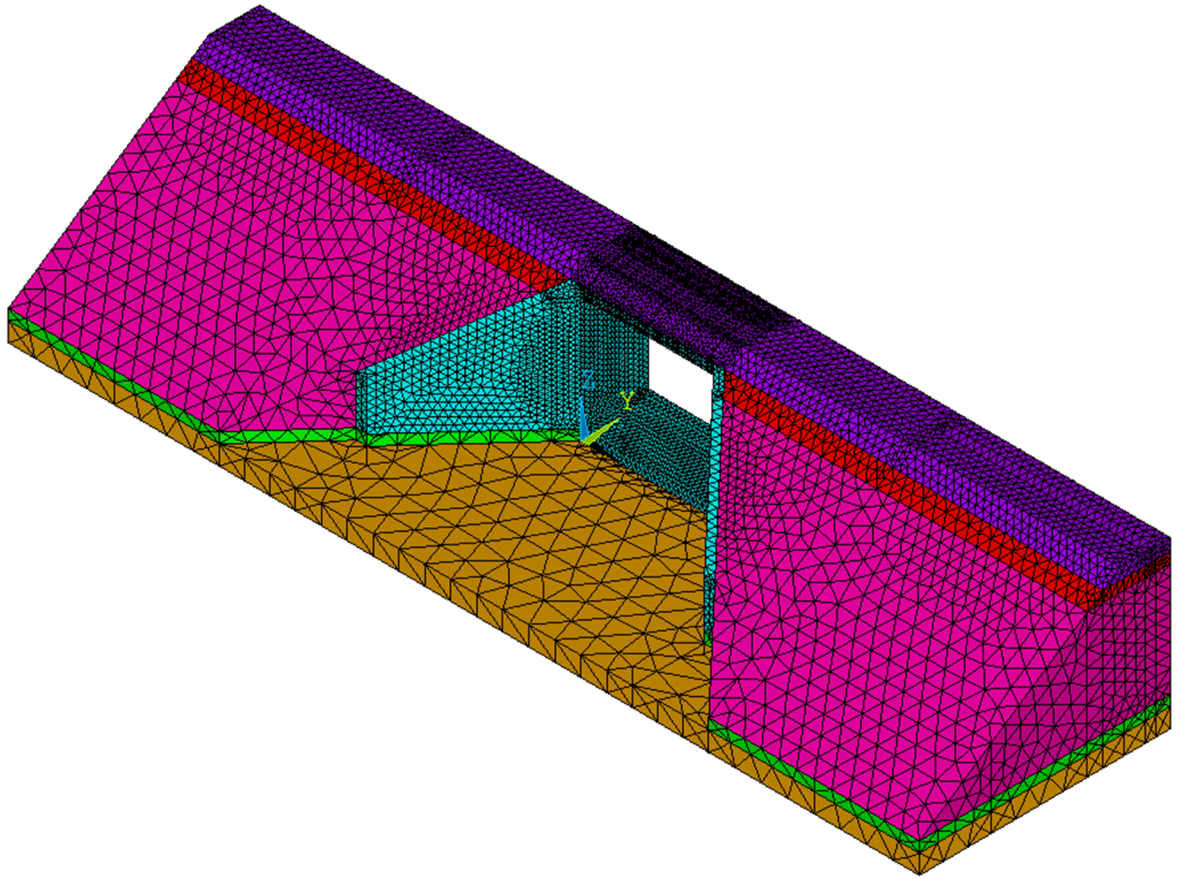


Figure 3.7 - 3D-Finite Element Mesh

## 4. STATIC AND DYNAMIC ACTIONS CONSIDERED IN THE MODEL

### 4.1. Static loads

The model used in this study for the train is the Load Model 71 (LM 71), taken from EN 1991-2, illustrated in next figure:

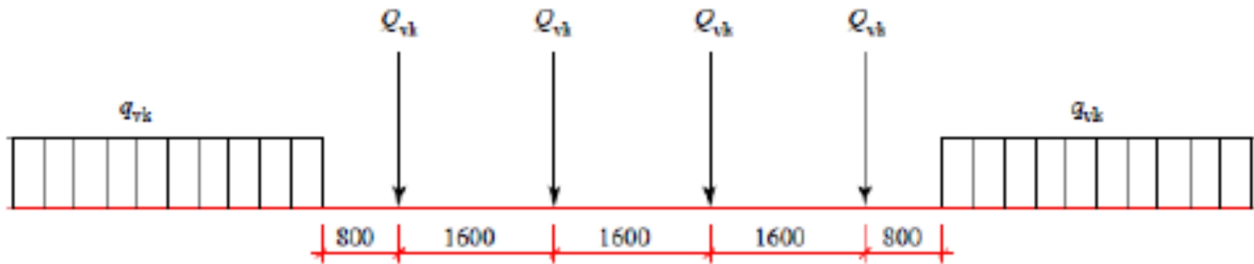


Figure 4.1 - Load Model 71 (LM71)

Load Model 71 represents the static effect of vertical loading due to normal rail traffic. The distributed load  $q_{vk}$  is 80 kN/m and the concentrated loads  $Q_{vk}$  are 250 kN/m. The distributed load is infinite and should be placed at the most unfavorable position. Because in this thesis was modeled just half of model, the values of loads were divided by two, which correspond for only one rail.

A point force in Load Model 71 may be distributed over three rail support points as shown in Figure 4.2:

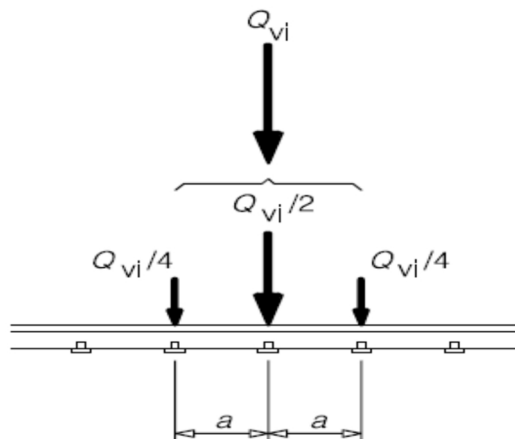


Figure 4.2 - Longitudinal distribution of a point force or wheel load by the rail

Where:

$Q_{vi}$  – is the point force on each rail due to Load Model 71;

$a$  – is the distance between rail support points.



For this thesis were made several assumptions: the distance (a) between sleepers is 60 cm and because the sleepers weren't modeled in finite element model, and to consider their existence, it was assumed a distribution area. This is the reason why the bridge deck and the ballast layer were divided in several pieces, with the width of piece equal with the width of the considered sleeper (25 cm) as shown in figure (Figure 4.3).

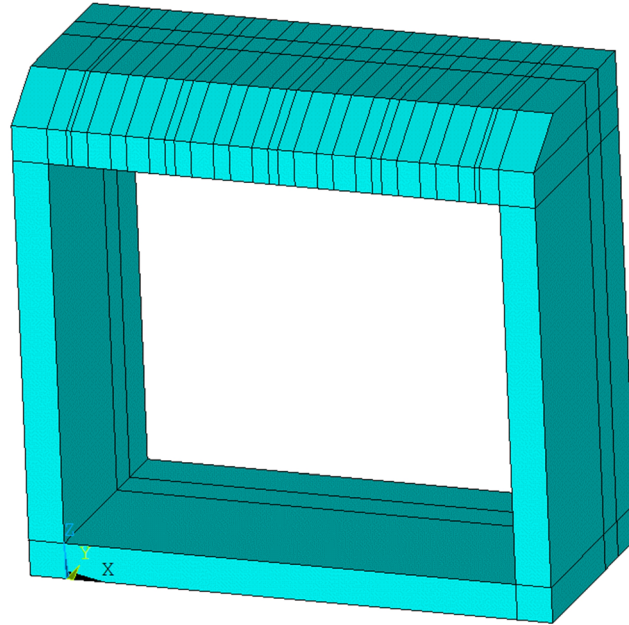


Figure 4.3 - The divided bridge deck and ballast layer

Thus, will be defined three kind of pressures acting on the bridge structure:

- 1 = 192300 N/m<sup>2</sup> is the pressure below concentrated load;
- 2 = 96150 N/m<sup>2</sup> is the pressure situated next to sleeper below concentrated load;
- di = 30770 N/m<sup>2</sup> is the pressure from uniformly distributed load;

All the computations for these pressures are presented in annex A3.

The distribution of loads, due to Load Model 71 above the bridge structure, is illustrated in the figure (Figure 4.4) and the pressure from uniformly distributed load was taken into consideration over a length equal with the length of the backfill material.

To define these loads, due to Load Model 71 in the 3D-FE Model, the following commands were used:

- "A" – defines an area by connecting keypoints;
- "SFA" – specifies surfaces loads on the selected areas;

For example, to define the pressure below the concentrated load, the following command lines are used:

"a,391,394,395,392" - to define the area of sleeper;

"sfa,3,,pres,P1" - to assign the pressure 1;

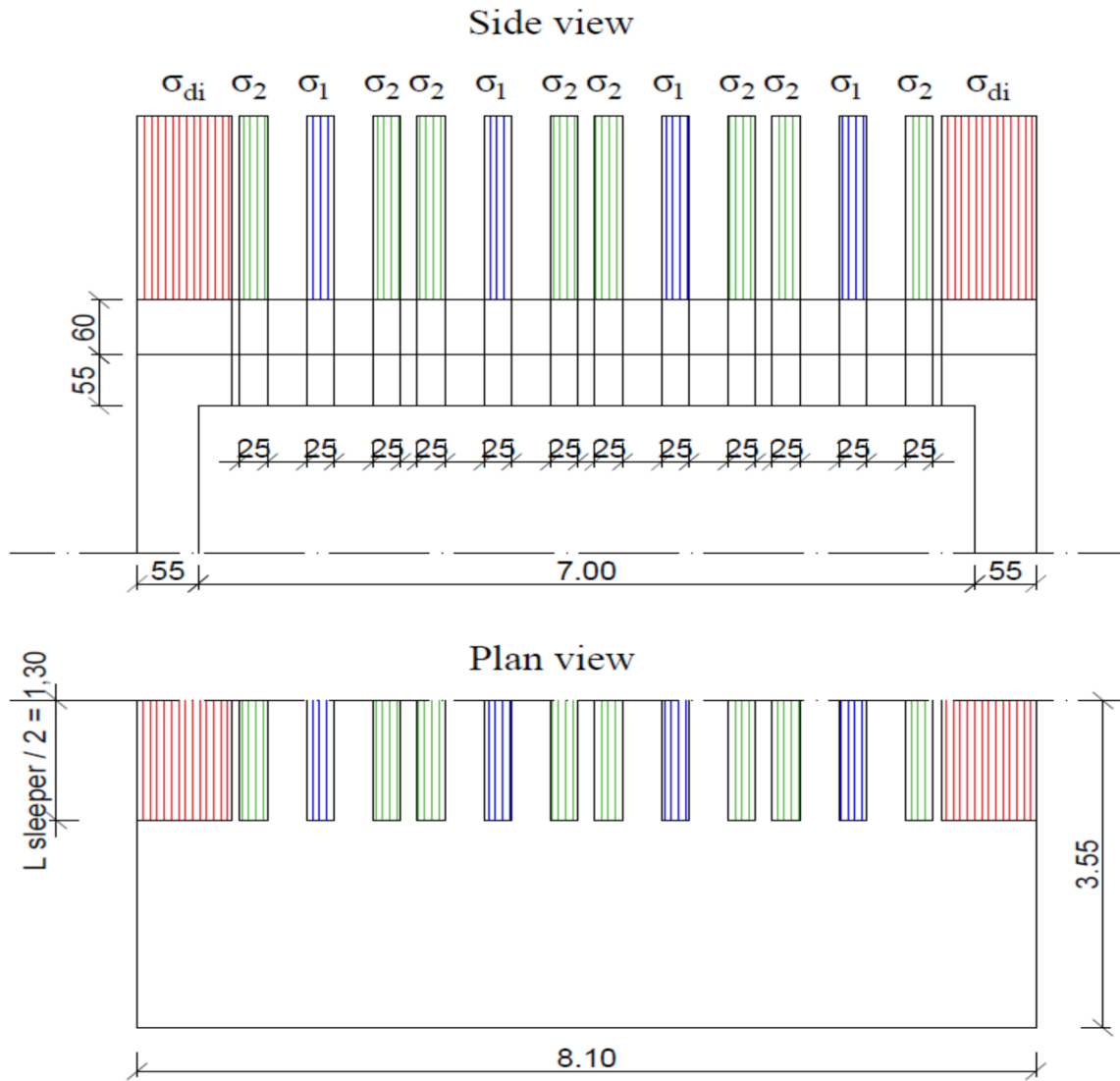


Figure 4.4 - The distribution of loads due to Load Model 71 considered in the 3D-FEM

## 4.2. Permanent loads

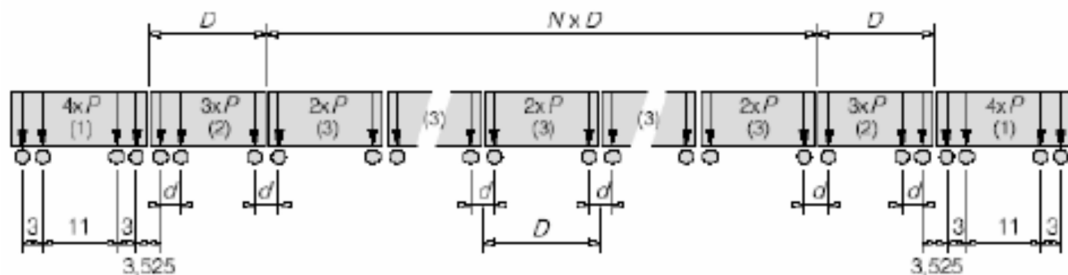
These permanent loads are due to the weight of the different elements of the bridge. The dead loads from concrete and ballast are considered with their characteristics densities (see Table 3.2) and the volumes are deduced from the dimensions of the elements. To take in account the weight of the sleepers and the rail, the density of the ballast was increased with 270 kg.

Other permanent loads were not considered in the analysis, such as: weight of the guardrail or parapets, electrical equipment, concrete protection or waterproofing membranes or future supplementary dead load.

### 4.3. Dynamic loads

Obviously, a static analysis is not sufficient when studying the behavior of bridges subjected to high speed trains. Therefore, the dynamic behavior of the structure shall be taken into account to study the real effects.

When considering the dynamic analysis of the bridge, only vertical actions are taken into account. Imposed train loads acting on the bridges, representing the dynamic effects of railway traffic, are taken from Eurocode. The train load models in Eurocode are a theoretical idealization of the high-speed trains. Furthermore, according to Eurocode, the dynamic analysis shall be undertaken using characteristic values of the train loading, the High Speed Load Model (HSLM). The HSLM consists of different train load configurations, with different characteristic axle loads and spacing between axles. The train configurations and the characteristic values are shown in Figure 4.5 and Table 4.1.



- (1) Power car (leading and trailing power cars identical)
- (2) End coach (leading and trailing and coaches identical)
- (3) Intermediate coach

Figure 4.5 - Train configurations of High Speed Lane Model – HSLM-A

Universal Train	Number of intermediate coaches N	Coach length D [m]	Bogie axle spacing d [m]	Point force P [kN]
A1	18	18	2.0	170
A2	17	19	3.5	200
A3	16	20	2.0	180
A4	15	21	3.0	190
A5	14	22	2.0	170
A6	13	23	2.0	180
A7	13	24	2.0	190
A8	12	25	2.5	190
A9	11	26	2.0	210
A10	11	27	2.0	210

Table 4.1 - Characteristics values of High Speed Lane Model – HSLM-A





A FORTRAN code together with a MATLAB code developed by Professor Pedro Museros Romero, is used to generate the train models and to carry out the dynamic analysis. Due to time restrictions, the dynamic analysis is carried in a simplified manner resorting to mode superposition, while in future developments such procedure should be improved in order to account for the time-domain interaction of soil and structure, and the wave transmission and energy dissipation through the boundaries of the numerical model.

#### 4.4. Thermal loading and rheological effects

Thermal loading contains two thermal effects that can induce stresses in the bridge. The first is a uniform temperature change, which results in an axial expansion or contraction, and the second is a differential temperature, which causes curvature. Like shrinkage, temperature change is an applied strain, not stress.

Shrinkage is the reduction in the length of a concrete element that occurs as the concrete sets and moisture are lost over time. The Eurocodes separate total shrinkage into two components: autogenous shrinkage and drying shrinkage.

Creep is the increase in deformation over time that occurs in the presence of a sustained stress. The Eurocodes give the creep coefficient as a function of the concrete strength and its tangent modulus, which, in turn, is a function of the cement type and the age of concrete at the first time of loading. Thus, creep can be reduced by delaying the first loading or using stronger concrete.

The movements due to temperature differences or creep/shrinkage can be a problem for frame or box bridges. The effect of deck shortening, relative to the supports, is to induce bending in the whole frame, as illustrated in figure (Figure 4.6). If some of this shortening is due to creep or shrinkage, there is the usual complexity and uncertainty associated with such calculations.

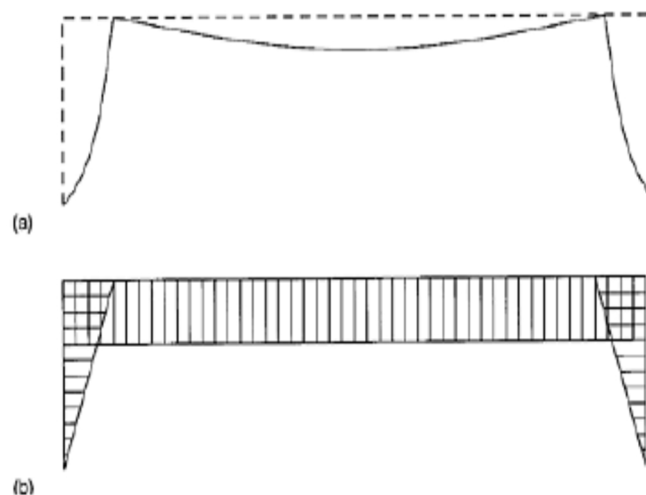


Figure 4.6 - Effect of thermal contraction of deck in frame bridge: a) deflected shape; b) distribution of bending moments



In this thesis, the thermal loading and rheological effects were considered in a simple manner using SAP2000 software. Therefore, for thermal loading just the effect of the uniform changes in temperature has been considered.

Because the studied bridge is a real example from Sweden [14], the location of the bridge is considered to be the same as in the mentioned article. The location of the bridge is in North of Sweden and was considered to be near the Umea city. The values of the maximum and minimum temperature was considered according to Table C-11 from “*Boverket mandatory provisions amending the board’s mandatory provisions and general recommendations (2011:10) on the application of European design standards (Eurocodes), BFS 2013:10 - EKS 9*” [2].

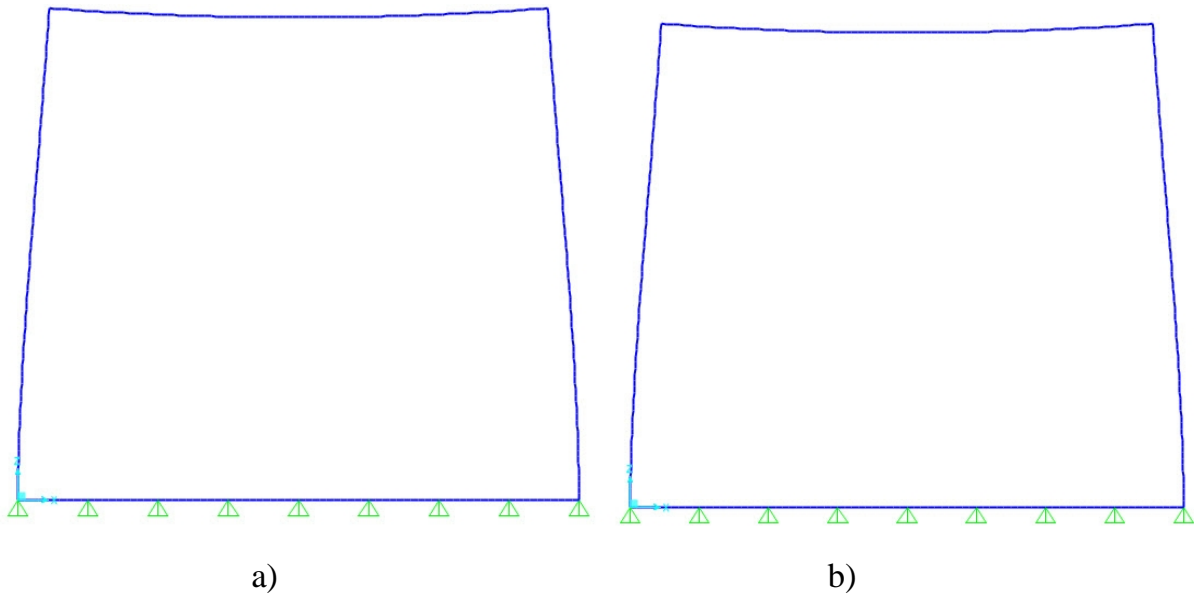


Figure 4.7 - Deformed shape due to: a) maximum negative temperature b) shrinkage

As expected, the deformed shapes are similar because the shrinkage effect produces the same effect as negative temperature, only the values of the displacements are different.

The results of the bending moment and axial force due to thermal load and shrinkage are presented in the following table:

The type of effect	Axial force (N)/m	Bending moment (N*m)/m
<b>Thermal loading (Contraction)</b>	18205.91	39941.05
<b>Shrinkage effect</b>	9273.52	20344.97

Table 4.2 - Results of internal forces due to thermal and shrinkage effect

All the computations of the thermal loading and rheological effects are given in annex A4.



## 4.5. Loads not considered in the model

For the same reason for which was created only half of the model and being a complex and parametric 3D Finite Element Model (FEM), the following loads were not considered in the analysis:

- Earthquake loads;
- Wind loads;
- Derailment, centrifugal forces, noising force, traction and braking force;
- Fatigue assessment;
- The static effects of vertical loading due to heavy freight traffic (model SW/2);
- The effects of the Load Model “Unloaded train”;
- The effects of eccentricity of vertical loads;

Also, the maintenance over the life of bridge and construction methods should also be studied to have a complete idea about the advantages of this type of bridge.

Obviously, for a real project, it is mandatory that these loads and aspects must be taken into consideration.

## 5. RESULTS OF THE ANALYSIS

### 5.1. Static analysis

The static analysis was performed using the Load Model 71 (LM 71) for live loads and the dead loads were automatically considered by software based on their densities. Static analysis assumes that the live loads are applied instantaneously on the bridge in most unfavorable position. The position and the intensity of these loads has been discussed in the previous chapter.

To determine the internal forces, in this thesis, four sections were chosen, having the configuration of figure below (Figure 5.1). For each section, just relevant stresses were chosen to determine the internal forces.

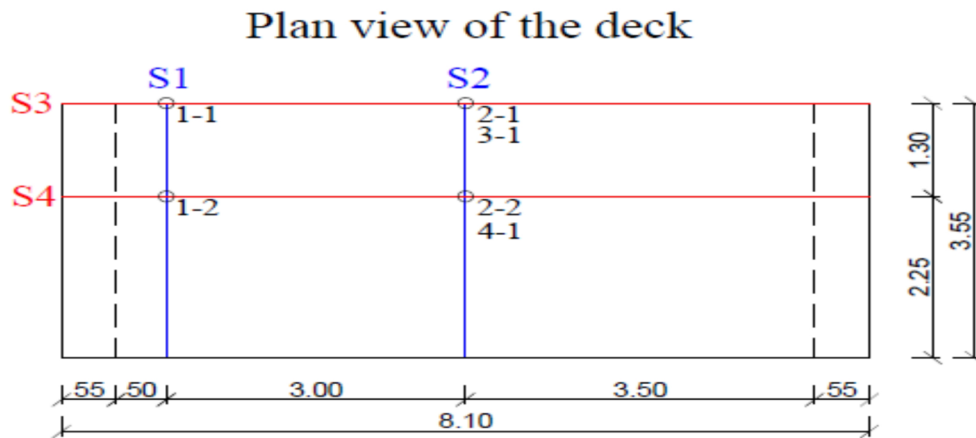


Figure 5.1 - Distribution of studied sections

Deflections, normal stresses and tangential stresses due to gravity loads were further analyzed for each section mentioned above.

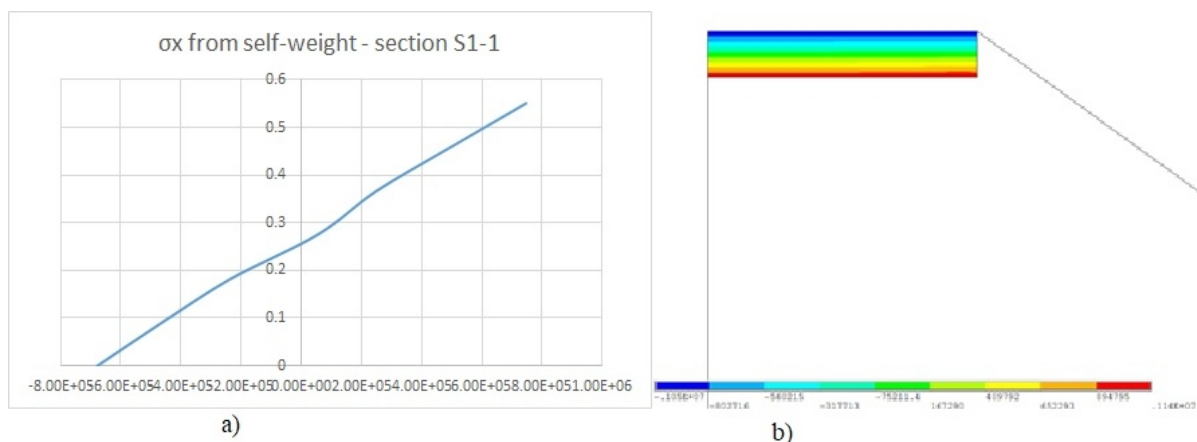


Figure 5.2 - The normal stress  $\sigma_x$  due to self-weight in section S1: a) distribution of normal stress in point S1-1; b) distribution of normal stress in deck's cross-section

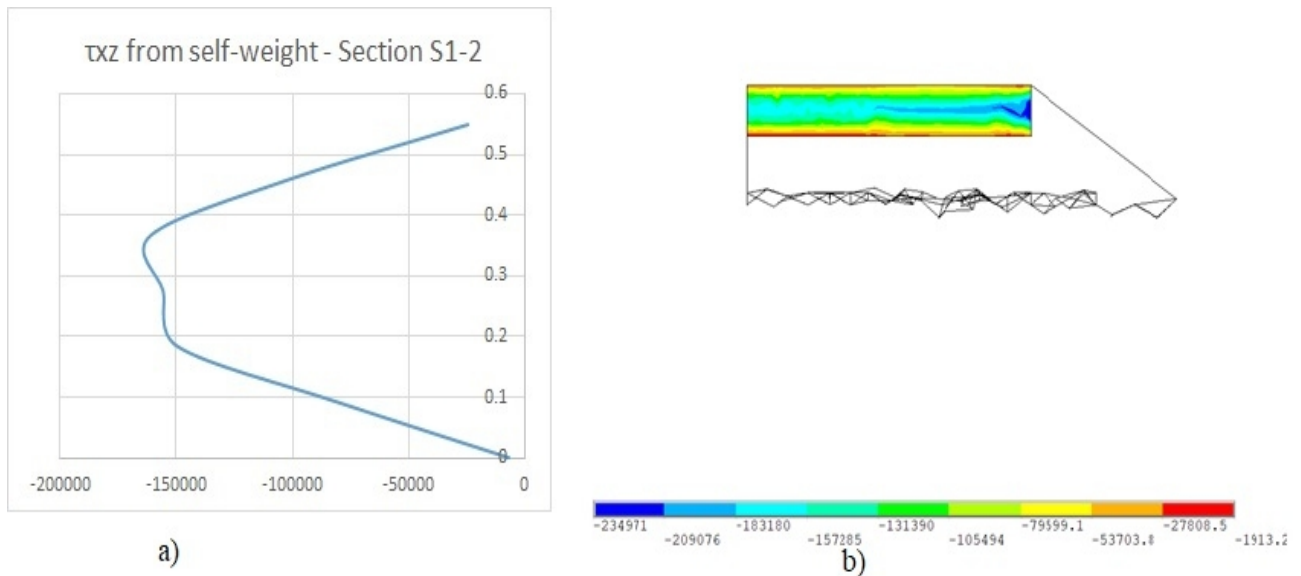


Figure 5.3 - The tangential stress  $\tau_{xz}$  due to self-weight in section S1: a) distribution of tangential stress in point S1-2; b) distribution of tangential stress in deck's cross-section

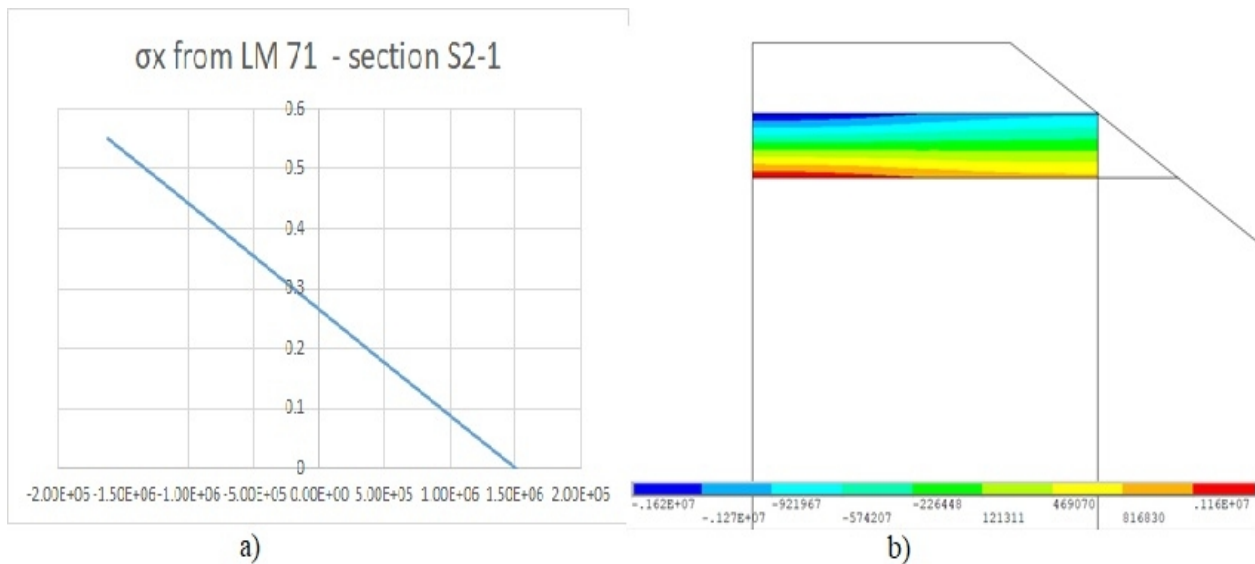


Figure 5.4 - The normal stress  $\sigma_x$  due to LM 71 in section S2: a) distribution of normal stress in point S2-1; b) distribution of normal stress in deck's cross-section

As can be seen in these graphs, the normal stresses (  $\sigma_x$  ) have a linear variation on the section and the tangential stresses (  $\tau_{xz}$  ) follow a parabolic variation, which are typical for rectangular sections.

A brief check of the results obtained in ANSYS has been done in parallel with SAP2000 software together with simple hand calculations. All verifications are presented in annex A1.

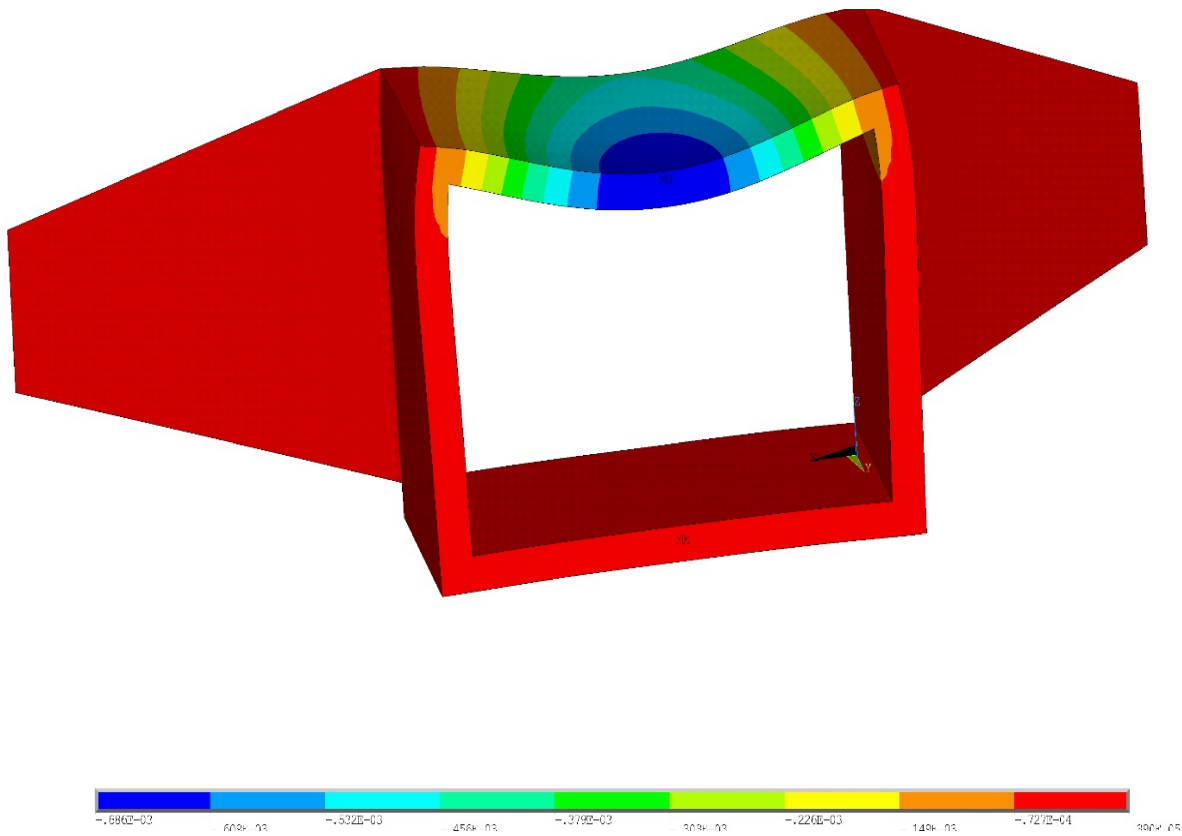


Figure 5.5 - The vertical displacements of the deck due to LM 71

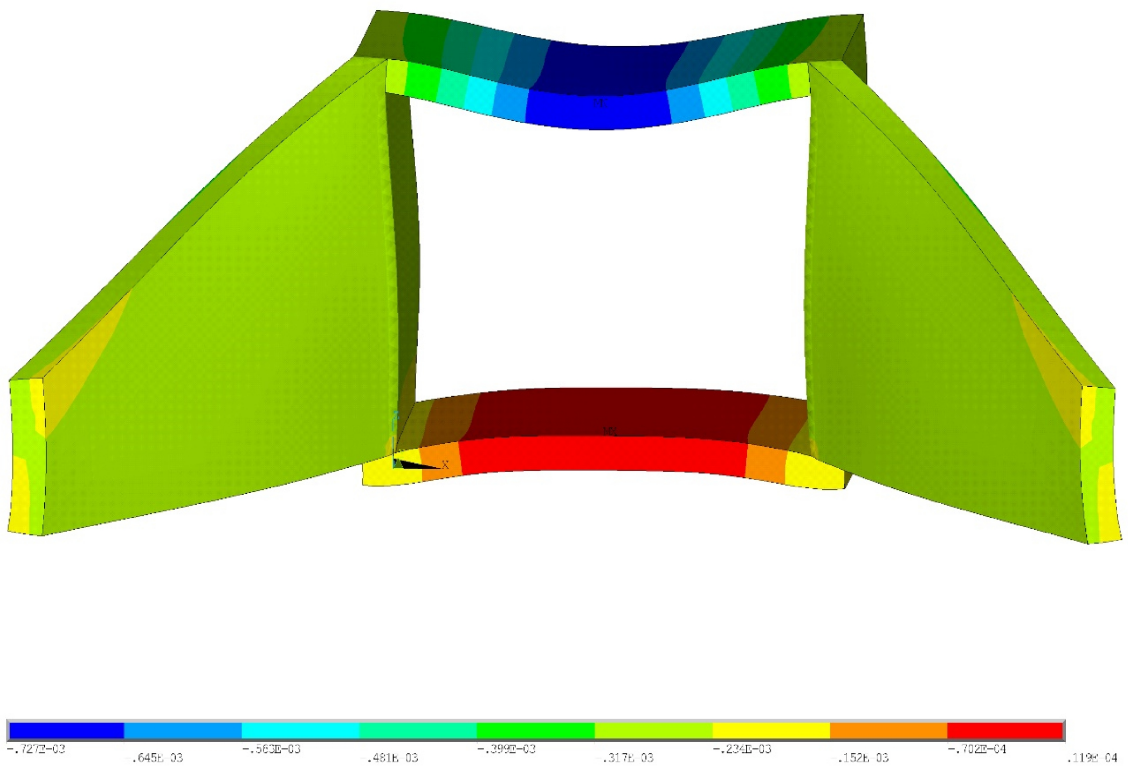


Figure 5.6 - The vertical displacements of the deck due to self-weight

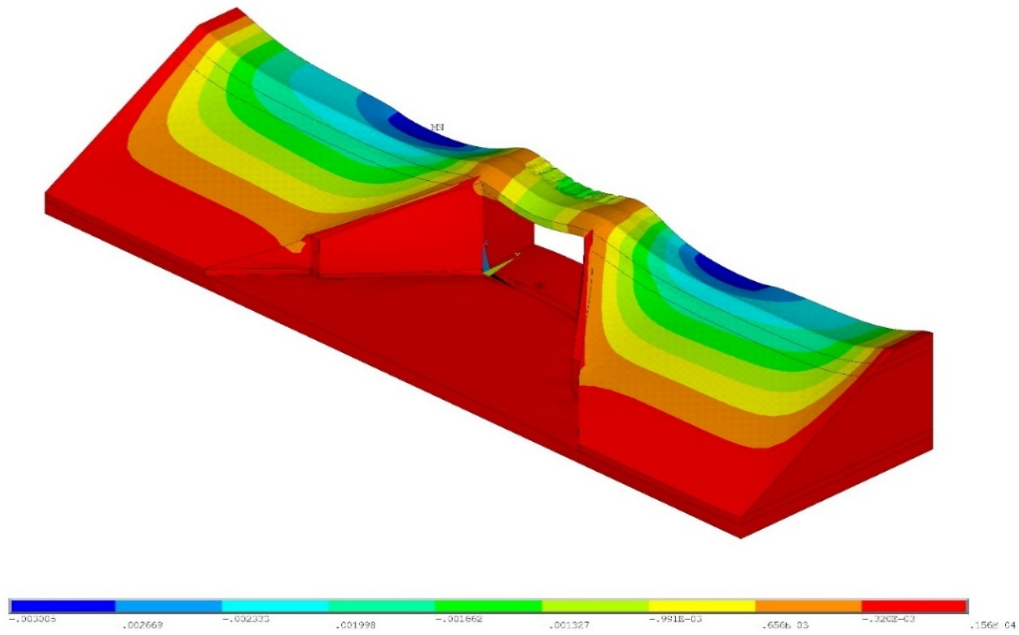


Figure 5.7 - The total vertical displacements of 3D-FE Model due to self-weight and LM 17

As expected, the largest vertical displacements appear on the backfill material next to the walls under the pressure from uniformly distributed load. Of course the reason is that the Young’s Modulus of the earthworks is much smaller compared to the Young’s Modulus of concrete structures. Also, a brief check of these displacements has been done, to validate them, and is presented in annex A2.

The results from static analysis with their characteristics values are presented in the following table (Table 5.1).

Span Length	Section - Point	Characteristics values due to Permanent Loads					Characteristics values due to Load Model (LM 71)				
		x (N/m <sup>2</sup> )		y (N/m <sup>2</sup> )	xz (N/m <sup>2</sup> )	yz (N/m <sup>2</sup> )	x (N/m <sup>2</sup> )		y (N/m <sup>2</sup> )	xz (N/m <sup>2</sup> )	yz (N/m <sup>2</sup> )
		top	bottom				top	bottom			
7 m	1--1	7.47E+05	6.78E+05	-	1.55E+05	-	4.55E+05	5.51E+05	-	2.54E+05	-
	1--2	7.62E+05	7.08E+05	-	1.56E+05	-	5.06E+05	5.81E+05	-	2.58E+05	-
	2--1	-	1.09E+06	-	-	-	1.62E+06	1.51E+06	-	-	-
	2--2	1.04E+06	1.09E+06	-	-	-	1.41E+06	1.31E+06	-	-	-
	3--1	-	-	3.56E+05	-	-	-	-	1.14E+06	-	-
	4--1	-	-	-	-	4370	-	-	-	-	5.23E+04

Table 5.1 - The characteristics values of stresses from static analysis

The stresses due to permanent loads have been evaluated considering that all the components of the embankments appeared simultaneously, but obviously it is not an accurate assessment. So, a brief analysis has been carried out at the mid-span to illustrate if the assessment of the

stresses, on each construction stage of the embankments, have a major influence on final stresses.

Hence, the construction have been divided in three stages:

Stage 1: The bridge structure and the wings were built on the sub-grade layer.

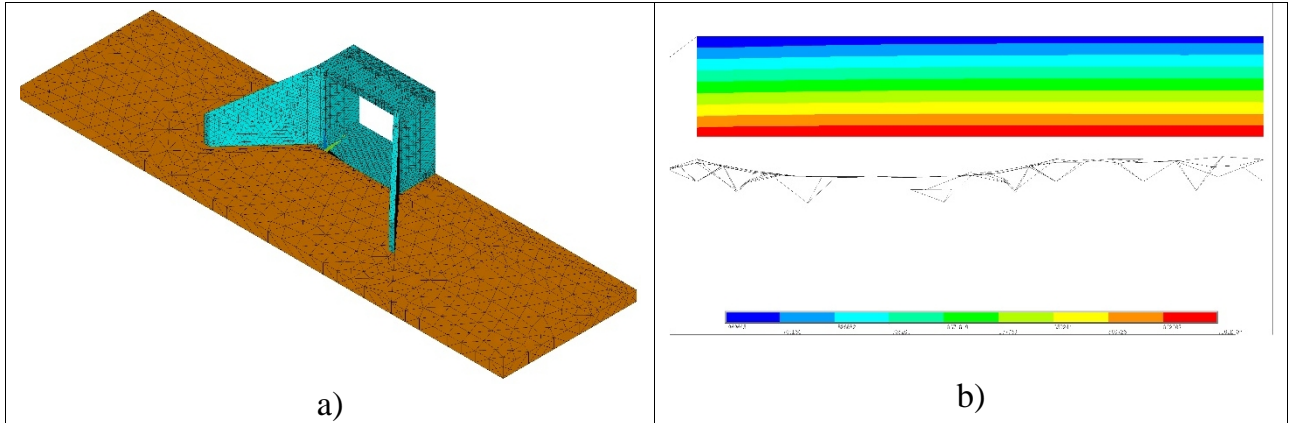


Figure 5.8 - Stage 1: a) the considered model; b) the normal stress (  $x$  ) at mid-span

Stage 2: Additionally, the backfill material, the filling material, the sub-soil layer and the sub-ballast layer were built.

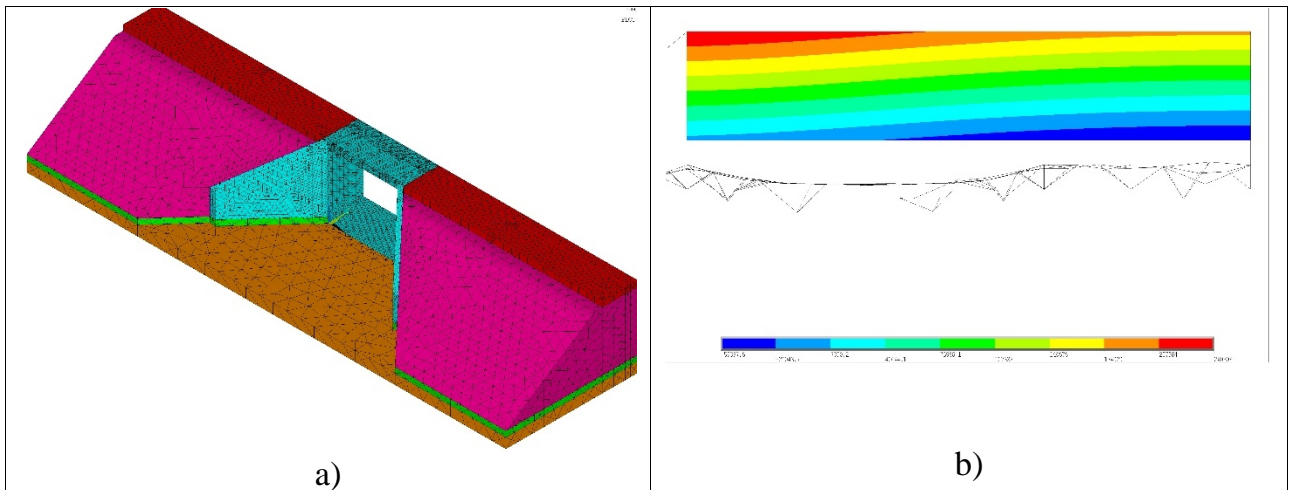


Figure 5.9 - Stage 2: a) the considered model; b) the normal stress (  $x$  ) at mid-span



Stage 3: Finally, the ballast layer was built.

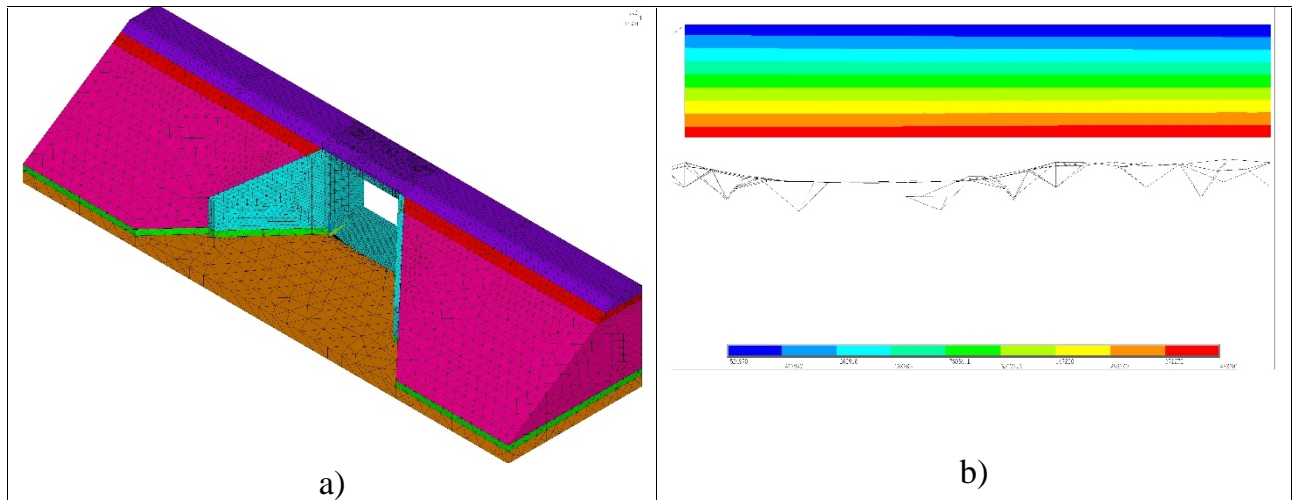


Figure 5.10 - Stage 3: a) the considered model; b) the normal stress ( $\sigma_x$ ) at mid-span

In the following table, a summary of the normal stresses at mid-span are presented, concerning the construction stages in parallel with the case when constructions stages were not considered.

Description	Normal stress at bottom edge (N/m <sup>2</sup> )	Normal stress at top edge (N/m <sup>2</sup> )
Stage 1	1020000	-876000
Stage 2	-59400	181000
Stage 3	483000	-525000
Total normal stresses from stages	1440000	-1220000
The model without construction stages	1094000	-1040000

Table 5.2 - The normal stress due to construction stages

Observing the values of total normal stresses due to permanent loads, taking into account construction stages, these are greater than the values when were not considered the construction stages. The difference between them are in the range 17% - 31%, which is quite important.

Therefore, in the design phase, the modelling of the embankments and the layers of substructure should be made on construction stages.

## 5.2. Dynamic analysis

As mentioned before, and due to time restrictions, the dynamic analysis is carried in a simplified manner resorting to mode superposition, while in future developments such procedure should be improved in order to account for the time-domain interaction of soil and



structure, and the wave transmission and energy dissipation through the boundaries of the numerical model.

For a mode superposition analysis, the natural frequencies and mode shapes are determined first. There are an infinite number of natural frequencies of mechanical system with continuously distributed mass. Only the lowest frequencies would have a practical application when studying the dynamic response of a bridge. The bridge structure reacts mainly with the frequencies near its own natural frequencies, when excitation forces are applied to a system over a wide spectrum of frequencies.

Also, Eurocode advises to check deck bridge acceleration for frequencies up to 30 Hz or 1,5 times the frequency of the first mode of vibration of the element. Since the first frequencies of interest are about 9-10 Hz, the modes up to 30 Hz have been considered in this thesis.

The ANSYS modal analysis is used to determine the natural frequencies and the mode shapes of bridge structure by exploiting the so-called “Block Lanczos” eigensolver.

Other important bridge parameters in dynamic analysis are structural damping and bridge mass. The magnitude of the vibrations depends heavily on structural damping, especially in proximity to resonance. Underrating the mass will lead to overestimation of the natural frequency of the structure and of the speed at which resonance occurs. At resonance, the maximum acceleration of a structure is inversely proportional to the distributed mass of the structure. The calculations of the bridge parameters are given in annex A7.

In order to determine the value of main bending frequency of the bridge deck ( $n_0$ ), a modal analysis of the bridge structure was performed in ANSYS software.

```
STEP=1
SUB =3
FREQ=18.2737
DMX =.005795
```

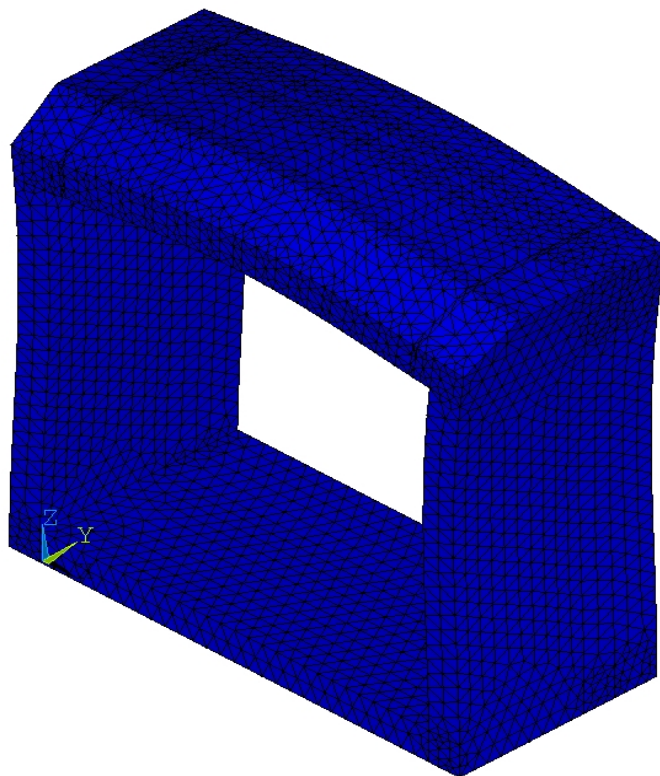


Figure 5.11 - The first natural bending frequency of the bridge deck



This value of first natural bending frequency,  $n_0=18.274$  (Hz) is used in formulae (C.6) from EN 1991-Part 2 - Annex C, to determine the “ factor.

The most important assumption was that a dynamic analysis was required for this bridge that carries traffic over 200 km/h.

Hence, the results of this dynamic analysis must be compared with the results of the static analysis enhanced by the dynamic factor. The most adverse load effects of this comparison must be used for the bridge design.

In order to perform the dynamic analysis of the model, the following step here is to extract the natural frequencies and mode shapes of the structure from 3D-Finite Element Model.

The first vertical mode shape is observed at the frequency of approximately 16.9 Hz and is showed in figure 5.12 and the rest of vertical mode shapes and their natural frequencies are illustrated in annex A8.

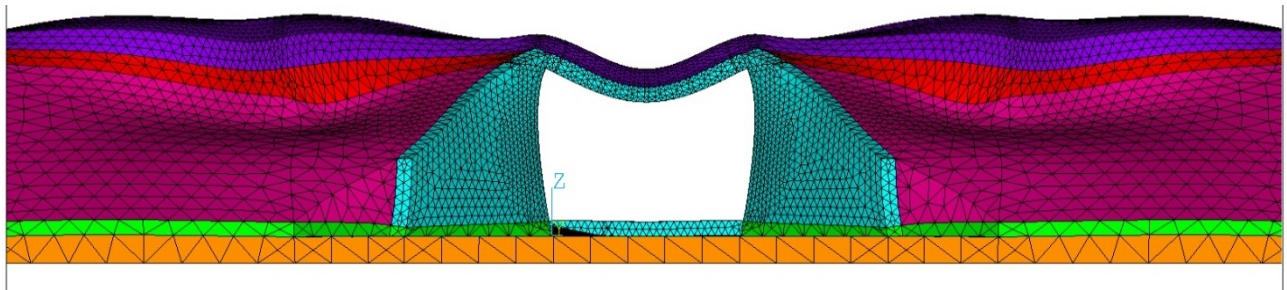


Figure 5.12 - The first vertical mode shape

In order to determine whether the calculated load effects from high-speed rail traffic (HSLM-A), are greater than those of normal rail traffic loading (LM 71) a dynamic analysis by mode superposition has been performed taking the values of natural frequencies up to 30 Hz.

The Train Model HSLM-A was used and the following values of dynamic increment,  $\phi'$ , were obtained as follows:

Dynamic increment $\phi'$	Universal Train
0.3313	A1
0.2213	A2
0.2822	A3
0.1767	A4
0.2865	A5
0.3544	A6
0.2946	A7
0.2039	A8
0.2915	A9
0.2859	A10

Table 5.3 - The values of dynamic increment corresponding to the HSLM-A



As can be seen, the maximum value of dynamic increment has been obtained for the universal train, A6.

The value of the static displacement was obtained from the graph below and corresponds to the value at minimum speed (100km/h), therefore the maximum static effect of HSLM-A is about 0.31 mm.

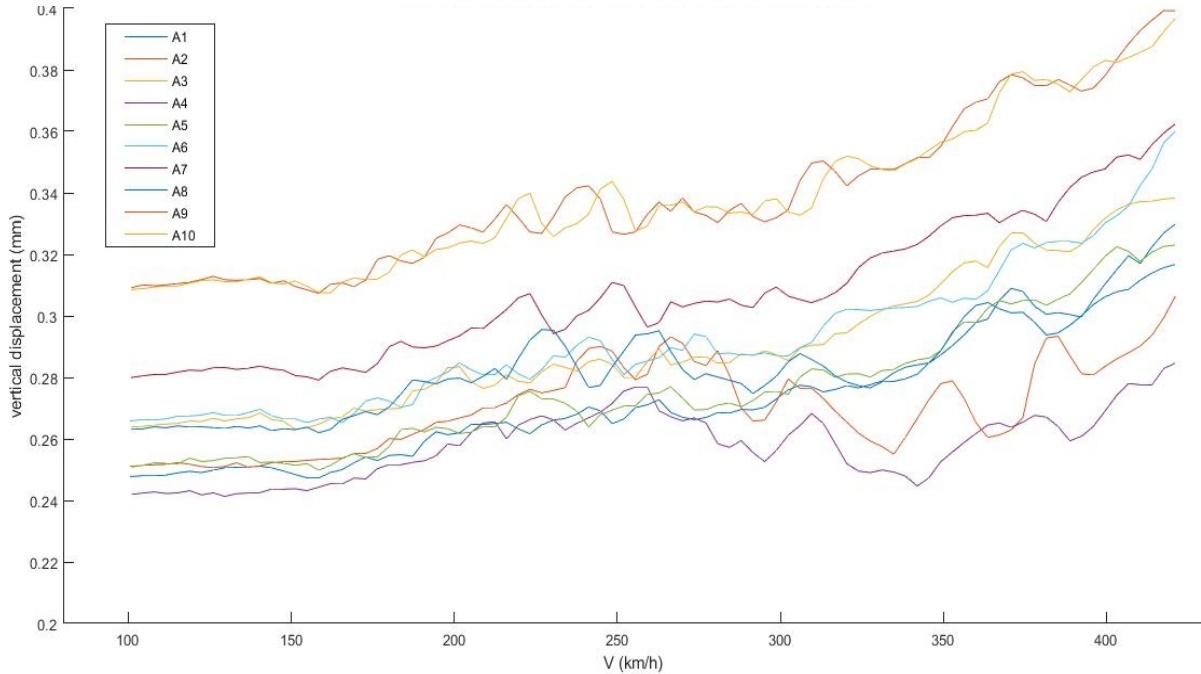


Figure 5.13 - Vertical displacements at mid-span due to train model HSLM-A for 7 meters span length

Further, these values are used in the Eq. (2.6) to compare the results with those from Eq.(2.7) in order to obtain the most unfavorable case. A brief overview about the results are presented in the table below. The calculation of the following factors, according to Annex C from EN 1991-2, are presented in detail in annex A10 of the thesis.

Type of effect	din	“	due to HSLM-A (mm)	Impact factor	due to LM71 (mm)	Value of the vertical displacement (mm)
<b>Dynamic - Eq 2.6</b>	0.3544	0.676	0.31	-	-	0.525
<b>Static - Eq 2.7</b>	-	-	-	1.34	0.686	0.919

Table 5.4 - The value of displacements due to static and dynamic analysis

According to the results in Table 5.4, for the ULS and SLS combinations, only the dynamic factor obtained using the Eq. (2.3) and factor  $\psi$ , will be considered to compute the internal forces.

## 6. COMBINATION OF EFFECTS FOR ULS AND SLS ASSESSMENT

### 6.1. Combinations of actions

The combinations of actions for this thesis will be carried out according to EN 1990 - Annex A2. This Annex A2 from EN 1990 gives rules and methods to establish combinations of actions for serviceability and ultimate limit states verifications (except fatigue verifications) with the recommended design value of permanent, variable and accidental actions and factors to be used in the design of railway bridges.

To determine the design value, two coefficients have to be included. The first one,  $\gamma$ , is a coefficient which takes into account the heavy or light railway traffic. This factor should be chosen among different values, depending on the country. In this study  $\gamma = 1,21$  is used; this value is commonly used in Spain. The second one is  $\psi$  factor which was calculated using the equation (Eq.2.3), for carefully maintained track.

The values of the coefficients for ULS and SLS verifications, are presented in the following table:

ULS - STR			SLS		Temperature	LM71	Factor		
Partial safety factor for			Partial safety factor for						
permanent action $G$	variable action $Q$	other variable action $Q$	permanent action $G$	variable action $Q$					
1.35	1.45	1.50	1.00	1.00	0.85	0.50	0.60	0.80	1.21

Table 6.1 - The coefficients used in ULS and SLS combinations

### 6.2. ULS assessment

For the check at the ULS, the maximum between STR-set A and STR-set B is used. The values from static analysis are combined in order to obtain the maximum values according to Table A2.4(B) from EN 1990 - Annex 2. The values of bending moment, shear force and axial force for each considered section have been determined. The maximum value of internal forces is given by “set B” combinations, and these values are presented in the following table:

Sections	Ultimate limit state - ULS			
	Mx (kN*m)/m	My (kN*m)/m	Sz (kN)/m	Nx (kN)/m
<b>S1-1</b>	155.079	-	283.427	576.436
<b>S1-2</b>	161.147	-	287.208	585.204
<b>S2-1</b>	301.346	-	-	564.595
<b>S2-2</b>	277.018	-	-	574.238
<b>S3-1</b>	-	155.103	-	-
<b>S4-1</b>	-	-	78.780	-

Table 6.2 - The values of internal forces at ULS combination

### 6.3. Computing of deck reinforcement

The design of reinforcements have been performed at ultimate limit state and the reinforcement of the deck was computed just for the case with span length = 7 m. The full calculation of reinforcements and the verifications at SLS combination are presented in Annex A5.

In this study, for deck verifications at SLS combinations, stress limitation and crack verification were performed.

For this thesis the following aspects have been considered:

- Concrete class: C35/45;
- Reinforcing steel: S500 (BST500B) – class of ductility B;
- Exposure class: XD3 Risk of chloride-induced corrosion (other than sea water);
- Relative humidity of the ambient environment : 80%;

The final reinforcement of the deck are summarized in the following table and reinforcement drawings are illustrated in annex A11.

Direction	Section	Reinforcement	Corresponding sectional area
Longitudinal	S1	16 s=200 mm on top	1005 mm <sup>2</sup> /m
Longitudinal	S2	20 s=200 mm on bottom	1571 mm <sup>2</sup> /m
Transversal	S3	16 s=225 mm on bottom 12 s=225 mm on top	894 mm <sup>2</sup> /m 503 mm <sup>2</sup> /m
Vertical (shear reinforcement)	-	12 s=300 mm 4 vertical links/meter	452 mm <sup>2</sup> /m

Table 6.3 - The summary of the deck reinforcement

Because in this thesis the reinforcement has been determined only for the deck, the reinforcement for the wall was assumed being the same as the one from end of the deck (S1-embedded section).

Every structural member can be subdivided in so-called B regions and D-regions. B stands for “Bernoulli” and corresponds to those parts of the member where the assumption of Bernoulli can be accepted (planar sections remain plan after load has applied). D stands for “Discontinuity” and corresponds to the regions where the assumption of Bernoulli is no longer valid, this is typically the region around:

- Changes in cross-section, openings, node in frames, connections between girders and beams (geometrical discontinuity);
- Isolated loads, supports, temperature changes, anchorage of prestressing tendons (static discontinuity).

In this thesis the checking of node frame of the bridge using the “Strut and Tie Model” has been performed and the calculation is presented in the Annex A6.

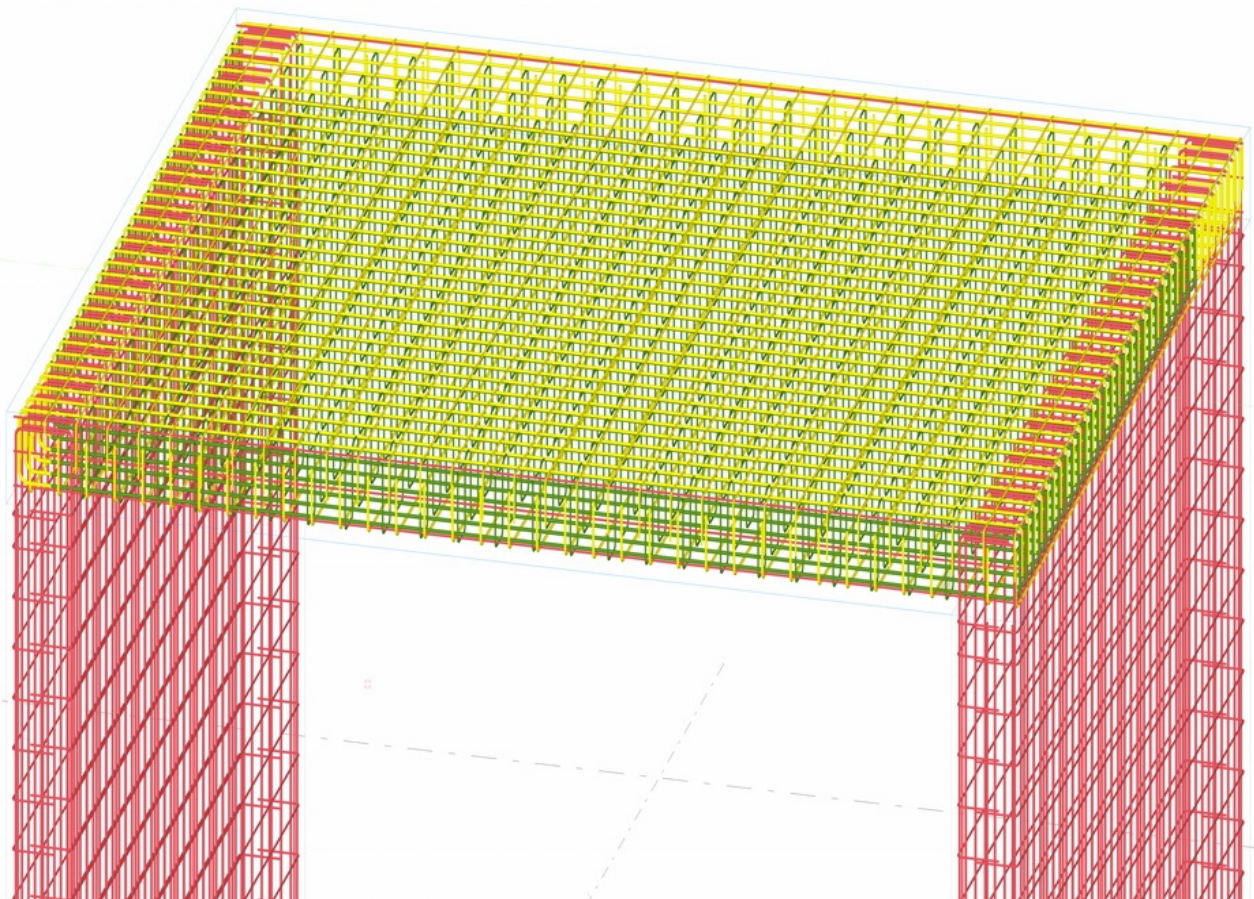


Figure 6.1 - The 3D-bridge reinforcement

#### 6.4. SLS assessment

For the check at the Serviceability Limit States, the combinations of actions were performed according to EN 1990 – Annex A2.

The vertical traffic loads applied to the bridge cause the deck to bend, resulting in a vertical displacement of every point on the surface of the deck. In general, maximum displacement



occurs in the middle of the deck or at mid-span. According to the European standard mentioned above, the deflections of the bridge should not exceed certain limits. The vertical deflection has two different limits: for traffic safety and for passenger comfort. For traffic safety, the EN 1990–A2 states for all structure configurations loaded with the classified characteristic vertical loading in accordance with EN 1991-2, clause 6.3.2, the maximum total vertical deflection measured along any track due to rail traffic actions should not exceed  $L/600$ .

For passenger comfort, the limitation depends on several parameters such as span length, configuration of the bridge and train speed. The vertical deflection should be determined with Load Model 71 multiplied by the factor  $= 1.34$  and with the value of  $\gamma$  taken as unity, in accordance with EN 1991-2 – Section 6. For a level of comfort “very good” and a maximum speed of 350 km/h the limitation of the bridge is  $L/\gamma = 1500$ .

The maximum deflections compared with their respective limits are presented in the following table:

	Deflection [mm]	Limit [mm]
Traffic safety	0.686	11.67 (L/600)
Passenger comfort	0.9192	4.67 (L/1500)

Table 6.4 - Deflections and their limits

As can be seen, all the deflections are under the limit values. The limit state is accomplished and there is no concern regarding the deflections. The longitudinal movements due to braking and traction forces were not considered in this thesis.

To ensure traffic safety, the verification of maximum peak deck acceleration, due to rail traffic actions, need to be regarded as a traffic safety requirement checked at the SLS for the prevention of the track instability. The maximum permitted peak design value of the bridge deck acceleration, determined along the track, must not exceed the recommended value given in EN 1990-Annex 2 – clause 4.4.2, which is:  $0.35g = 3.50 \text{ m/s}^2$ .

In the following graph are illustrated the values of the bridge deck acceleration at mid-span due to Train Model HSLM-A.



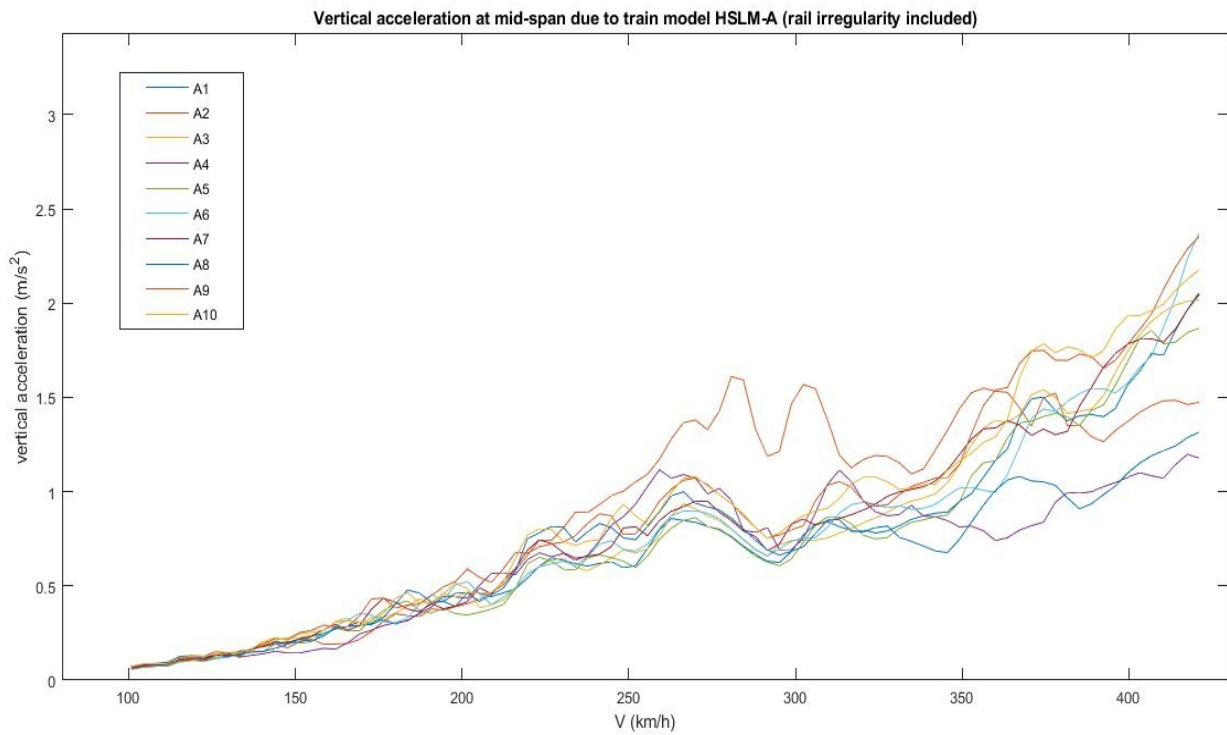


Figure 6.2 - Vertical acceleration of the bridge deck at mid-span due to HSLM-A

As can be seen, even if certain peaks of resonance phenomena are present, all the values of acceleration are under the limit value, so the limit state is fulfilled.

In this study, the frequent combination is used to check cracking. It has been considered just the section from the mid-span of the deck. The verification of the cracking is given in annex A5, with satisfactory results.

## 7. SENSITIVITY ANALYSIS FOR DIFFERENT SPAN LENGTHS

### 7.1. Static effects for 10 m and 13 m span lengths

The great advantage of a parametric model programmed in ANSYS is that only a few changes are needed to modify the input variables and obtain the desired models with different span lengths (10 meters and 13 meters). The same slenderness ratio has been adopted between span and deck thickness. The results of stresses and displacements for each case are illustrated in the next table.

Characteristics values due to Permanent Loads							Deflection (mm)
			x (N/m <sup>2</sup> )		y (N/m <sup>2</sup> )		
			top	bottom			
<b>SPAN LENGTH</b>	7	<b>Section - Point</b>	1--1	7.47E+05	-6.78E+05	-	0.726
			1--2	7.62E+05	-7.08E+05	-	
			2--1	-1.04E+06	1.09E+06	-	
			2--2	-1.04E+06	1.09E+06	-	
			3--1	-	-	3.56E+05	
	10	<b>Section - Point</b>	1--1	9.99E+05	-9.25E+05	-	1.294
			1--2	1.04E+06	-9.83E+05	-	
			2--1	-1.54E+06	1.52E+06	-	
			2--2	-1.54E+06	1.53E+06	-	
			3--1	-	-	2.82E+05	
	13	<b>Section - Point</b>	1--1	1.28E+06	-1.20E+06	-	2.110
			1--2	1.34E+06	-1.27E+06	-	
			2--1	-2.01E+06	1.93E+06	-	
			2--2	-2.02E+06	1.94E+06	-	
			3--1	-	-	2.47E+05	

Table 7.1 - The value of normal stresses and vertical deflection due to permanent loads

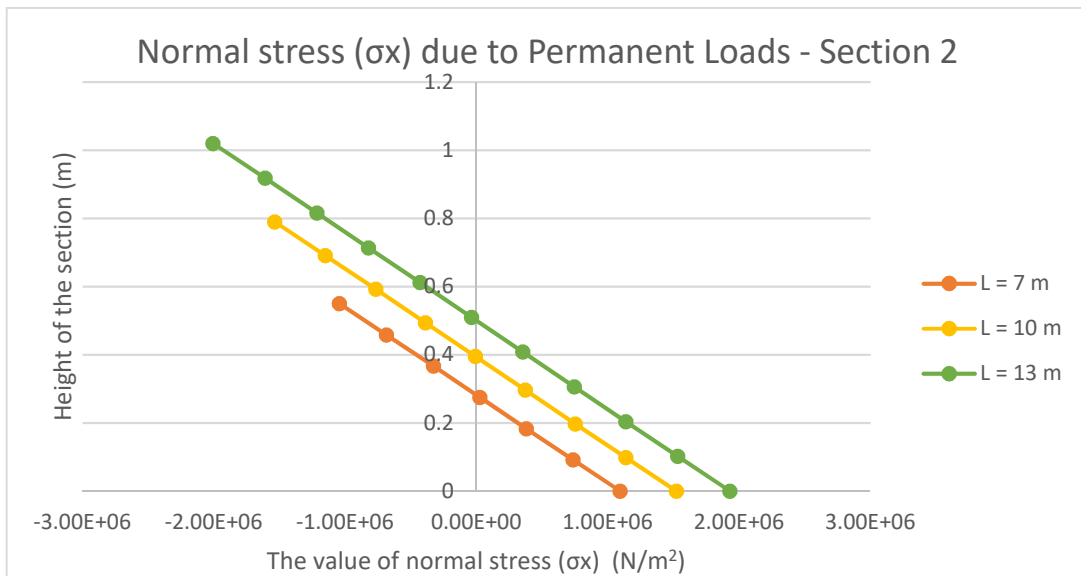


Figure 7.1 - Variation of normal stresses on the section due to permanent loads

As expected, with the increase of deck height and length, the normal stresses and deflection at mid-span, due to permanent loads, also have increased. But the value of normal stresses due to Load Model 71 does not respect the same rule, as can be observed the values are decreased. The reason is that if the depth of the section increases the section resistance increases also. Thus, due to variable loads, a stress reduction is happening.

Characteristics values due to Load Model 71							Deflection (mm)
			x (N/m <sup>2</sup> )		y (N/m <sup>2</sup> )		
			top	bottom			
SPAN LENGTH	7	Section	1--1	4.55E+05	-5.51E+05	-	0.686
			1--2	5.06E+05	-5.81E+05	-	
			2--1	-1.62E+06	1.51E+06	-	
			2--2	-1.41E+06	1.31E+06	-	
			3--1	-	-	1.14E+06	
	10	Section	1--1	6.21E+05	-6.59E+05	-	0.898
			1--2	6.48E+05	-6.84E+05	-	
			2--1	-1.40E+06	1.29E+06	-	
			2--2	-1.33E+06	1.23E+06	-	
			3--1	-	-	7.30E+05	
	13	Section	1--1	6.44E+05	-6.63E+05	-	1.084
			1--2	6.77E+05	-6.97E+05	-	
			2--1	-1.33E+06	1.21E+06	-	
			2--2	-1.29E+06	1.18E+06	-	
			3--1	-	-	5.03E+05	

Table 7.2 - The value of normal stresses and vertical deflection due to Load Model 71

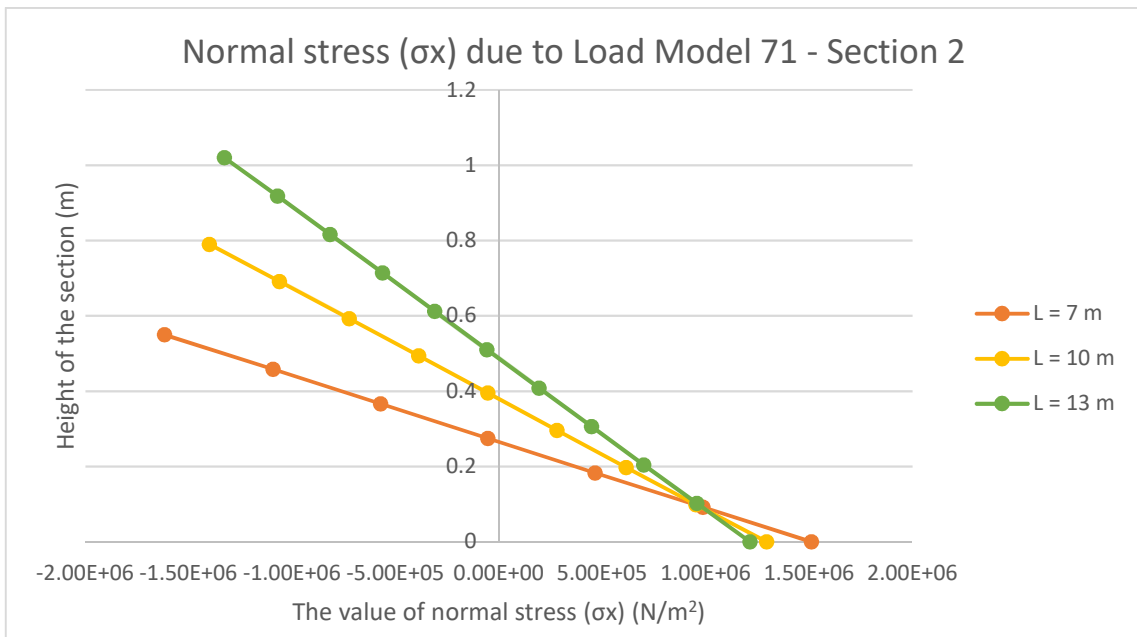


Figure 7.2 - Variation of normal stresses on the section due to Load Model 71

Below are presented the values of bending moment in the studied sections, for each span length.

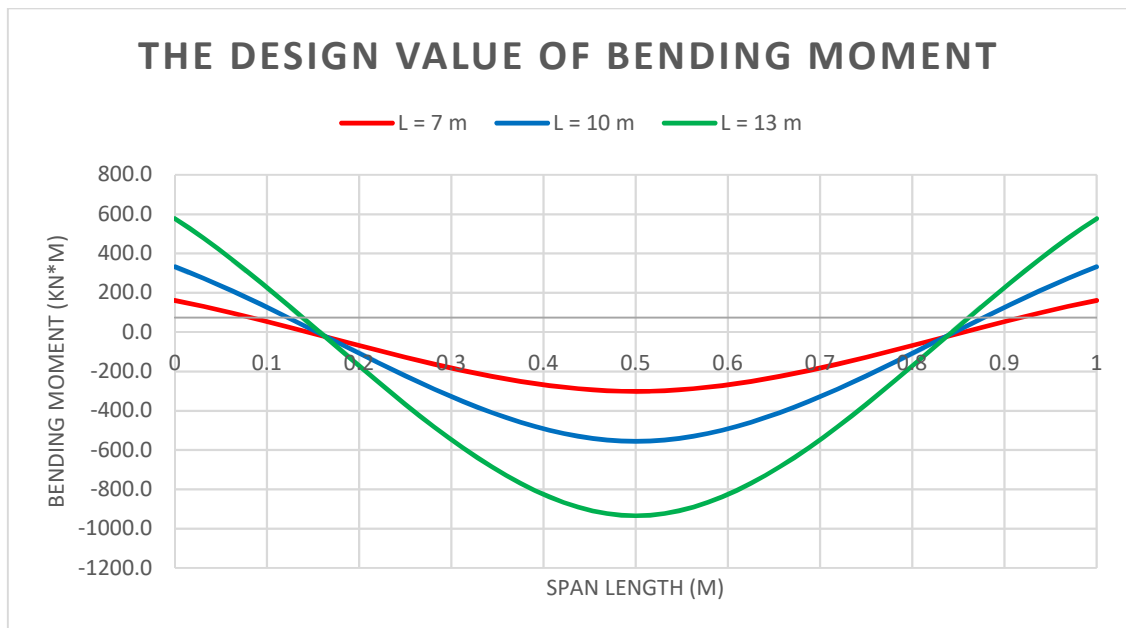


Figure 7.3 - The bending moment in deck slab

The value of bending moment, for 7 meters span length bridge, at mid-span represents about 65 % of the total value of bending moment and, if the span length increases to 10 meters, this percentage represents approximately 63 % of the total value. In the end, if the length increases to 13 meters, this percentage reaches about 61% of the total value of bending moment. This phenomenon is explained by the fact that increasing the stiffness of the frame node this will lead to higher stresses in that zone.



The maximum deflections, compared with their respective limits for all cases studied in this thesis, are presented in the following table:

Criteria	Span length = 7 meters			Span length = 10 meters			Span length = 13 meters		
	Deflection (mm)	Limit (mm)	Dynamic factor	Deflection (mm)	Limit (mm)	Dynamic factor	Deflection (mm)	Limit (mm)	Dynamic factor
Traffic Safety	0.686	11.67	1.34	0.898	16.67	1.30	1.084	21.67	1.26
Passenger comfort	0.919	4.67		1.167	6.67		1.366	8.67	

Table 7.3 - Deflections and their limits

As can be seen, all the deflections are under the limit values. The limit state is fulfilled and there is no concern regarding the deflections.

## 7.2. Dynamic effects for 10 m and 13 m span lengths

Firstly, a summary of the bridge parameters studied in this thesis are given in the following table. As can be observed, the structural damping does not have important changes of the value for different span length, but for the mass of the deck bridge it's clear that the value was increased, although the thickness of the ballast layer has been kept the same for all three bridges.

Bridge parameters	7 meters span length	10 meters span length	13 meters span length
Mass of the deck (kg)	57600	103600	161200
Structural damping (%)	2.41	2.20	1.99

Table 7.4 - Bridge parameters for studied bridges

Further, first vertical mode shape and natural frequency for the studied bridges are illustrated in next figure.

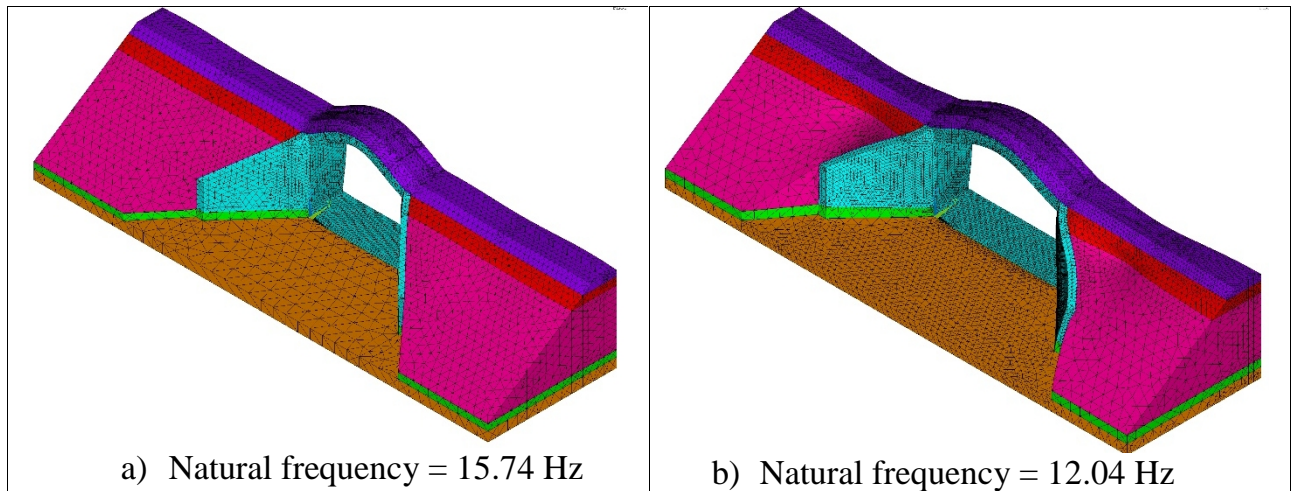


Figure 7.4 - The mode shapes of the bridge for a) 10 meters span length; b) 13 meters span length

A summary of the first twenty natural frequencies for all three spans length are presented in the table (Table 7.5). The influence of the soil stiffness and the soil density on the natural frequencies is not investigate in this thesis.

Natural frequencies (Hz)		
L = 7m	L = 10m	L = 13m
9.45443	9.52053	9.56279
10.6105	10.8688	10.8763
10.8766	10.8769	11.1608
11.6063	11.5973	11.5025
12.0018	11.873	11.7685
12.2444	12.1078	12.0407
12.3584	12.3326	12.1025
13.5499	13.6615	12.8162
13.5677	13.679	13.8645
14.5026	14.5033	13.897
14.6487	14.7268	14.502
14.7241	14.8908	14.6506
14.7339	15.0392	14.9937
15.2273	15.6147	15.106
15.516	15.6225	16.0261
16.1277	15.7451	16.0767
16.1346	16.4538	16.732
16.9459	16.4609	16.7743
17.4756	17.1822	17.3136
17.547	17.3641	17.4841

Table 7.5 - Natural frequencies from the FE-analysis.

In order to determine whether the calculated load effects from high-speed rail traffic, including HSLM, are greater than those of normal rail traffic loading (LM 71), a dynamic analysis has been performed considering the values of natural frequencies up to 30 Hz for bridges with 10 and 13 meters span length.

The Train Model HSLM-A was used and the following values of dynamic increment,  $\phi'$ , were obtained for both bridges, as follows:

10 meters span length		13 meters span length	
Dynamic increment {'	Universal Train	Dynamic increment {'	Universal Train
0.2787	A1	0.3416	A1
0.1525	A2	0.1295	A2
0.2976	A3	0.2054	A3
0.1933	A4	0.1816	A4
0.6201	A5	0.2259	A5
0.6720	A6	0.1975	A6
0.4455	A7	0.1964	A7
0.2988	A8	0.1030	A8
0.3297	A9	0.1209	A9
0.2613	A10	0.1247	A10

Table 7.6 - The values of dynamic increments corresponding to the HSLM-A trains

As can be seen, the maximum value of dynamic increment for the bridge with 10 meters span length has been obtained for the universal train A6, and for the bridge with 13 meters span length has been obtained for the universal train A1.

In order to determine the most adverse effects, according to Eurocode, the value of the static displacement due to HSLM-A trains was obtained from the graphs below and the summary of the results determined in the annex A10 are presented in the Table 7.7

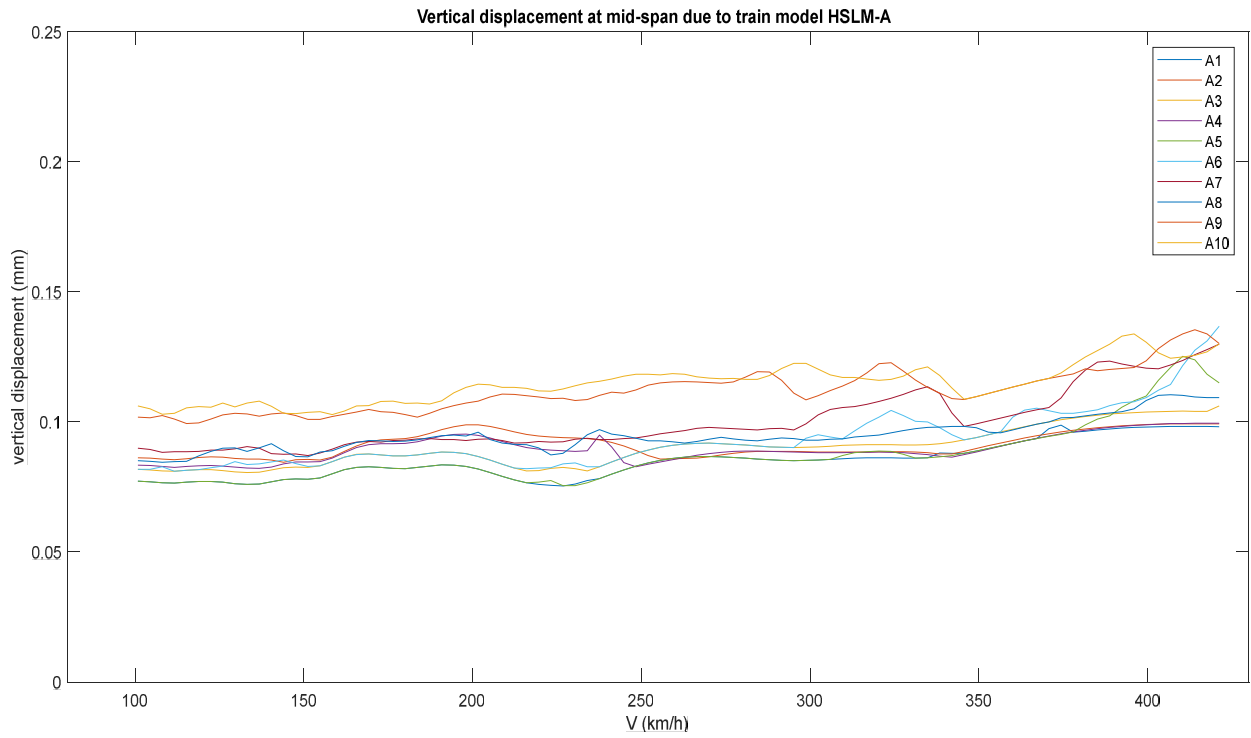


Figure 7.5 - Vertical displacements at mid-span due to train model HSLM-A for 10 meters span length

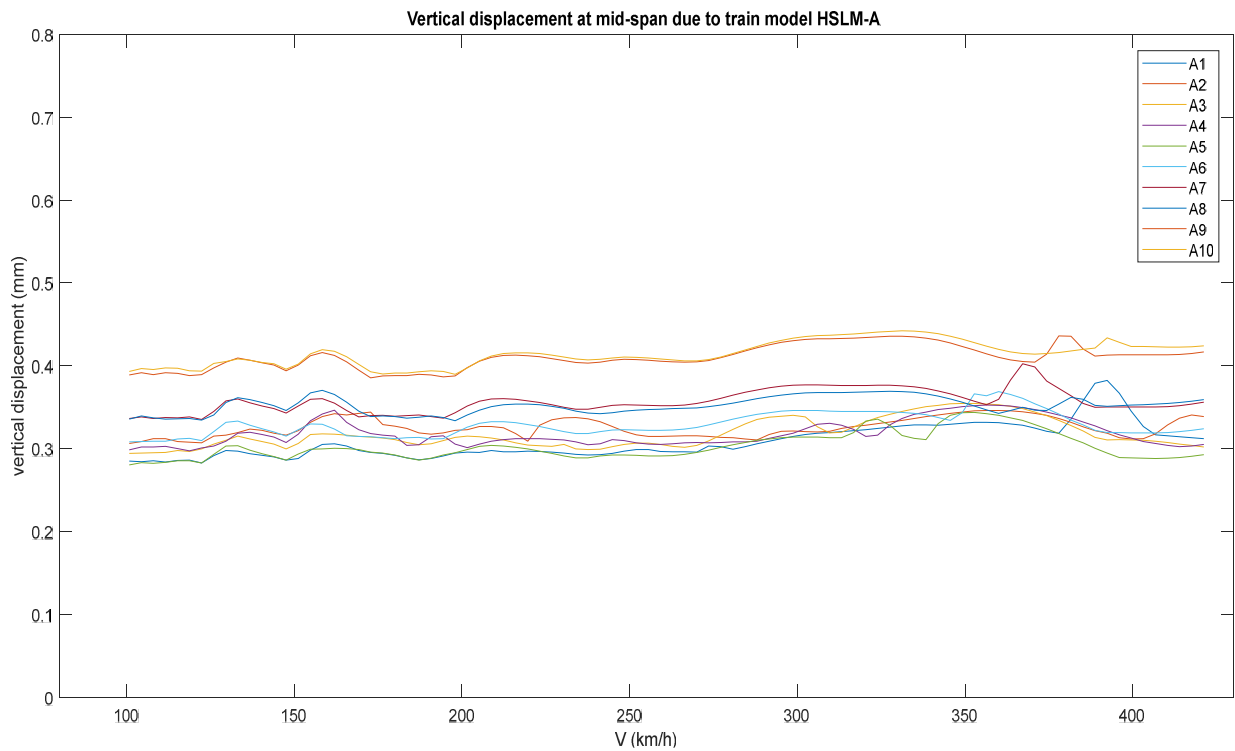


Figure 7.6 - Vertical displacements at mid-span due to train model HSLM-A for 13 meters span length





Span length	Type of effects	‘din	“	from HSLM-A (mm)		from LM71 (mm)	Value
10 m.	Dynamic	0.672	0.495	0.11	-	-	0.211
	Static	-	-	-	1.30	0.898	1.167
13 m.	Dynamic	0.342	0.364	0.39		-	0.594
	Static	-	-	-	1.26	1.084	1.366

Table 7.7 - The value of displacements due to static and dynamic analysis for 10 and 13 meters span length

As can be observed, the dynamic factor determined from dynamic analysis has a small value than the value from static analysis. So, in this case to determine the design value of internal forces the dynamic factor resulted from static analysis should be consider further.

Obviously, the maximum acceleration of the slab must be checked at the serviceability limit state (SLS), as a request for traffic requirement for prevention of track instability. In the following graphs are illustrated the values of the deck acceleration at mid-span due to Train Model HSLM-A at different speeds.

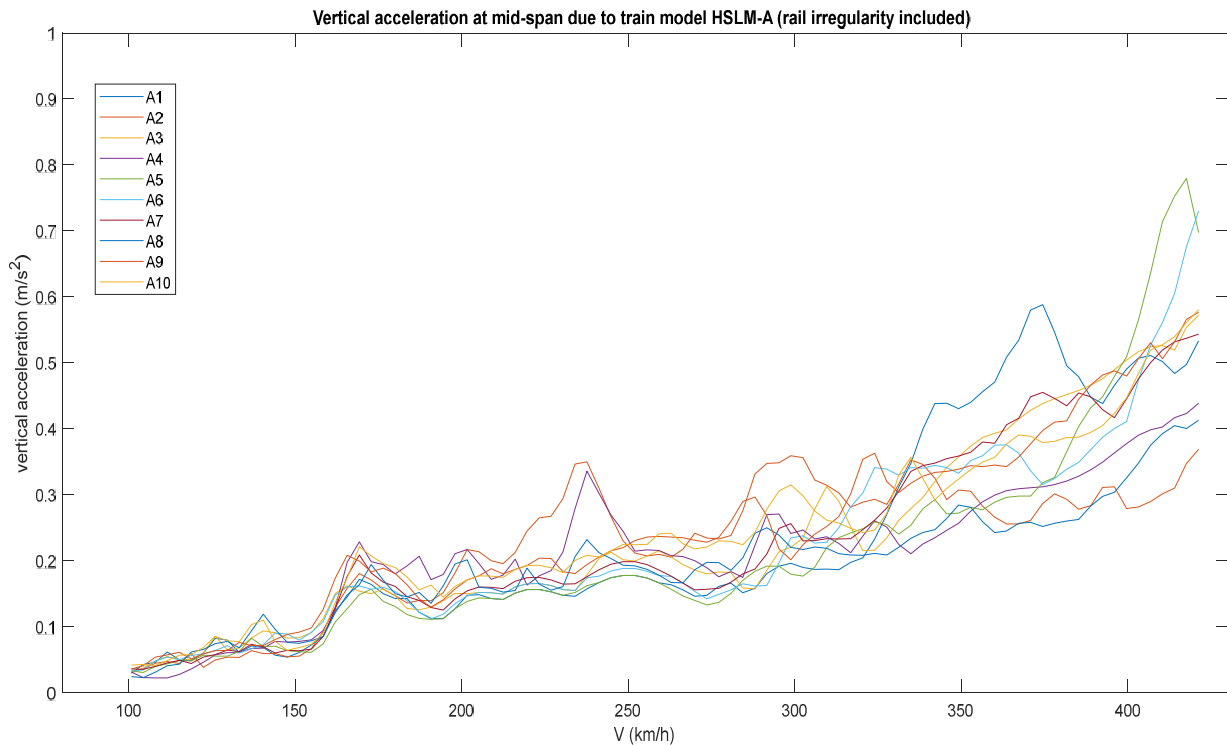


Figure 7.7 - Vertical acceleration of the bridge deck at mid-span due to HSLM-A for 10 meters span length

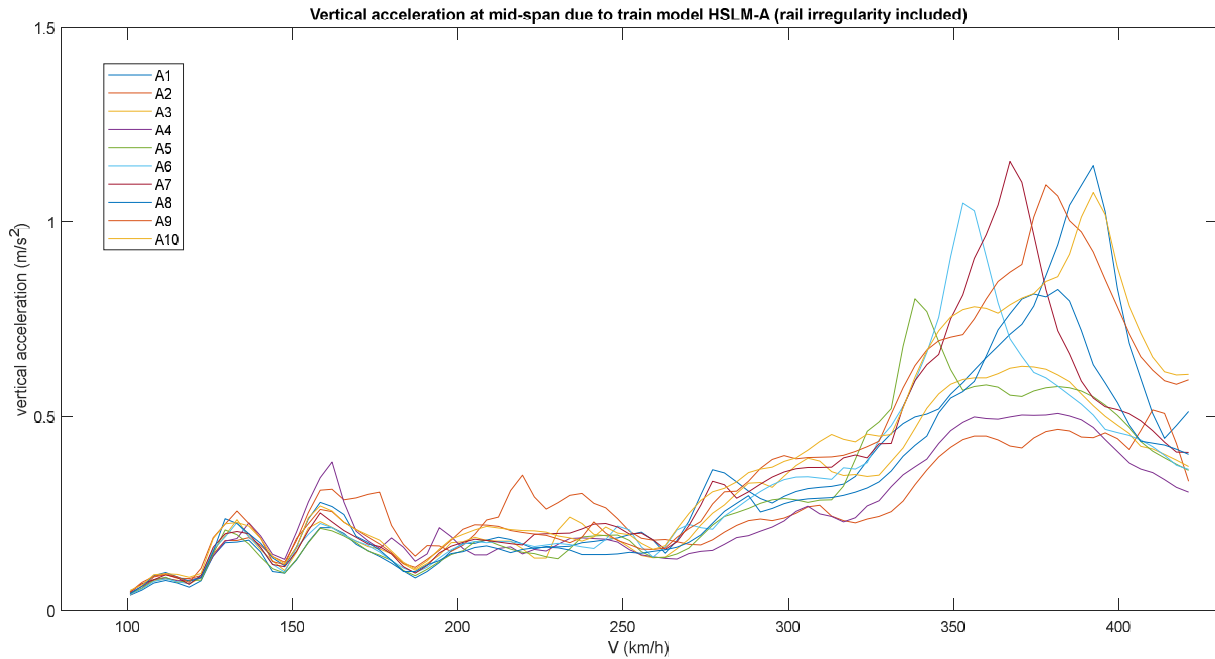


Figure 7.8 - Vertical acceleration of the bridge deck at mid-span due to HSLM-A for 13 meters span length

Looking at the shapes of the graphs, it can be concluded that, for the bridge with 10 meters span length, the value of the vertical acceleration reaches the limits at a speed close to 250 km/h. Therefore, at this span length, for trains' speed up to 250 km/h, the verification concerning vertical acceleration is satisfied. For the bridge with 13 meters span length, the vertical acceleration is under the limit value, so the limit state is fulfilled.

Watching the variations of the vertical accelerations for all three span length, can be seen that, for the bridge with 10 meters span length, the value has exceeded the limit value, according to Eurocode. Thus, here it can be drawn the conclusion regarding the type of boundary conditions. In this model, the boundary conditions have been defined having fixed horizontal, vertical and rotational degrees of freedom of the nodes, instead of absorbing boundaries. This fact was also an assumption used in the model, because for a realistic behavior, the boundary conditions should allow waves to exit from the domain without being reflected back in a non realistic way and corrupting the solutions.

## 8. CONCLUSIONS AND FUTURE DEVELOPMENT

### 8.1. Conclusions

A 3D-Finite Element Model was built up for three different span lengths. The model is parametric, based on an ASCII input file for the ANSYS program. In this way, it is very easy to change any dimensions or properties with minimum effort.

The eigenfrequencies and mode shapes of the structure were investigated. Also the vertical accelerations on the deck and the vertical displacements were computed under the passage of high-speed trains as prescribed by EN 1991-2.

Regarding the dynamic analysis, the following conclusions were obtained:

- The maximum vertical acceleration limit from Eurocode, which is  $3,50 \text{ m/s}^2$ , is not exceeded for the bridges between 7 and 13 meters span length, when natural frequencies up to 30 Hz are taken into account.
- For the studied bridges, the value of calculated loads effects due to high-speed rail traffic (HSLM-A), are smaller than those of normal rail traffic loading (LM71).

It is important to note that is recommended to use absorbing boundaries or non-reflecting boundaries for the bottom layer of the model, in order to avoid waves to reflect back in the model. In this regard, the results from the mode superposition analysis can be considered only as a first approach.

Concerning the static analysis, the following conclusions can be formulated:

- Observing the value of the stresses in the studied sections, it can be deduced that the thickness of the slab might be optimized because the resistance of the section is higher. In this case the slenderness ratio is about 1/13, so it may be reduced somewhat for this kind of structures.
- The 3D Finite Element Model allows to assess, in an accurate way, the stresses and the displacements in any point of the structure.
- The values of total normal stresses due to permanent loads, taking into account construction stages, are greater than the values obtained when the construction stages were not considered. The difference between them are in the range 17% - 31%, which is of practical relevance. .
- Also, the thermal and rheological effects have an important influence on the final value of internal forces, especially the value of bending moment is significant and should be considered in the ULS and SLS combinations.
- As expected, the stresses due to Load Model 71 have decreased with the increasing of slab thickness and span length.
- The vertical deflection at mid-span, due to Load Model 71, is below the limits and both criteria regarding traffic safety and passenger comfort are accomplished.



## 8.2. Future development

Regarding this master thesis, because several assumptions were considered, here are some suggestions to improve the 3D-Finite Element Model of the concrete frame bridges:

- In order to have a more accurate distribution of loads through rail and sleepers, it's necessary to model them using 3D solid elements.
- In order to obtain fully realistic results, when a dynamic analysis needs to be carried out, absorbing boundaries and a complete time-domain soli-structure interaction analysis is required.
- For double-track bridges, an entire 3D model would be useful to reflect the real behavior of such structures.
- The influence of different soil parameters (e.g. Young's modulus, Poisson's ratio and density) can be studied very easily using this model as well.
- Also, the influence of stiffness of the frame corner could be studied in order to evaluate more accurately the distribution of stresses around that zone.
- The loads which were not considered in this study, could be taken into account according to Eurocode (e.g. fatigue, derailment, braking and traction forces, wind load, earthquake load and so on).
- Finally, real scale field measurements would be of great interest to calibrate the 3D-Finite Element Model (FEM).

## BIBLIOGRAPHY

1. ANSYS Mechanical APDL for Finite Element Analysis. Mary K. Thompson, John M. Thompson. ISBN 978-0-12-812981-4. Butterworth-Heinemann. 1<sup>st</sup> edition 2017;
2. Boverket mandatory provisions amending the board's mandatory provisions and general recommendations (2011:10) on the application of European design standards (Eurocodes), BFS 2013:10 - EKS 9;
3. Bridge deck analysis - Second edition. Eugene J. O'Brien, Damien L. Keogh, Alan J. O'Connor. ISBN 978-1-4822-2724-6. CRC Press. Taylor & Francis Group. 2015;
4. Bridges for High-Speed Railways. R. Calçada, R. Delgado, A. C. e Matos. ISBN 978-0-415-47147-3. Published 2008;
5. Designers' guide to EN 1991-2, EN 1991-1-1, -1-3 to -1-7 and EN 1990 Annex A2. J.-A. Calgaro, M. Tschumi and H. Gulvanessian. ISBN 0-7277-3158-6. First published 2010;
6. Designers' guide to EN 1992-1-1 and EN 1992-1-2. Eurocode 2: Design of concrete structures. General rules and rules for buildings and structural fire design. A. W. Beeby and R.S. Narayanan. ISBN 0-7277-3150-0. First published 2005. Reprinted with amendments 2009;
7. Designers' guide to EN 1992-2. Eurocode 2: Design of concrete structures. Part 2: Concrete bridges. C. R. Hendy and D. A. Smith. ISBN 0-7277-3159-3. First published 2007;
8. Dynamic response of underpasses for high-speed train lines. J. Vega, A. Fraile, E. Alarcon, L. Hermanns. Journal of Sound and Vibration 331 (2012) 5125-5140;
9. Dynamics of Railway Bridges. Ladislav Fryba. ISBN 80-200-0544-7. Academia Prague 1996;
10. EN 1990. Eurocode: Basis of structural design;
11. EN 1990. Eurocode: Basis of structural design - Annex A2: Application for bridges;
12. EN 1991-2. Eurocode 1: Actions on structures - Part 2: Traffic loads on bridges;
13. EN 1992-1-1. Eurocode 2: Design of concrete structures - Part 1-1: General rules and rules for buildings;
14. EN 1992-2. Eurocode 2: Design of concrete structures - Part 2: Concrete bridges;
15. Identification of soil-structure interaction effect in a portal frame railway bridge through full-scale dynamic testing. Abbas Zangeneh, Christoffer Svedholm, Andreas Andersson, Costin Pacoste, Raid Karoumi. Engineering Structures 159(2018)299-309;
16. Master Thesis: "Dynamic Analysis of a Railway Bridge subjected to High Speed Trains". Lena Björklund, Royal Institute of Technology Stockholm, Sweden, 2004;
17. Master Thesis: "Dynamic response of railway bridges subjected to high speed trains. Parametrical case studies". Marcus Hjelm and Niclas Karlsson, Chalmers University of Technology Göteborg, Sweden, 2016;
18. Reinforced concrete design to Eurocode 2 (EC2). W. H. Mosley, R. Hulse, J. H. Bungey. ISBN 978-0-333-60878-4. First published 1996;
19. <https://www.ansys.com/>;
20. <https://www.sharcnet.ca/Software/Ansys/17.0/en>;

## ANNEXES

### Annex A1. Verification of bridge model in SAP 2000 software

A verification of the results obtained in ANSYS was performed in parallel with SAP 2000. The model has been represented only by the bridge structure without any loads. The section where the checks were performed is the mid-span of the bridge and the normal stress and the vertical deflection have been checked.

Computing the normal stress ( $\sigma_x$ ) at the mid-span of the bridge :

$$h_d := 0.55\text{m} \quad \text{height of the deck;}$$

$$w_d := 3.55\text{m} \quad \text{width of the deck}$$

$$I_y := \frac{w_d \cdot h_d^3}{12} = 0.049\text{m}^4 \quad \text{moment of inertia;}$$

$$z_{\max} := \frac{h_d}{2} = 0.275\text{m} \quad \text{distance from gravity point of section to the external edge of section;}$$

$$A_d := h_d \cdot w_d = 1.953\text{m}^2 \quad \text{the cross section area;}$$

$$N_{\text{mid}} := -3442\text{N} \quad \text{axial force at mid-span from SAP 2000;}$$

$$M_{Y,\text{mid}} := 184950.15\text{N}\cdot\text{m} \quad \text{bending moment at mid-span from SAP 2000;}$$

Normal stresses at mid-span

$$\sigma_{x,t} := \frac{N_{\text{mid}}}{A_d} - \frac{M_{Y,\text{mid}}}{I_y} \cdot z_{\max} = -1050991.5 \frac{\text{N}}{\text{m}^2}$$

$$\sigma_{x,b} := \frac{N_{\text{mid}}}{A_d} + \frac{M_{Y,\text{mid}}}{I_y} \cdot z_{\max} = 1015731.1 \frac{\text{N}}{\text{m}^2}$$

Normal stresses at mid-span from ANSYS

$$\sigma_{x_t} := -1010000 \frac{\text{N}}{\text{m}^2}$$

$$\sigma_{x_b} := 971070 \frac{\text{N}}{\text{m}^2}$$

Differences between ANSYS and SAP 2000:

$$pm_t := \frac{\sigma_{x_t}}{\sigma_{x,t}} - 1 = -3.9\%$$

$$pm_b := \frac{\sigma_{x,b}}{\sigma_{x,b}} - 1 = -4.397\%$$

As can be observed, the differences between SAP2000 and ANSYS are less than 5%, so the results are acceptable.

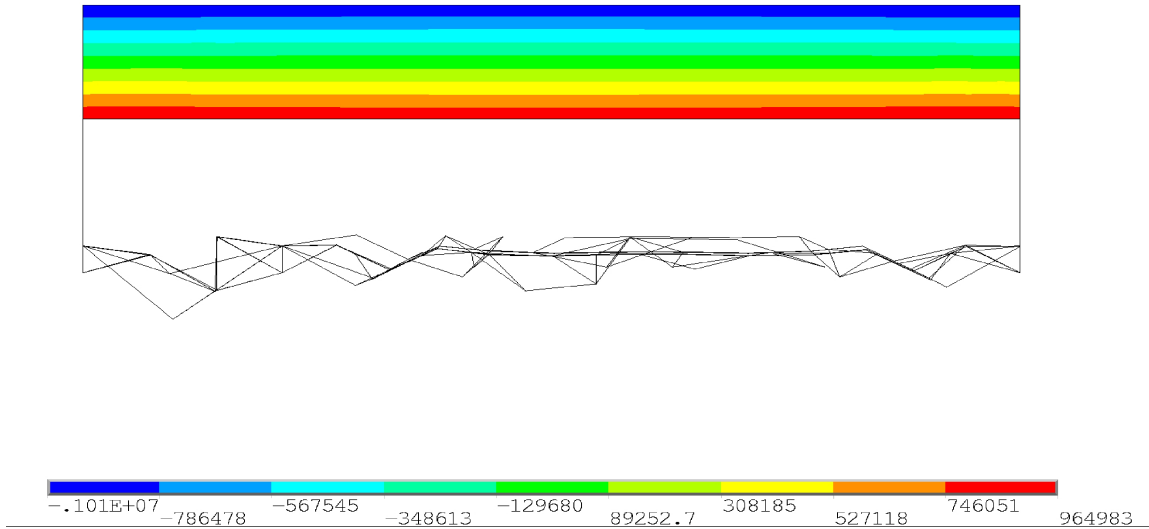


Figure A1.1 – The normal stress (sigma x) at the mid-span (ANSYS)

Also, a check of the vertical displacement at mid-span was performed. As can be seen below, the results from both software are similar.

1 = 0.558 mm. the vertical displacement from ANSYS;

2 = 0.594 mm. the vertical displacement from SAP2000;

DMX = .558E-03  
 SMN = -.558E-03  
 SMX = .847E-05

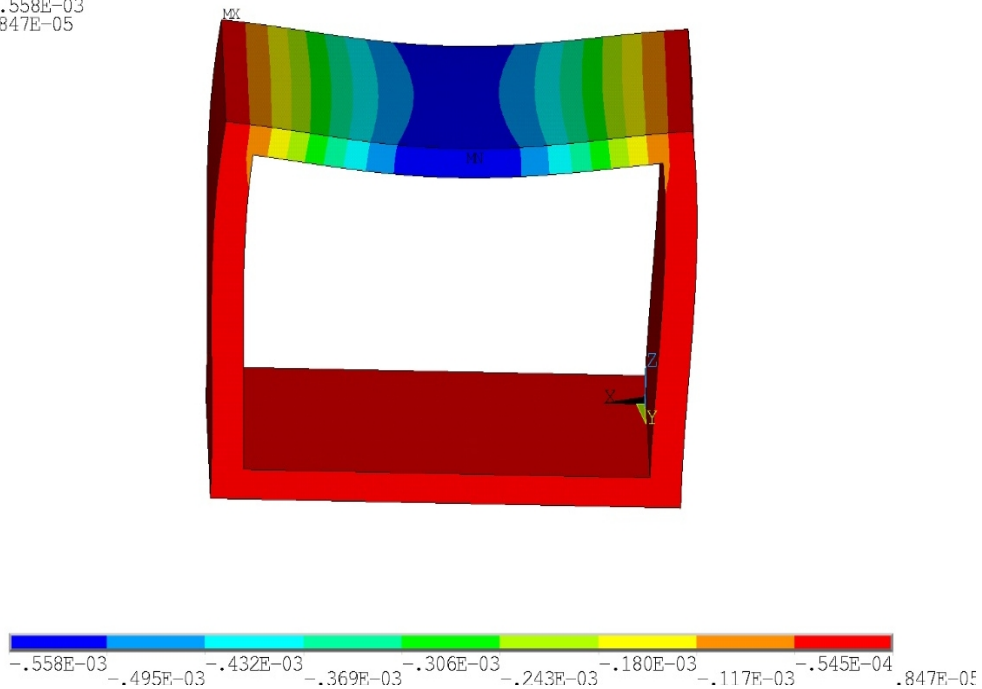


Figure A1.2 – The vertical displacement of the bridge (ANSYS)

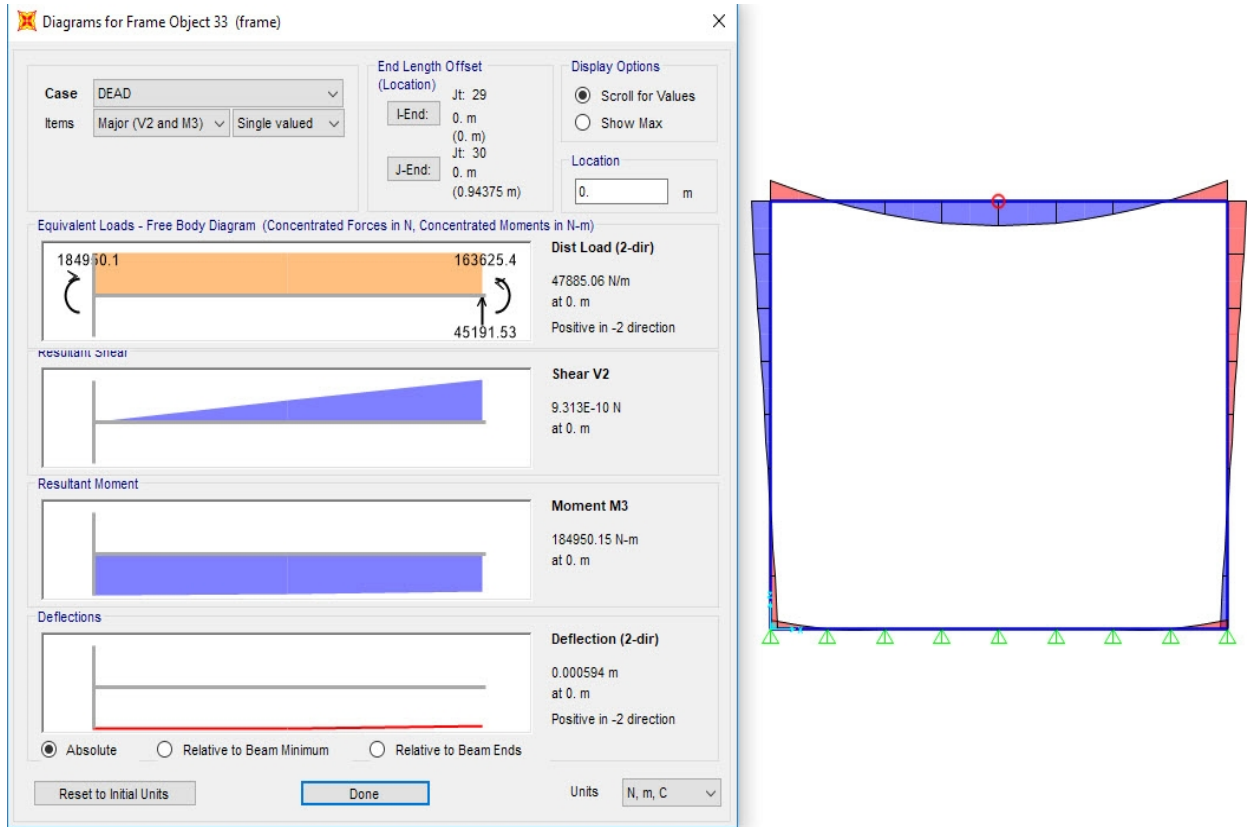


Figure A1.3 – The vertical displacement and internal forces of the bridge (SAP2000)



## Annex A2. Verification of settlement of the embankment's layer

In order to check the value of the settlements for different layers of embankment, it was performed a short hand calculation of the vertical settlement for filling material and sub-grade layer as a comparison with the results from ANSYS.

Filling material:

$$E_{\text{soil}} := 8 \cdot 10^7 \frac{\text{N}}{\text{m}^2} \quad \text{Young's modulus of the layer}$$

$$L_{\text{soil}} := 11.1\text{m} \quad \text{length of the layer}$$

$$B_{\text{soil}} := 3.55\text{m} \quad \text{width of the soil}$$

$$H_{\text{soil}} := 5.9\text{m} \quad \text{height of the soil}$$

$$A_{\text{soil}} := L_{\text{soil}} \cdot B_{\text{soil}} = 39.405\text{m}^2 \quad \text{cross section area of the soil}$$

$$\rho_{\text{soil}} := 1900 \frac{\text{kg}}{\text{m}^3}$$

$$\gamma_s := \rho_{\text{soil}} \cdot g = 18.639 \frac{\text{kN}}{\text{m}^3}$$

$$w_s := \gamma_s \cdot A_{\text{soil}} = 734.47 \frac{\text{kN}}{\text{m}} \quad \text{the load from layer's weight}$$

$$N(x) := -w_s \cdot x$$

The vertical displacement of layer:

$$\delta_{\text{soil}} := \int_0^{H_{\text{soil}}} \frac{N(x)}{E_{\text{soil}} \cdot A_{\text{soil}}} dx = -4.055\text{mm}$$

The vertical displacement of layer (ANSYS)

$$\delta_{\text{soilA}} := 3.885\text{mm}$$

The result of settlement obtained by hand calculation is close with the value from ANSYS software.

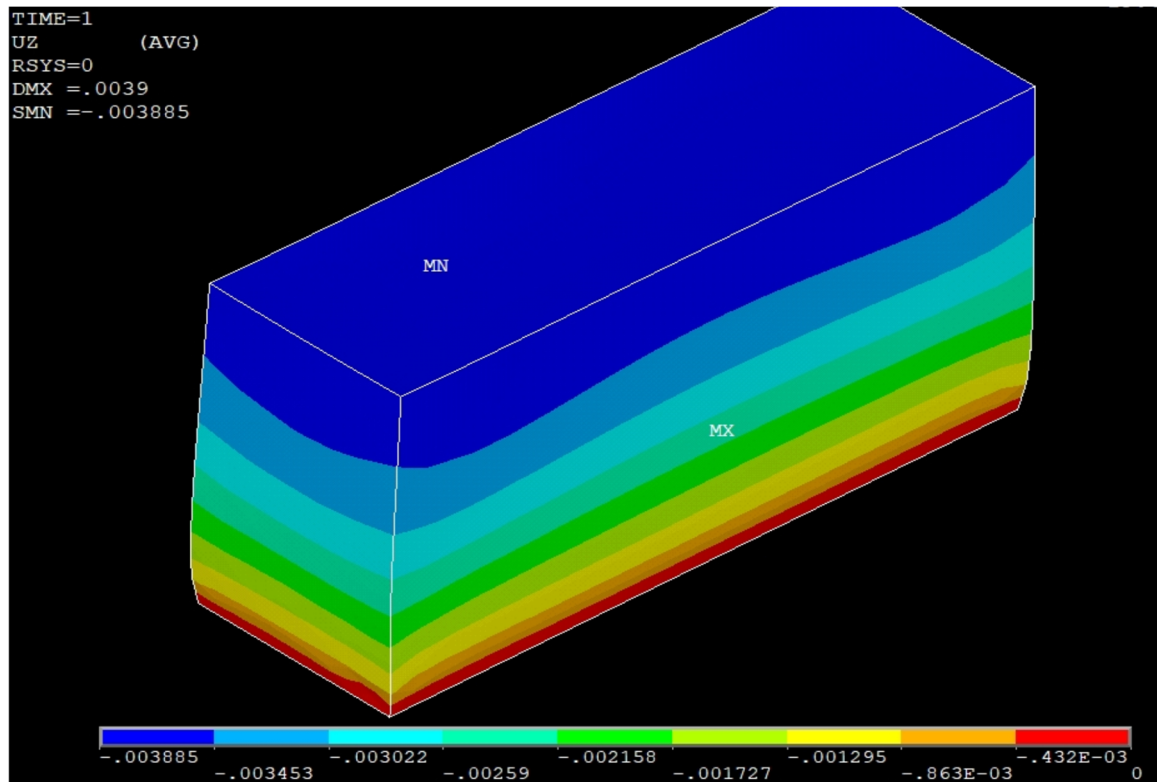


Figure A2.1 – The settlement of the filling material (ANSYS)

Another check was performed for sub-grade layer.

$$E_{\text{soil}} := 2.85 \cdot 10^8 \text{ Pa}$$

Young's modulus of the layer

$$L_{\text{soil}} := 11.1 \text{ m}$$

length of the layer

$$B_{\text{soil}} := 3.55 \text{ m}$$

width of the layer

$$H_{\text{soil}} := 1 \text{ m}$$

height of the layer

$$A_{\text{soil}} := L_{\text{soil}} \cdot B_{\text{soil}} = 39.405 \text{ m}^2$$

cross section area of the layer

$$\rho_{\text{soil}} := 1900 \frac{\text{kg}}{\text{m}^3}$$

$$\gamma_s := \rho_{\text{soil}} \cdot g = 18.639 \frac{\text{kN}}{\text{m}^3}$$

$$w_s := \gamma_s \cdot A_{\text{soil}} = 734.47 \frac{\text{kN}}{\text{m}}$$

the load from layer's weight

$$N(x) := -w_s \cdot x$$

The vertical displacement of layer:

$$\delta_{\text{soil}} := \int_0^{H_{\text{soil}}} \frac{N(x)}{E_{\text{soil}} \cdot A_{\text{soil}}} dx = -0.033 \text{ mm}$$

The vertical displacement of layer (ANSYS)

$$\delta_{\text{Ansys}} := 0.0312 \text{ mm}$$

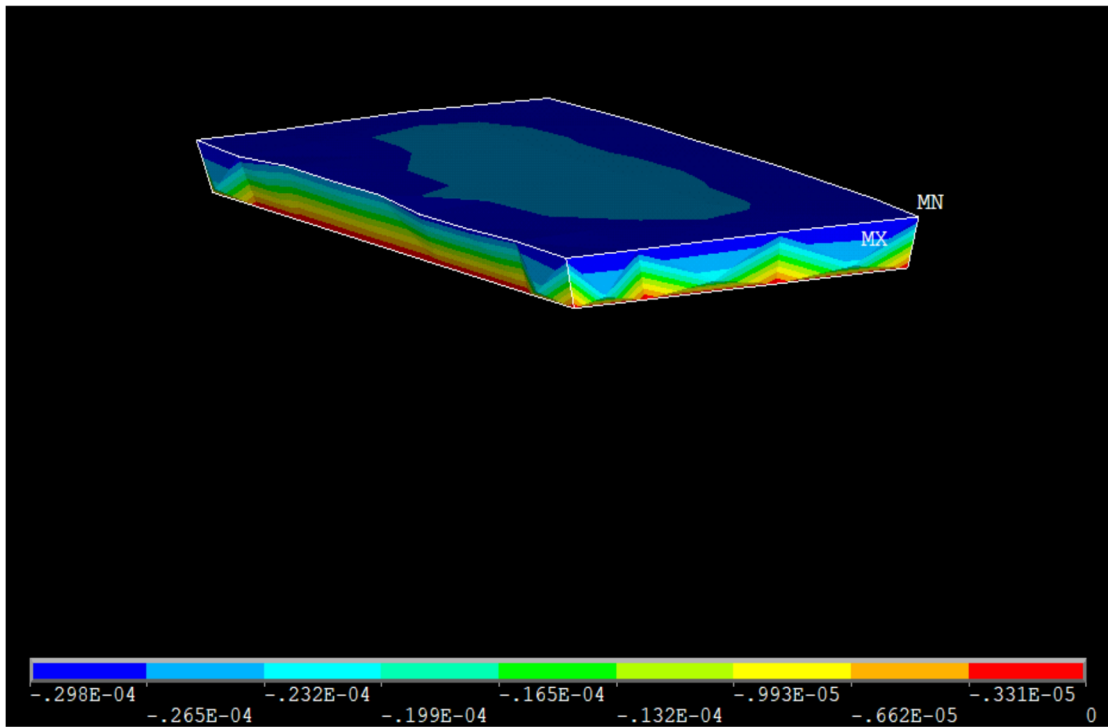


Figure A2.2 – The settlement of the sub-grade layer (ANSYS)

As can be seen, the results obtained in both ways are quite similar, thus the model is accepted.

## Annex A3. Computation of the pressure below sleepers due to Load Model 71 (LM71)

In order to take into account the distribution of loads due to Load Model 71 (LM71), through rail and sleepers, the pressures below to the sleepers have been calculated. These values of pressures have been assigned to the 3D-FE Model.

### The pressures from concentrated load:

$$Q_{vi} := \frac{250}{2} \text{ kN} = 125 \text{ kN}$$

the value of concentrated load from LM71 vehicle for each rail

$$w_s := 250 \text{ mm}$$

width of sleeper

$$Le_s := \frac{2600 \text{ mm}}{2} = 1.3 \text{ m}$$

length of sleeper

$$A_s := w_s \cdot Le_s = 0.325 \text{ m}^2$$

The pressure in sleeper below concentrated load:

$$\sigma_1 := \frac{Q_{vi}}{2 \cdot A_s} = 1.923 \times 10^5 \text{ Pa}$$

The pressure in sleeper situated next to sleeper below concentrated load:

$$\sigma_2 := \frac{Q_{vi}}{4 \cdot A_s} = 9.615 \times 10^4 \text{ Pa}$$

### The pressures from uniformly distributed load:

$$q_{vk} := \frac{80 \text{ kN}}{2 \text{ m}} = 40 \frac{\text{kN}}{\text{m}}$$

the uniformly distributed load for each rail

$$\sigma_{di} := \frac{q_{vk}}{Le_s} = 3.077 \times 10^4 \cdot \text{Pa}$$

the pressure from uniformly distributed load

## Annex A4. Thermal loading and rheological effects assessment

The thermal and rheological effects were determined in a simple manner, modelling the bridge structure in SAP2000 software, with the same dimensions as the 3D-FE Model.

### Thermal loading:

$T_0 := 10$  the reference temperature

The location of bridge is near the Umea city, Sweden

$T_{e.min} := -38$  the minimum temperature

$T_{e.max} := 29$  the maximum temperature

The characteristics values of the maximum contraction and expansion range of the uniform bridge temperature component are respectively:

$\Delta T_{N.con} := T_0 - T_{e.min} = 48$  EN 1991-5-eq.6.1

$\Delta T_{N.exp} := T_{e.max} + T_0 = 39$  EN 1991-5-eq.6.2

$\alpha_T := 10 \cdot 10^{-6}$  coefficient of thermal expansion for concrete

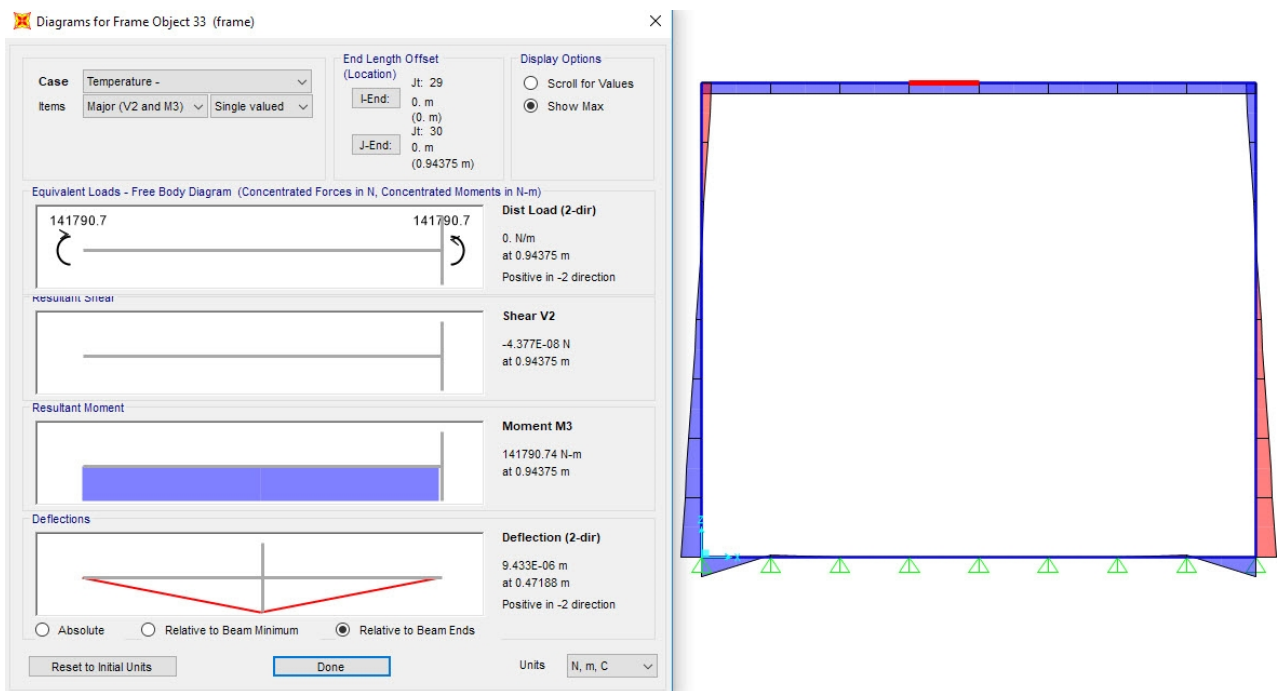


Table A4.1 – Bending moment due to negative temperature

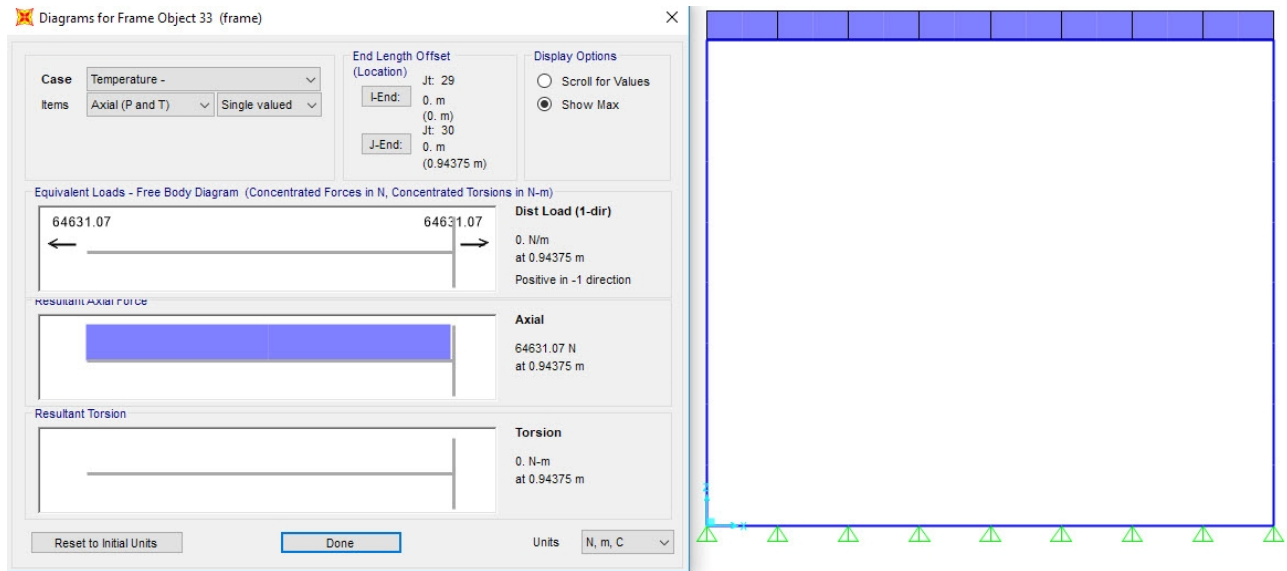


Table A4.2 – Axial force due to negative temperature

**Creep assessment:**

RH := 80 relative humidity

$$\alpha_1 := \left(\frac{35}{f_{cm}}\right)^{0.7} = 0.866 \qquad \alpha_2 := \left(\frac{35}{f_{cm}}\right)^{0.2} = 0.96$$

h<sub>0</sub> := 550

The factor which allows the effect of relative humidity on the national creep coefficient

$$\phi_{RH} := 1 + \frac{\left(1 - \frac{RH}{100}\right)}{0.1 \cdot \sqrt[3]{h_0}} = 1.244$$

The factor which allows for the effect of concrete strength on the notional creep coefficient

$$\beta_{f_{cm}} := \frac{16.8}{\sqrt{f_{cm}}} = 2.562$$

The effect of concrete age at loading on the notional creep coefficient is given by the following factor:

t<sub>0</sub> := 30 for loading at 30 days

$$\beta_{t_0} := \frac{1}{\left(0.1 + t_0^{0.20}\right)} = 0.482$$

$$\beta_H := 1.5 \cdot \left[1 + (0.012 \cdot RH)^{18}\right] \cdot h_0 + 250 = 1.471 \times 10^3$$

$$\beta_H \leq 1500 = 1$$

$$t := 365 \cdot 100$$



$$t_s := 1$$

$$t_0 = 30$$

$$\beta_{c,t,t_0} := \left( \frac{t - t_0}{\beta_H + t - t_0} \right)^{0.3} = 0.988$$

The final creep coefficient is:

$$\phi_0 := \phi_{RH} \beta_{fcm} \beta_{t_0} = 1.537$$

$$\phi_{t,t_0} := \phi_0 \beta_{c,t,t_0} = 1.518$$

## Shrinkage assessment:

Shrinkage assessment for time = 100 years

$$t = 3.65 \times 10^4$$

Autogenous shrinkage:

$$\beta_{as} := 1 - e^{(-0.2 \cdot t^{0.5})} = 1$$

$$\varepsilon_{ca,\infty} := 2.5 (f_{ck} - 10) \cdot 10^{-6} = 6.25 \times 10^{-5}$$

$$\varepsilon_{ca,t} := \beta_{as} \cdot \varepsilon_{ca,\infty} = 6.25 \times 10^{-5}$$

Drying shrinkage:

$$\left[ \text{linterp} \left[ \begin{pmatrix} 20 \\ 40 \end{pmatrix}, \begin{pmatrix} 0.30 \\ 0.24 \end{pmatrix}, f_{ck} \right] \right] = 0.26$$

for RH=80%

$$\varepsilon_{cd,0} := \frac{0.26}{1000}$$

$$k_h := 0.70$$

$$t_s = 1$$

the day when the shrinkage starts

$$u := 0.5 + 7.1 + 0.5$$

$$A_{co} := 7.1 \cdot 0.55 = 3.905$$

$$h_0 := 2 \frac{A_{co}}{u} = 0.964$$

$$\beta_{ds,\infty,ts} := \frac{(t - t_s)}{(t - t_s) + 0.04 \sqrt{h_0^3}} = 1$$

$$\varepsilon_{cd,\infty} := \beta_{ds,\infty,ts} \cdot k_h \cdot \varepsilon_{cd,0} = 1.82 \times 10^{-4}$$

The total shrinkage for time =100 years is:



$$\epsilon_{cs,\infty} := \epsilon_{cd,\infty} + \epsilon_{ca,t} = 2.445 \times 10^{-4}$$

In order to be able to assess the effect of the shrinkage in SAP2000, it has been determined the temperature which produces the same effect as strain due to shrinkage.

$$\text{temp} := \frac{\epsilon_{cs,\infty}}{\alpha_T} = 24.45$$

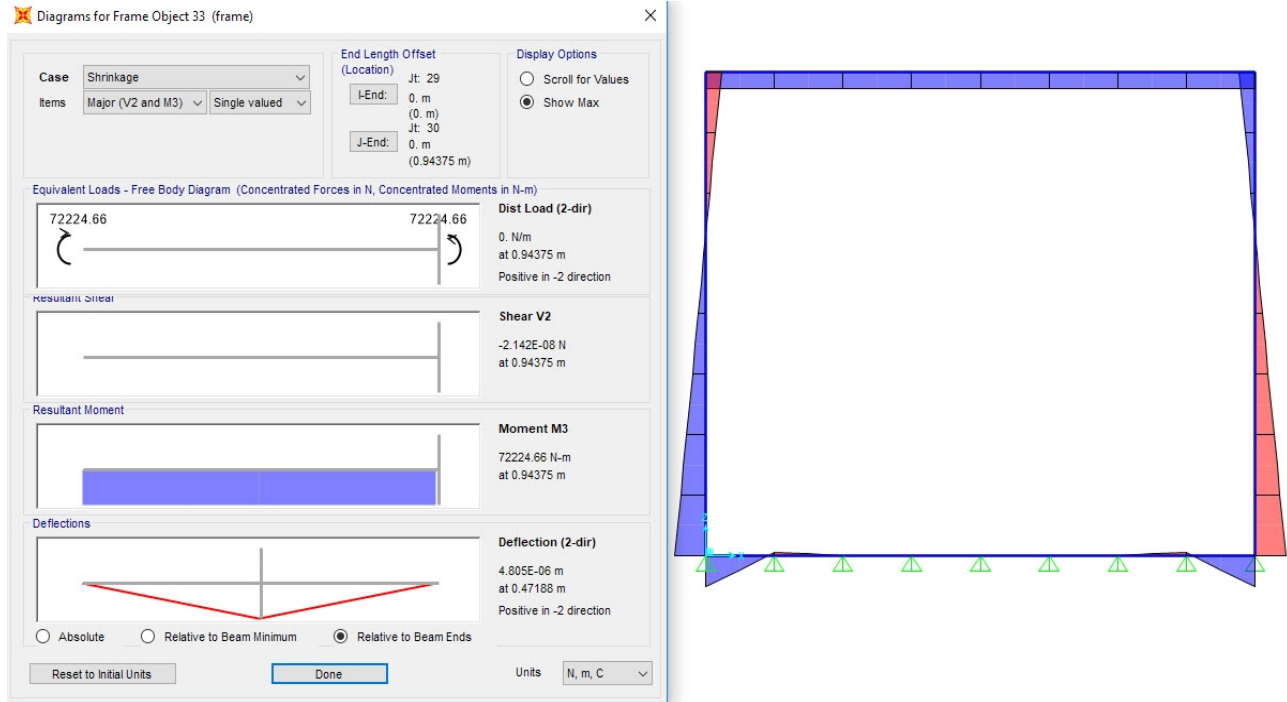


Table A4.3 – Bending moment due to shrinkage

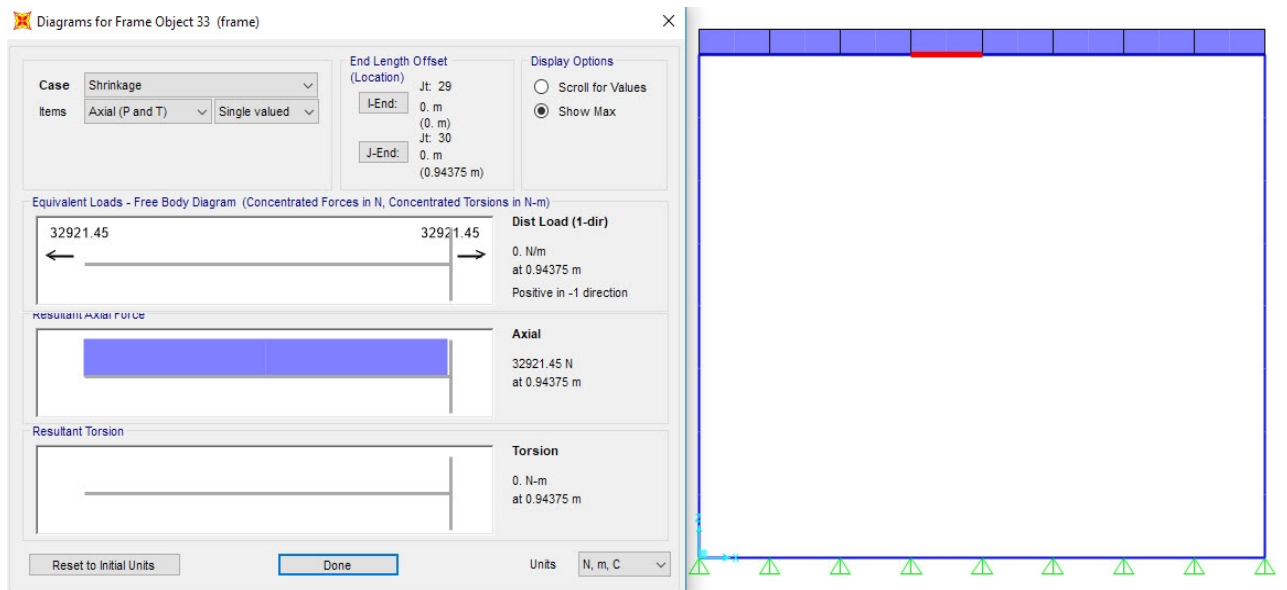


Table A4.4 – Axial force due to shrinkage



## Annex A5. Computing the deck reinforcement

The reinforcement of deck was made according to EN 1992-1 and EN 1992-2. The designed bending moment is the moment obtained in the ULS combination.

### Mid-span section (S2):

1. Recommended values of material factors according to clause 2.4 from SR-EN 1992-1

$$\gamma_c := 1.5$$

2. Materials according to clause 3 from SR-EN 1992-1

Concrete class: C35/45	$f_{ck} := 35\text{MPa}$	$f_{ctm} := 3.2\text{MPa}$	$E_{cm} := 34\text{GPa}$
$f_{ctk0.05} := 2.2\text{MPa}$	$f_{ctk0.95} := 4.2\text{MPa}$		
$\alpha_{cc} := 0.85$	$\alpha_{ct} := 1.0$	$\lambda := 0.8$	$\eta := 1.0$

The design compressive strength for concrete

$$f_{cd} := \alpha_{cc} \cdot \frac{f_{ck}}{\gamma_c} = 19.833 \cdot \text{MPa}$$

The design tensile strength for concrete

$$f_{ctd} := \frac{\alpha_{ct} \cdot f_{ctk0.05}}{\gamma_c} = 1.467 \cdot \text{MPa}$$

Reinforcing steel: B500B:

$$f_{yk} := 500\text{MPa}$$

$$E_s := 200\text{GPa}$$

$$k := 1.08$$

The minimum value for B class of ductility

$$f_{yd} := \frac{f_{yk}}{\gamma_s} = 434.783 \cdot \text{MPa}$$

The design tensile strength for steel

3. Concrete cover: according to clause 4.4 from SR-EN 1992-1

The minimum cover

$$c_{\min} := \max(25\text{mm}, 30\text{mm} + 0 - 0 - 0, 10\text{mm}) = 30 \cdot \text{mm}$$

$$\Delta c_{\text{dev}} := 10\text{mm}$$

The recommended value for bridges

$$c_{\text{nom}} := c_{\min} + \Delta c_{\text{dev}} = 40 \cdot \text{mm}$$

The nominal cover



#### 4. Longitudinal reinforcement of concrete slab

$h_s := 550\text{mm}$  height of slab  
 $b_s := 1000\text{mm}$  considered width of slab  
 $M_{Ed,x} := 301.346\text{kN}\cdot\text{m}$  maximum applied ULS bending moment

Assuming rectangular concrete stress block:

$\beta := 0.400$   
 $\Phi_s := 16\text{mm}$  considered size bar  
 $d_1 := \frac{\Phi_s}{2} + c_{nom} = 48\cdot\text{mm}$   
 $d := h_s - d_1 = 502\cdot\text{mm}$

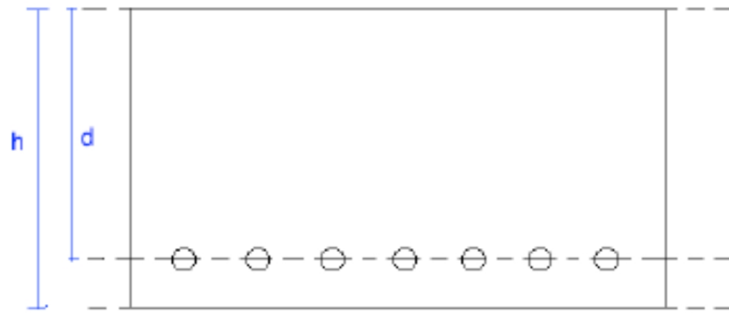


Figure A5.1 – Effective depth of the slab

$$K_{av} := \frac{M_{Ed,x}}{b_s \cdot d^2 \cdot f_{cd}} = 0.06$$

$$\text{ratio}_{x,d} := \frac{1 - \sqrt{1 - 4\beta \cdot K_{av}}}{2 \cdot \beta} = 0.062$$

Check limit from next equation to ensure reinforcement is yielding:

$$Eq := \frac{1}{\left( \frac{f_{yk}}{\gamma_s \cdot E_s \cdot \varepsilon_{cu3}} + 1 \right)} = 0.617$$

" SINGLY REINFORCED " if  $|\text{ratio}_{x,d}| < |Eq|$  = " SINGLY REINFORCED "  
 " DOUBLY REINFORCED " otherwise

$x := 0.062 \cdot d = 31.124\cdot\text{mm}$  depth of compression concrete  
 $z := d - \beta \cdot x = 489.55\cdot\text{mm}$  lever arm



Minimum reinforcement area required

$$A_{s.req} := \frac{M_{Ed.x} \cdot \gamma_s}{f_{yk} \cdot z} = 1.416 \times 10^3 \cdot \text{mm}^2$$

Minimum longitudinal reinforcement area

$$A_{s.min} := \max\left(0.0013 \cdot b_s \cdot d, \frac{0.26 \cdot f_{ctm} \cdot b_s \cdot d}{f_{yk}}\right) = 835.328 \cdot \text{mm}^2$$

Maximum longitudinal reinforcement area

$$A_{s,max} := 0.04 \cdot b_s \cdot d = 2.008 \times 10^4 \cdot \text{mm}^2$$

Maximum spacing for main reinforcement (Smax):

$$S_{max} := \min(3 \cdot h_s, 400\text{mm}) = 400 \cdot \text{mm}$$

$$A_s := 1570\text{mm}^2$$

Steel area of longitudinal reinforcement-> 20/200mm

The moment resistance with this steel area:

$$M_{Rd} := A_s \cdot f_{yd} \cdot d \cdot \left(1 - \frac{f_{yd} \cdot A_s}{2 \cdot \eta \cdot f_{cd} \cdot b_s \cdot d}\right) = 330.923 \cdot \text{kN} \cdot \text{m}$$

$$\left| \begin{array}{l} \text{" VERIFY " if } |M_{Ed.x}| < |M_{Rd}| = \text{" VERIFY "} \\ \text{" NOT VERIFY " otherwise} \end{array} \right.$$

$$x_{eff} := \frac{A_s \cdot f_{yd}}{\lambda \cdot b_s \cdot \eta \cdot f_{cd}} = 43.022 \cdot \text{mm}$$

$$\left| \begin{array}{l} \text{" VERIFY " if } \frac{x_{eff}}{d} < \frac{1}{\left(\frac{f_{yk}}{\gamma_s \cdot E_s \cdot \varepsilon_{cu3}} + 1\right)} = \text{" VERIFY "} \\ \text{" NOT VERIFY " otherwise} \end{array} \right.$$

From the reinforcing steel stress-strain idealization:

$$\varepsilon_{s.yield} := \frac{f_{yk}}{\gamma_s \cdot E_s} = 2.174 \times 10^{-3}$$

And from strain diagram:



To ensure yielding:

" Yielding " if  $\varepsilon_s \geq \varepsilon_{s,yield}$  = " Yielding "  
 " NO Yielding " otherwise

$$\varepsilon_s := \varepsilon_{cu3} \cdot \left( \frac{d}{x_{eff}} - 1 \right) = 0.037$$

5. Shear reinforcement

$$V_{Ed} := 78.78 \text{ kN}$$

Design value shear force at ULS

$$A_{sI} := A_s = 1.57 \times 10^3 \cdot \text{mm}^2$$

$$\rho_1 := \frac{A_s}{b_s \cdot d} = 3.127 \times 10^{-3}$$

The percentage of longitudinal reinforcement

" Verify " if  $0.02 \geq \rho_1$  = " Verify "  
 " NO Verify " otherwise

$$k := 1 + \sqrt{\left( \frac{200 \text{ mm}}{d} \right)} = 1.631$$

" Verify " if  $2 \geq k$  = " Verify "  
 " NO Verify " otherwise

$$C_{Rdc} := \frac{0.18}{\gamma_c} = 0.12$$

Assuming the shear reinforcement to be fully stressed:

$$v_1 := 0.6 \cdot \left( 1 - \frac{f_{ck}}{250} \right) = 0.516$$

$$V_{Rdc} := \min \left[ \left[ C_{Rdc} \cdot k \cdot \left( 100 \cdot \rho_1 \cdot f_{ck} \right)^{\frac{1}{3}} \cdot \frac{\text{N}}{\text{mm}^2} \right] \cdot b_s \cdot d, 0.5 \cdot b_s \cdot d \cdot v_1 \cdot f_{cd} \right] = 218.179 \cdot \text{kN}$$

" NO Shear Reinforcement " if  $|V_{Ed}| < |V_{Rdc}|$  = " NO Shear Reinforcement "  
 " SHEAR REINFORCEMENT IS NEEDED " otherwise

Thus, the section of the deck from mid-span does not requires shear reinforcement.


**Anchorage of longitudinal reinforcement ( 20):**

$$f_{ctd} = 1.467 \cdot \text{MPa}$$

$$\eta_1 := 0.7$$

$$\eta_2 := 1$$

Ultimate bond stress is:

$$f_{bd} := 2.25 \cdot \eta_1 \cdot \eta_2 \cdot f_{ctd} = 2.31 \cdot \text{MPa}$$

$$\sigma_{sd} := f_{yd} = 434.783 \cdot \text{MPa}$$

Basic anchorage length:

$$l_{b.rqd} := \frac{\Phi_s}{4} \cdot \frac{\sigma_{sd}}{f_{bd}} = 941.088 \cdot \text{mm}$$

$$\alpha_1 := 1$$

$$\alpha_2 := 1$$

$$\alpha_3 := 1$$

$$\alpha_4 := 0.7$$

$$\alpha_5 := 1$$

$$l_{b.min} := \max(0.6 \cdot l_{b.rqd}, 10 \cdot \Phi_s, 100 \text{mm}) = 564.653 \cdot \text{mm}$$

The design anchorage length is:

$$l_{bd} := \max(\alpha_1 \cdot \alpha_2 \cdot \alpha_3 \cdot \alpha_4 \cdot \alpha_5 \cdot l_{b.rqd}, l_{b.min}) = 658.762 \cdot \text{mm}$$

The value of the design anchorage length is rounded at 660 mm.

## Serviceability Limit State

For the Serviceability Limit State (SLS) the following verifications have been performed in this thesis: stress limitation and crack control.

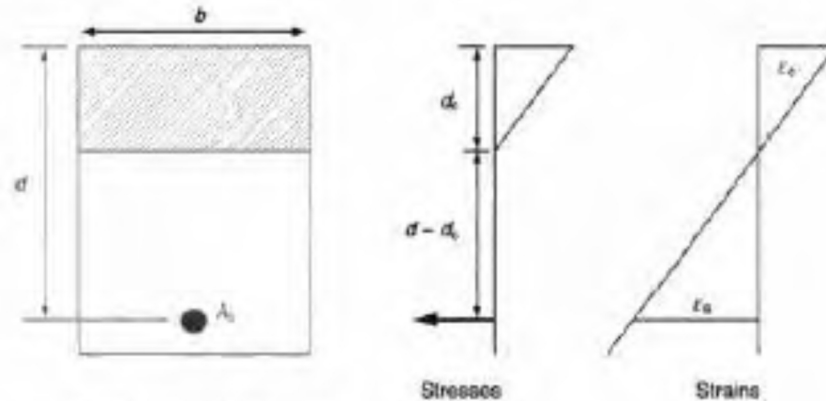


Figure A5.2 – Notation for a rectangular section

Stress Limitation:

$$M_{SLS} := 195649 \text{ N} \cdot \text{m}$$

$$I_y := \frac{b_s \cdot d^3}{12} = 1.054 \times 10^6 \cdot \text{cm}^4$$

$$y := \frac{d}{2} = 0.251 \text{ m}$$

depth of neutral axis

For the un-cracked section the tensile and compressive stress at the top and bottom of the section are:

$$\sigma_{\text{top}} := \left( \frac{M_{SLS} \cdot y}{I_y} \right) = 4.658 \cdot \text{MPa}$$

$$\sigma_{\text{bot}} := \sigma_{\text{top}} = 4.658 \cdot \text{MPa}$$

" Section is cracked " if  $\sigma_{\text{bot}} \geq f_{\text{ctm}}$  = " Section is cracked "  
" Section is NOT cracked " otherwise

Stresses therefore will be calculated ignoring concrete in tension.

1. First, a check is performed at an age when the bridge first opens, assuming minimal creep has occurred, and therefore the short-term-modulus is used for all loading:

$$E_s = 200 \cdot \text{GPa}$$

$$E_{\text{cm}} = 34 \cdot \text{GPa}$$

$$A_s = 20.1 \cdot \text{cm}^2$$

$$E_{\text{c.eff}} := E_{\text{cm}} = 34 \cdot \text{GPa}$$

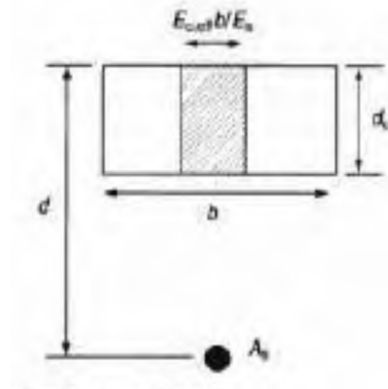


Figure A5.3 – Cracked section transformed to steel units

The depth of concrete in compression is:

$$d_c := \frac{-A_s \cdot E_s + \sqrt{(A_s \cdot E_s)^2 + 2 \cdot b_s \cdot A_s \cdot E_s \cdot E_{c,eff} \cdot d}}{b_s \cdot E_{c,eff}} = 97.769 \cdot \text{mm}$$

The cracked second moment of area in steel units is:

$$I_c := A_s \cdot (d - d_c)^2 + \frac{1}{3} \cdot \frac{E_{c,eff}}{E_s} \cdot b_s \cdot d_c^3 = 3.077 \times 10^8 \cdot \text{mm}^4$$

$$W_c := \frac{I_c}{d_c} = 3.517 \times 10^3 \cdot \text{cm}^3$$

The concrete stress at the top of the section is:

$$\sigma_c := \frac{E_{c,eff}}{E_s} \cdot \left( \frac{M_{SLS}}{W_c} \right) = 9.458 \cdot \text{MPa}$$

The compression limit at top edge is:

$$\sigma_{c,adm} := k_1 \cdot f_{ck} = 21 \cdot \text{MPa}$$

$$k_1 = 0.6$$

$$\left| \begin{array}{l} \text{" Verify " if } \sigma_{c,adm} \geq \sigma_c \\ \text{" NOT Verify " otherwise} \end{array} \right. = \text{" Verify "}$$

The reinforcement stress is:

$$\sigma_s := \frac{M_{SLS} \cdot (d - d_c)}{I_c} = 263.554 \cdot \text{MPa}$$

$$k_3 := 0.8$$

$$f_{yk} = 500 \cdot \text{MPa}$$

The tensile limit under the characteristic combination is:



$$\sigma_{s.adm} := k_3 \cdot f_{yk} = 400 \cdot \text{MPa}$$

" Verify " if  $\sigma_{s.adm} \geq \sigma_s$  = " Verify "  
 " NOT Verify " otherwise

2. Second check is performed after all the creep has taken place. The creep factor is  $\phi_{creep} = 1.515$ . This is used to calculate an effective modulus of elasticity for the concrete:

$$M_{dead} := 22.74\%$$

$$M_{live} := 77.26\%$$

$$E_{c.eff} := \frac{(M_{dead} + M_{live}) \cdot E_{cm}}{M_{live} + (1 + \phi_{creep}) \cdot M_{dead}} = 25.288 \cdot \text{GPa}$$

The depth of concrete in compression is:

$$d_c := \frac{-A_s \cdot E_s + \sqrt{(A_s \cdot E_s)^2 + 2 \cdot b_s \cdot A_s \cdot E_s \cdot E_{c.eff} \cdot d}}{b_s \cdot E_{c.eff}} = 99.925 \cdot \text{mm}$$

The cracked second moment of area in steel units is:

$$I_c := A_s \cdot (d - d_c)^2 + \frac{1}{3} \cdot \frac{E_{c.eff}}{E_s} \cdot b_s \cdot d_c^3 = 2.959 \times 10^8 \cdot \text{mm}^4$$

$$W_c := \frac{I_c}{d_c} = 2.961 \times 10^3 \cdot \text{cm}^3$$

The concrete stress at the top of the section is:

$$\sigma_c := \frac{E_{c.eff}}{E_s} \cdot \left( \frac{M_{SLS}}{W_c} \right) = 8.355 \cdot \text{MPa}$$

The compression limit at top edge is:

$$\sigma_{c.adm} := k_1 \cdot f_{ck} = 21 \cdot \text{MPa}$$

$$k_1 = 0.6$$

" Verify " if  $\sigma_{c.adm} \geq \sigma_c$  = " Verify "  
 " NOT Verify " otherwise

The reinforcement stress is:

$$\sigma_s := \frac{M_{SLS} \cdot (d - d_c)}{I_c} = 265.883 \cdot \text{MPa}$$

$$k_3 := 0.8$$





$$f_{yk} = 500 \cdot \text{MPa}$$

The tensile limit under the characteristic combination is:

$$\sigma_{s.adm} := k_3 \cdot f_{yk} = 400 \cdot \text{MPa}$$

$$\left| \begin{array}{l} \text{" Verify " if } \sigma_{s.adm} \geq \sigma_s = \text{" Verify "} \\ \text{" NOT Verify " otherwise} \end{array} \right.$$

Thus, the stresses in the deck are below the limits and so it's ensure normal conditions of use and the assumptions made in design model remains valid (linear-elastic behavior).

### Control of crack widths by direct calculation

$$d = 502 \cdot \text{mm}$$

$$x := d_c = 111.434 \cdot \text{mm}$$

$$c_{nom} = 40 \cdot \text{mm}$$

$$h_{c.eff} := \min \left[ 2.5 \cdot (h_s - d), \frac{h_s}{2}, \frac{(h_s - x)}{3} \right] = 120 \cdot \text{mm}$$

The effective tension area is:

$$A_{c.eff} := b_s \cdot h_{c.eff} = 1.2 \times 10^5 \cdot \text{mm}^2$$

$$\rho_{p.eff} := \frac{A_s}{A_{c.eff}} = 0.01308$$

$$k_1 := 0.80$$

$$k_2 := 0.5$$

The maximum final crack spacing is:

$$s_{r_{max}} := 3.4 \cdot c + 0.425 \cdot k_1 \cdot k_2 \cdot \frac{\Phi_s}{\rho_{p.eff}} = 395.873 \cdot \text{mm}$$

$$\sigma_s = 265.883 \cdot \text{MPa}$$

$$k_t := 0.50$$

$$f_{ct.eff} := f_{ctm} = 3.2 \cdot \text{MPa}$$

$$\alpha_c := \frac{E_s}{E_{cm}} = 5.882$$



$$\Delta\varepsilon := \varepsilon_{sm} - \varepsilon_{cm}$$

$$\Delta\varepsilon := \frac{\sigma_s - k_t \cdot \frac{f_{ct,eff}}{\rho_{p,eff}} \cdot (1 + \alpha_c \cdot \rho_{p,eff})}{E_s} = 6.709 \times 10^{-4}$$

Therefore the maximum crack width is:

$$w_k := s_{r,max} \cdot \Delta\varepsilon = 0.266 \cdot \text{mm}$$

$$w_{k,lim} := 0.30 \text{ mm}$$

$$\left| \begin{array}{l} \text{" Verify " if } w_{k,lim} \geq w_k = \text{" Verify "} \\ \text{" NOT Verify " otherwise} \end{array} \right.$$

Thus, the maximum crack width is under the limit value. There is no problem concerning the cracks.

### **Embedded section (S1) – section next to the wall:**

1.Recommended values of material factors according to clause 2.4 from SR-EN 1992-1

$$\gamma_c := 1.5 \quad \text{For concrete}$$

$$\gamma_s := 1.15 \quad \text{For reinforcing steel}$$

2.Materials according to clause 3 from SR-EN 1992-1

Concrete class: C35/45

$$f_{ck} := 35\text{MPa}$$

$$f_{ctm} := 3.2\text{MPa}$$

$$f_{ctk0.05} := 2.2\text{MPa}$$

$$f_{ctk0.95} := 4.2\text{MPa}$$

$$E_{cm} := 34\text{GPa}$$

$$\alpha_{cc} := 0.85$$

$$\alpha_{ct} := 1.0$$

$$\lambda := 0.8$$

$$\eta := 1.0$$

The design compressive strength for concrete

$$f_{cd} := \alpha_{cc} \cdot \frac{f_{ck}}{\gamma_c} = 19.833 \cdot \text{MPa}$$

The design tensile strength for concrete

$$f_{ctd} := \frac{\alpha_{ct} \cdot f_{ctk0.05}}{\gamma_c} = 1.467 \cdot \text{MPa}$$

Reinforcing steel: B500B:

$$f_{yk} := 500 \text{MPa}$$

$$\varepsilon_{cu3} := 0.0035$$

$$E_s := 200 \text{GPa}$$

$$f_{yd} := \frac{f_{yk}}{\gamma_s} = 434.783 \cdot \text{MPa}$$

The design tensile strength for steel

3. Concrete cover: according to clause 4.4 from SR-EN 1992-1

$$c_{\min} := \max(25 \text{mm}, 30 \text{mm} + 0 - 0 - 0, 10 \text{mm}) = 30 \cdot \text{mm} \quad \text{The minimum cover}$$

$$\Delta c_{\text{dev}} := 10 \text{mm} \quad \text{The recommended value for bridges}$$

$$c_{\text{nom}} := c_{\min} + \Delta c_{\text{dev}} = 40 \cdot \text{mm} \quad \text{The nominal cover}$$

4. Longitudinal reinforcement of concrete slab

$$h_s := 550 \text{mm} \quad \text{height of slab}$$

$$b_s := 1000 \text{mm} \quad \text{considered width of slab}$$

$$M_{\text{Ed},x} := 161147.5 \text{N} \cdot \text{m} \quad \text{maximum applied ULS bending moment}$$

$$\beta := 0.400 \quad \text{assuming rectangular concrete stress block}$$

$$\Phi_s := 16 \text{mm} \quad \text{considered size bar}$$

Distance from bottom edge of slab to geometric center of bars

$$d_1 := \frac{\Phi_s}{2} + c_{\text{nom}} = 48 \cdot \text{mm}$$

$$d := h_s - d_1 = 502 \cdot \text{mm} \quad \text{effective depth of slab}$$

$$K_{\text{av}} := \frac{M_{\text{Ed},x}}{b_s \cdot d^2 \cdot f_{cd}} = 0.032$$

$$\text{ratio}_{x,d} := \frac{1 - \sqrt{1 - 4\beta \cdot K_{\text{av}}}}{2 \cdot \beta} = 0.033$$



Check limit from next equation to ensure reinforcement is yielding:

$$\text{Eq} := \frac{1}{\left( \frac{f_{yk}}{\gamma_s \cdot E_s \cdot \varepsilon_{cu3}} + 1 \right)} = 0.617$$

" SINGLY REINFORCED " if  $|\text{ratio}_{x,d}| < |\text{Eq}|$  = " SINGLY REINFORCED "  
 " DOUBLY REINFORCED " otherwise

$$x := 0.033 \cdot d = 16.566 \cdot \text{mm}$$

depth of compression concrete

$$z := d - \beta \cdot x = 495.374 \cdot \text{mm}$$

lever arm

Minimum reinforcement area required

$$A_{s,\text{req}} := \frac{M_{\text{Ed},x} \cdot \gamma_s}{f_{yk} \cdot z} = 748.201 \cdot \text{mm}^2$$

Minimum longitudinal reinforcement area

$$A_{s,\text{min}} := \max \left( 0.0013 \cdot b_s \cdot d, \frac{0.26 \cdot f_{ctm} \cdot b_s \cdot d}{f_{yk}} \right) = 835.328 \cdot \text{mm}^2$$

Maximum longitudinal reinforcement area

$$A_{s,\text{max}} := 0.04 \cdot b_s \cdot d = 2.008 \times 10^4 \cdot \text{mm}^2$$

Maximum spacing for main reinforcement ( $S_{\text{max}}$ ):

$$S_{\text{max}} := \min(3 \cdot h_s, 400\text{mm}) = 400 \cdot \text{mm}$$

Minimum spacing for longitudinal reinforcement ( $S_{\text{min}}$ ):

$$S_{\text{min}} := \max(\Phi_s, \Phi_s + 5\text{mm}, 20\text{mm}) = 21 \cdot \text{mm}$$

$$A_s := 1005 \text{mm}^2$$

Steel area of longitudinal reinforcement-> 16/200mm

The moment resistance with this steel area:

$$M_{\text{Rd}} := A_s \cdot f_{yd} \cdot d \cdot \left( 1 - \frac{f_{yd} \cdot A_s}{2 \cdot \eta \cdot f_{cd} \cdot b_s \cdot d} \right) = 214.539 \cdot \text{kN} \cdot \text{m}$$

" VERIFY " if  $|M_{\text{Ed},x}| < |M_{\text{Rd}}|$  = " VERIFY "  
 " NOT VERIFY " otherwise

$$x_{\text{eff}} := \frac{A_s \cdot f_{yd}}{\lambda \cdot b_s \cdot \eta \cdot f_{cd}} = 27.539 \cdot \text{mm}$$



$$\left| \begin{array}{l} \text{" VERIFY " if } \frac{x_{\text{eff}}}{d} < \frac{1}{\left( \frac{f_{yk}}{\gamma_s \cdot E_s \cdot \varepsilon_{cu3}} + 1 \right)} = \text{" VERIFY " } \\ \text{" NOT VERIFY " otherwise} \end{array} \right.$$

From the reinforcing steel stress-strain idealization:

$$\varepsilon_{s,\text{yield}} := \frac{f_{yk}}{\gamma_s \cdot E_s} = 2.174 \times 10^{-3}$$

And from strain diagram

$$\varepsilon_s := \varepsilon_{cu3} \cdot \left( \frac{d}{x_{\text{eff}}} - 1 \right) = 0.06$$

To ensure yielding:

$$\left| \begin{array}{l} \text{" Yielding " if } \varepsilon_s \geq \varepsilon_{s,\text{yield}} = \text{" Yielding " } \\ \text{" NO Yielding " otherwise} \end{array} \right.$$

## Shear reinforcement

$$V_{Ed} := 287208.6\text{N} \quad \text{Design value shear force at ULS}$$

$$A_{s1} := A_s = 1.005 \times 10^3 \cdot \text{mm}^2$$

$$\rho_1 := \frac{A_{s1}}{b_s \cdot d} = 0.002$$

The percentage of longitudinal reinforcement

$$\left| \begin{array}{l} \text{" Verify " if } 0.02 \geq \rho_1 = \text{" Verify " } \\ \text{" NO Verify " otherwise} \end{array} \right.$$

$$k := 1 + \sqrt{\left( \frac{200\text{mm}}{d} \right)} = 1.631$$

$$\left| \begin{array}{l} \text{" Verify " if } 2 \geq k = \text{" Verify " } \\ \text{" NO Verify " otherwise} \end{array} \right.$$

$$C_{Rdc} := \frac{0.18}{\gamma_c} = 0.12$$

Assuming the shear reinforcement to be fully stressed:

$$v_1 := 0.6 \cdot \left( 1 - \frac{f_{ck}}{250} \right) = 0.516$$

The design shear resistance of the section without shear reinforcement

$$V_{Rdc} := \min \left[ \left[ C_{Rdc} \cdot k \cdot \left( 100 \cdot \rho_l \cdot f_{ck} \right)^{\frac{1}{3}} \cdot \frac{N}{\text{mm}^2} \right] \cdot b_s \cdot d, 0.5 \cdot b_s \cdot d \cdot v_1 \cdot f_{cd} \right] = 188.033 \cdot \text{kN}$$

" NO Shear Reinforcement "if  $|V_{Ed}| < |V_{Rdc}|$  = " IS REQUIRED Shear Reinforcement  
" IS REQUIRED Shear Reinforcement "otherwise

If there are considered link bars inclined at an angle of  $90^\circ$  and a strut angle of  $45^\circ$ , the following relationship must be used:

$$\alpha_{cw} := 1$$

$$\alpha := 90\text{deg} \quad \text{for non-prestressed structure}$$

$$\theta_1 := 45\text{deg}$$

$$\cot(\theta_1) = 1$$

$$\tan(\theta_1) = 1$$

$$f_{cd} = 19.833 \cdot \text{MPa}$$

$$z_w := 0.9 \cdot d = 45.18 \cdot \text{cm}$$

For the vertical shear reinforcement, the design value of the maximum shear force, which can be sustained by the member, limited by crushing of the compression struts:

$$V_{Rd,max} := \frac{\alpha_{cw} \cdot b_s \cdot z_w \cdot v_1 \cdot f_{cd}}{(\cot(\theta_1) + \tan(\theta_1))} = 2.312 \times 10^3 \cdot \text{kN}$$

$$\frac{A_{sw}}{s} \geq \frac{V_{Rds}}{z_w \cdot f_{yd} \cdot \cot(\theta_1)}$$

It is assumed that  $V_{rds} = V_{ed}$ , so;

$$\frac{V_{Ed}}{z_w \cdot f_{yd} \cdot \cot(\theta_1)} = 1.462 \cdot \frac{\text{mm}^2}{\text{mm}}$$

If it considered  $s = 300$  mm:

$$s := 300 \text{ mm}$$



$$A_{sw} := \left( \frac{V_{Ed}}{z_w \cdot f_{yd} \cdot \cot(\theta_1)} \right) \cdot s = 438.632 \cdot \text{mm}^2$$

The area of the shear reinforcement for one meter of slab is:

$$A_{sw} := 452 \text{mm}^2 \quad 4 \quad 12 \text{ mm}$$

So, for the vertical shear reinforcement, the design value of shear force, which can be sustained by the yielding shear reinforcement:

$$V_{Rd.s} := \frac{A_{sw}}{s} \cdot z_w \cdot f_{yd} \cdot \cot(\theta_1) = 295.962 \cdot \text{kN}$$

$$\left| \begin{array}{l} \text{" VERIFY " if } |V_{Ed}| < |V_{Rd.s}| \\ \text{" NOT VERIFY " otherwise} \end{array} \right. = \text{" VERIFY "}$$

#### **Anchorage of longitudinal reinforcement ( 16):**

$$f_{ctd} = 1.467 \cdot \text{MPa}$$

$$\eta_1 := 0.7$$

$$\eta_2 := 1$$

Ultimate bond stress is:

$$f_{bd} := 2.25 \cdot \eta_1 \cdot \eta_2 \cdot f_{ctd} = 2.31 \cdot \text{MPa}$$

$$\sigma_{sd} := f_{yd} = 434.783 \cdot \text{MPa}$$

Basic anchorage length:

$$l_{b.rqd} := \frac{\Phi_s}{4} \cdot \frac{\sigma_{sd}}{f_{bd}} = 752.87 \cdot \text{mm}$$

$$\alpha_1 := 1$$

$$\alpha_2 := 1$$

$$\alpha_3 := 1$$

$$\alpha_4 := 0.7$$

$$\alpha_5 := 1$$

$$l_{b.min} := \max(0.6 \cdot l_{b.rqd}, 10 \cdot \Phi_s, 100 \text{mm}) = 451.722 \cdot \text{mm}$$

The design anchorage length is:



$$l_{bd} := \max(\alpha_1 \cdot \alpha_2 \cdot \alpha_3 \cdot \alpha_4 \cdot \alpha_5 \cdot l_{b.rqd}, l_{b.min}) = 527.009 \cdot \text{mm}$$

The value of the design anchorage length is rounded at 530 mm.

### Transversal reinforcement (S3)

$$M_{Ed.y} := 155103.6 \text{ N}\cdot\text{m} \quad \text{maximum applied ULS bending moment in Y direction}$$

Assuming rectangular concrete stress block:

$$\beta := 0.400$$

$$\Phi_s := 16 \text{ mm} \quad \text{considered size bar}$$

$$d_1 := \Phi_s + c_{nom} + \frac{16 \text{ mm}}{2} = 64 \cdot \text{mm}$$

distance from bottom edge of slab to geometric center of bars

$$d := h_s - d_1 = 486 \cdot \text{mm}$$

effective depth of slab

$$K_{av} := \frac{M_{Ed.y}}{b_s \cdot d^2 \cdot f_{cd}} = 0.033$$

$$\text{ratio}_{x.d} := \frac{1 - \sqrt{1 - 4\beta \cdot K_{av}}}{2 \cdot \beta} = 0.034$$

Check limit from next equation to ensure reinforcement is yielding:

$$Eq := \frac{1}{\left( \frac{f_{yk}}{\gamma_s \cdot E_s \cdot \varepsilon_{cu3}} + 1 \right)} = 0.617$$

$$\left| \begin{array}{l} \text{" SINGLY REINFORCED " if } |\text{ratio}_{x.d}| < |Eq| \\ \text{" DOUBLY REINFORCED " otherwise} \end{array} \right. = \text{" SINGLY REINFORCED "}$$

$$x := 0.034 \cdot d = 16.524 \cdot \text{mm} \quad \text{depth of compression concrete}$$

$$z := d - \beta \cdot x = 479.39 \cdot \text{mm} \quad \text{lever arm}$$

Minimum reinforcement area required

$$A_{s.req} := \frac{M_{Ed.y} \cdot \gamma_s}{f_{yk} \cdot z} = 744.15 \cdot \text{mm}^2$$

Minimum longitudinal reinforcement area





$$A_{sl_{min}} := \max\left(0.0013 \cdot b_s \cdot d, \frac{0.26 \cdot f_{ctm} \cdot b_s \cdot d}{f_{yk}}\right) = 808.704 \cdot \text{mm}^2$$

Maximum longitudinal reinforcement area

$$A_{sl_{max}} := 0.04 \cdot b_s \cdot d = 1.944 \times 10^4 \cdot \text{mm}^2$$

Maximum spacing for main reinforcement (Smax):

$$S_{max} := \min(3 \cdot h_s, 400\text{mm}) = 400 \cdot \text{mm}$$

$$A_s := 840\text{mm}^2 \quad \text{Steel area of longitudinal reinforcement} \rightarrow 16/250\text{mm}$$

The moment resistance with this steel area:

$$M_{Rd} := A_s \cdot f_{yd} \cdot d \cdot \left(1 - \frac{f_{yd} \cdot A_s}{2 \cdot \eta \cdot f_{cd} \cdot b_s \cdot d}\right) = 174.133 \cdot \text{kN} \cdot \text{m}$$

$$\left| \begin{array}{l} \text{" VERIFY " if } |M_{Ed,y}| < |M_{Rd}| = \text{" VERIFY "} \\ \text{" NOT VERIFY " otherwise} \end{array} \right.$$

$$x_{eff} := \frac{A_s \cdot f_{yd}}{\lambda \cdot b_s \cdot \eta \cdot f_{cd}} = 23.018 \cdot \text{mm}$$

$$\left| \begin{array}{l} \text{" VERIFY " if } \frac{x_{eff}}{d} < \frac{1}{\left(\frac{f_{yk}}{\gamma_s \cdot E_s \cdot \varepsilon_{cu3}} + 1\right)} = \text{" VERIFY "} \\ \text{" NOT VERIFY " otherwise} \end{array} \right.$$

From the reinforcing steel stress-strain idealization:

$$\varepsilon_{s,yield} := \frac{f_{yk}}{\gamma_s \cdot E_s} = 2.174 \times 10^{-3}$$

And from strain diagram

$$\varepsilon_s := \varepsilon_{cu3} \cdot \left(\frac{d}{x_{eff}} - 1\right) = 0.07$$

To ensure yielding:

$$\left| \begin{array}{l} \text{" Yielding " if } \varepsilon_s \geq \varepsilon_{s,yield} = \text{" Yielding "} \\ \text{" NO Yielding " otherwise} \end{array} \right.$$

### Annex A6. D-region verification

For the frame corner of the bridge structure, the following “strut and tie” model has been chosen:

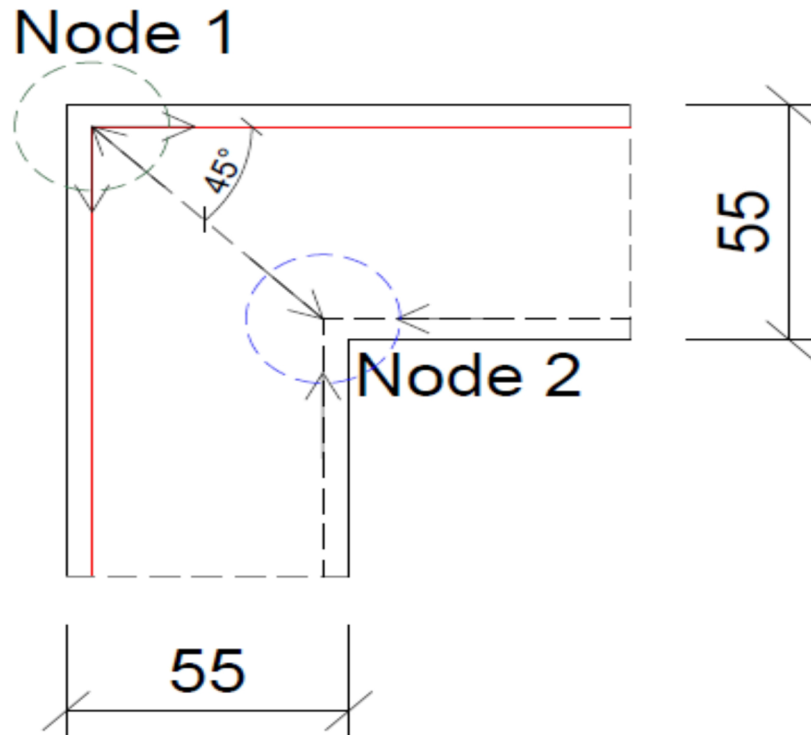


Figure A6.1 – Strut and tie model for corner joint

$$A_s := 1005 \text{ mm}^2$$

Total area of reinforcement

$$f_{yd} := 435 \frac{\text{N}}{\text{mm}^2}$$

The design yield strength

$$x := 27.539 \text{ mm}$$

The depth of compression section

$$\lambda := 0.8$$

$$b := 1000 \text{ mm}$$

$$f_{ck} := 35 \frac{\text{N}}{\text{mm}^2}$$

$$\phi_s := 16 \text{ mm}$$

$$k_3 := 0.75$$

$$k_2 := 0.85$$

$$f_{cd} := \frac{f_{ck}}{1.5} = 23.333 \frac{\text{N}}{\text{mm}^2}$$

$$F_s := A_s \cdot f_{yd} = 4.372 \times 10^5 \text{ N}$$

$$F_c := F_s = 4.372 \times 10^5 \text{ N}$$

## First check - Compression tension node with reinforcement provided in two directions (C-T-T type)

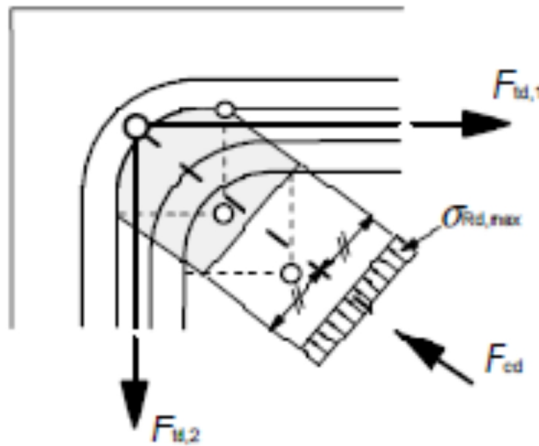


Figure A6.2 – Concrete compression stress verification in a compression-tension node with anchored ties provided in more than one direction

The force in strut:

$$F_{\text{strut}} := \frac{F_s}{\cos(45\text{deg})} = 6.183 \times 10^5 \text{ N}$$

$$b_{\text{radius}} := 4 \cdot \frac{\phi_s}{2} = 32 \text{ mm}$$

The considered bend radius

The width of strut in this point is:

$$w_{\text{strut1}} := \sqrt{2} \cdot \left( b_{\text{radius}} + \frac{\phi_s}{2} \right) = 56.569 \text{ mm}$$

The design value is:

$$\sigma_{\text{strut1}} := \frac{F_{\text{strut}}}{b \cdot w_{\text{strut1}}} = 10.929 \frac{\text{N}}{\text{mm}^2}$$

$$\nu_1 := \left( 1 - \frac{f_{\text{ck}}}{250 \text{ MPa}} \right) = 0.86$$

$$\sigma_{\text{Rd,max1}} := k_3 \cdot \nu_1 \cdot f_{\text{cd}} = 15.05 \frac{\text{N}}{\text{mm}^2}$$

" VERIFY " if  $\sigma_{\text{strut1}} < \sigma_{\text{Rd,max1}}$  = " VERIFY "  
" NOT VERIFY " otherwise



**Second check – Compression node without ties (C-C-C type)**

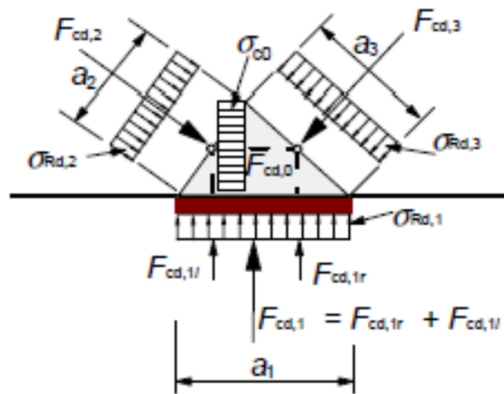


Figure A6.3 – Concrete compression stress verification in a compression node without ties

$$w_{strut2} := \frac{x}{\cos(45deg)} = 38.946mm$$

The design value is:

$$\sigma_{strut2} := \frac{F_{strut}}{b \cdot w_{strut2}} = 15.875 \frac{N}{mm^2}$$

$$\sigma_{Rd,max2} := k_2 \cdot \nu_1 \cdot f_{cd} = 17.057 \frac{N}{mm^2}$$

" VERIFY " if  $\sigma_{strut2} < \sigma_{Rd,max2}$  = " VERIFY "  
 " NOT VERIFY " otherwise

The values of stresses are under the limit value, so is no problem regarding the stresses.

## Annex A7. Bridge parameters

### Case with 7 meters span length

#### Mass of the bridge:

$L_{\text{bridge}} := 7\text{m}$	inner span length
$\rho_{\text{ballast}} := 1800 \frac{\text{kg}}{\text{m}^3}$	density of the ballast which includes the mass of sleepers and rail
$A_{\text{ballast}} := 1.86\text{m}^2$	cross section area of ballast prism
$\rho_{\text{concrete}} := 2500 \frac{\text{kg}}{\text{m}^3}$	density of concrete

#### The cross-section dimensions of deck

$b_s := 3.55\text{m}$	
$h_s := 0.55\text{m}$	
$A_{\text{deck}} := b_s \cdot h_s = 1.953\text{m}^2$	cross section area of deck

#### The total mass of the deck is:

$$M_{\text{deck}} := A_{\text{ballast}} \cdot L_{\text{bridge}} \cdot \rho_{\text{ballast}} + A_{\text{deck}} \cdot L_{\text{bridge}} \cdot \rho_{\text{concrete}} = 5.76 \times 10^4 \text{ kg}$$

#### Structural damping

Bridge type	Damping ratio, %	
	Span $L < 20$ m	Span $L > 20$ m
Steel and composite	$0.5+0.125(20-L)$	0.5
Prestressed concrete	$1.0+0.070(20-L)$	1.0
Filler beam and reinf. concr.	$1.5+0.070(20-L)$	1.5

Table A7.1 – Damping coefficient for bridge structures, assumed for dynamic analysis in design purpose

$$L_b := 7$$

#### The damping of the bridge is:

$$\zeta := 1.5 + 0.07 \cdot (20 - L_b) = 2.41$$



## Case with 10 meters span length

### Mass of the bridge:

$$L_{\text{bridge}} := 10\text{m} \quad \text{inner span length}$$

The cross-section dimensions of deck

$$b_s := 3.55\text{m}$$

$$h_s := 0.79\text{m}$$

$$A_{\text{deck}} := b_s \cdot h_s = 2.805\text{m}^2 \quad \text{cross section area of deck}$$

The total mass of the deck is:

$$M_{\text{deck}} := A_{\text{ballast}} \cdot L_{\text{bridge}} \cdot \rho_{\text{ballast}} + A_{\text{deck}} \cdot L_{\text{bridge}} \cdot \rho_{\text{concrete}} = 1.036 \times 10^5 \text{ kg}$$

### Structural damping

$$L_b := 10$$

The damping of the bridge is:

$$\zeta := 1.5 + 0.07 \cdot (20 - L_b) = 2.2$$

## Case with 13 meters span length

$$L_{\text{bridge}} := 13\text{m} \quad \text{inner span length}$$

The cross-section dimensions of deck

$$b_s := 3.55 \text{ m}$$

$$h_s := 1.02 \text{ m}$$

$$A_{\text{deck}} := b_s \cdot h_s = 3.621\text{m}^2 \quad \text{cross section area of deck}$$

The total mass of the deck is:

$$M_{\text{deck}} := A_{\text{ballast}} \cdot L_{\text{bridge}} \cdot \rho_{\text{ballast}} + A_{\text{deck}} \cdot L_{\text{bridge}} \cdot \rho_{\text{concrete}} = 1.612 \times 10^5 \text{ kg}$$

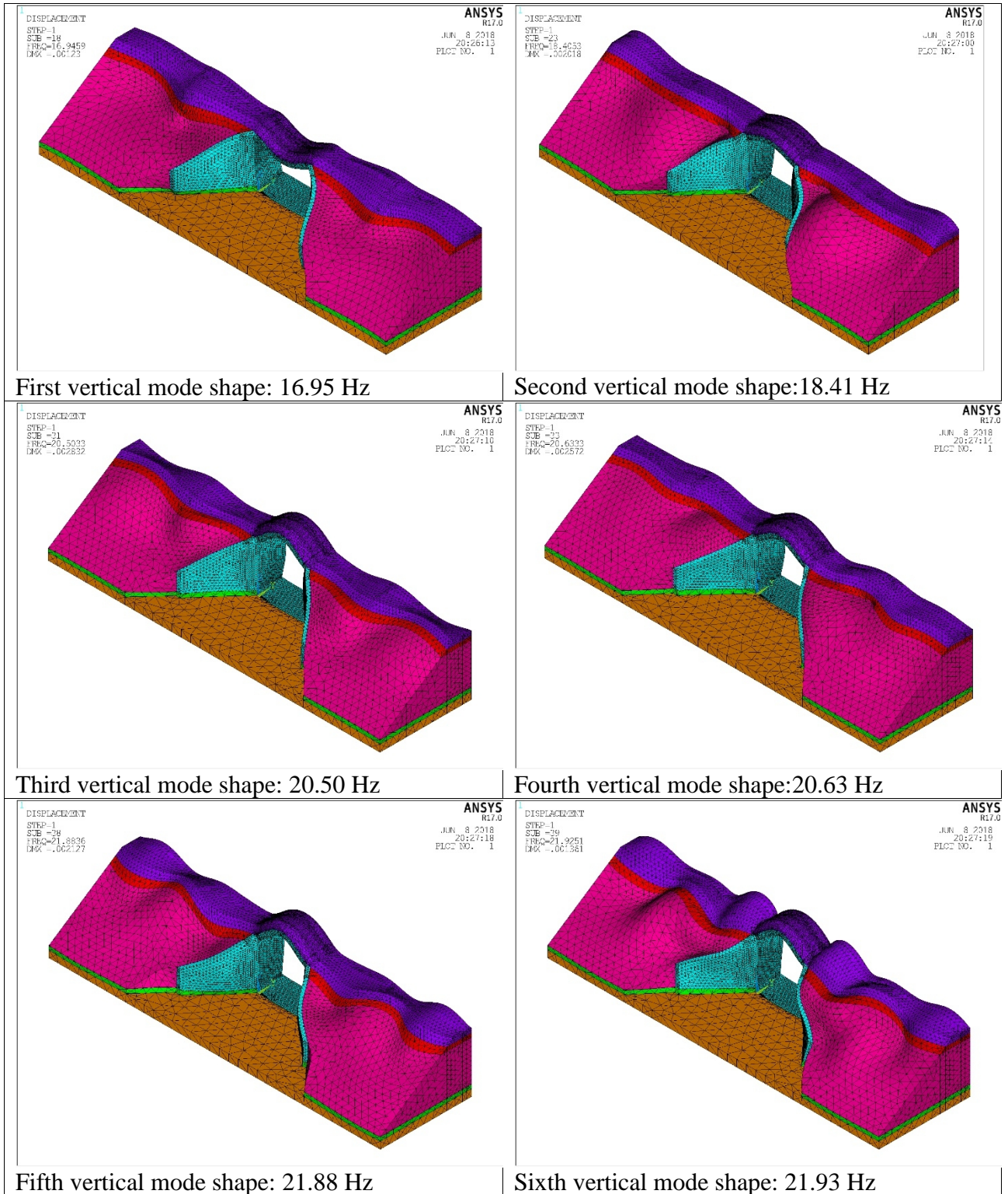
### Structural damping

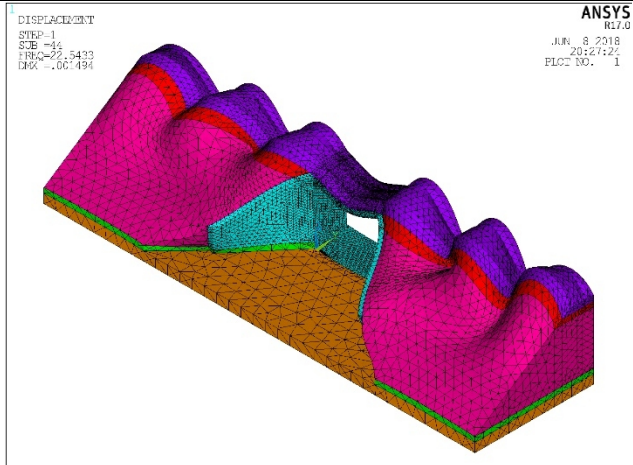
$$L_b := 13$$

The damping of the bridge is:

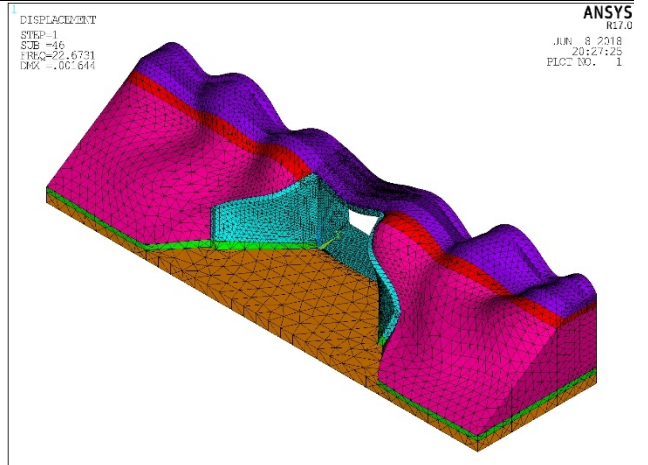
$$\zeta := 1.5 + 0.07 \cdot (20 - L_b) = 1.99$$

## Annex A8. Vertical mode shapes and natural frequencies for 7 meters span length

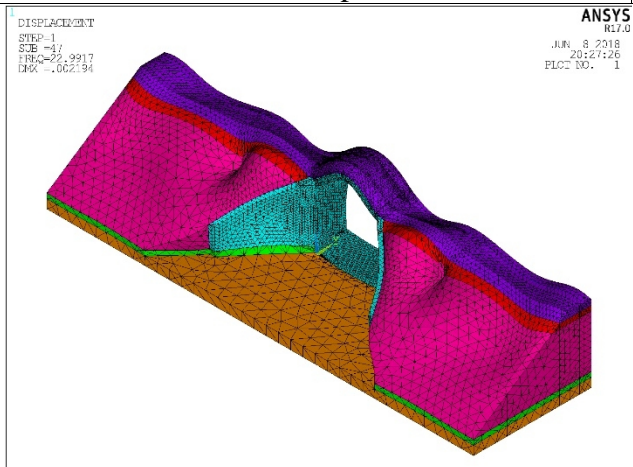




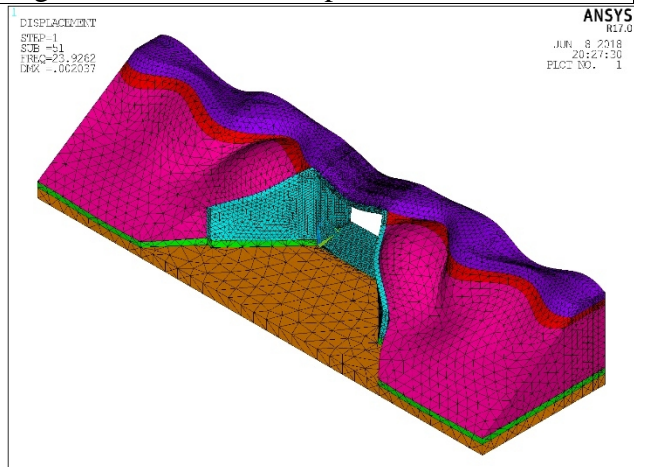
Seventh vertical mode shape: 22.54 Hz



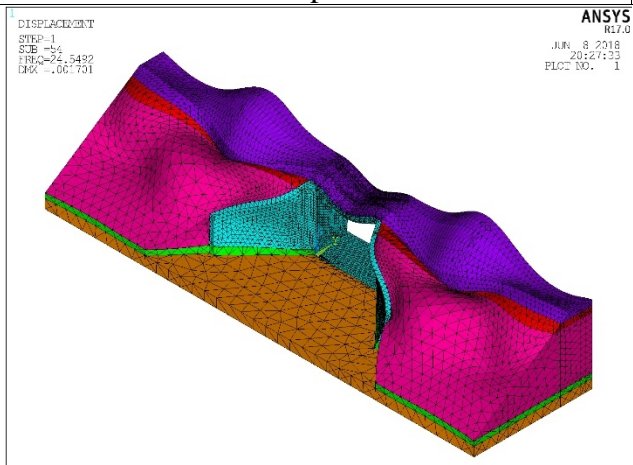
Eighth vertical mode shape: 22.67 Hz



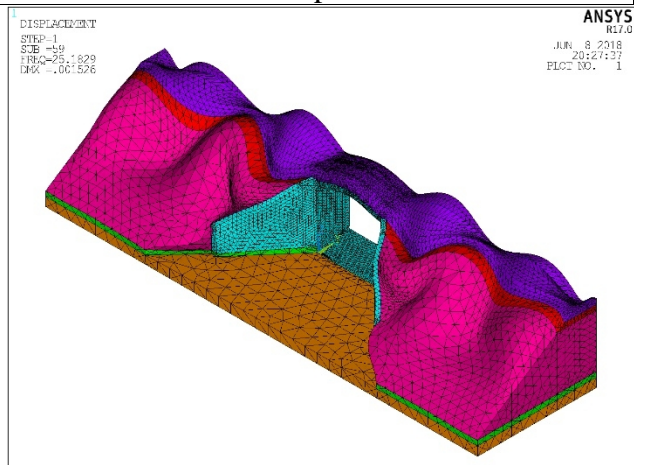
Ninth vertical mode shape: 22.99 Hz



Tenth vertical mode shape: 23.93 Hz

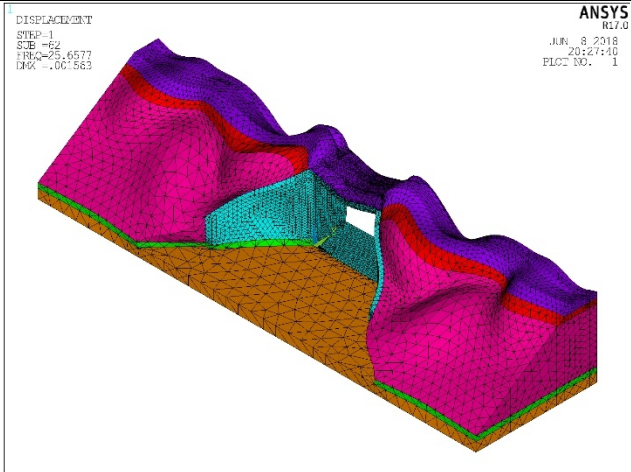


Eleventh vertical mode shape: 24.54 Hz

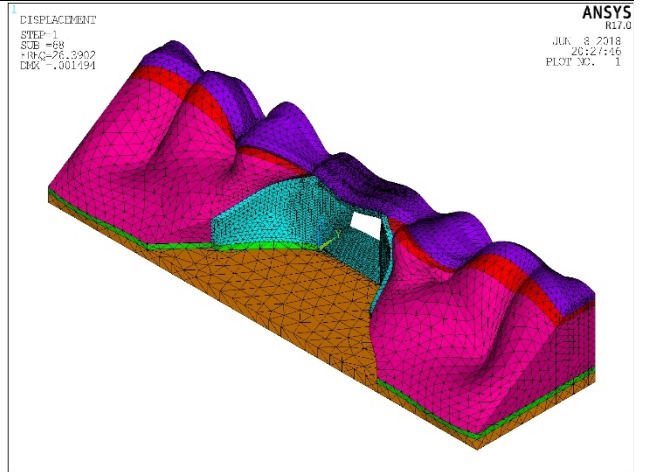


Twelfth vertical mode shape: 25.18 Hz

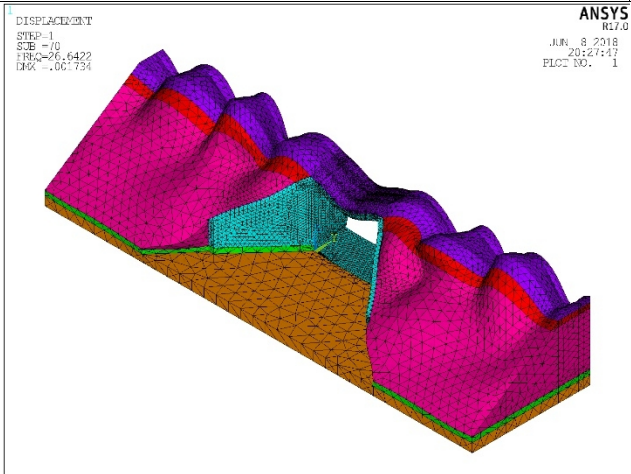




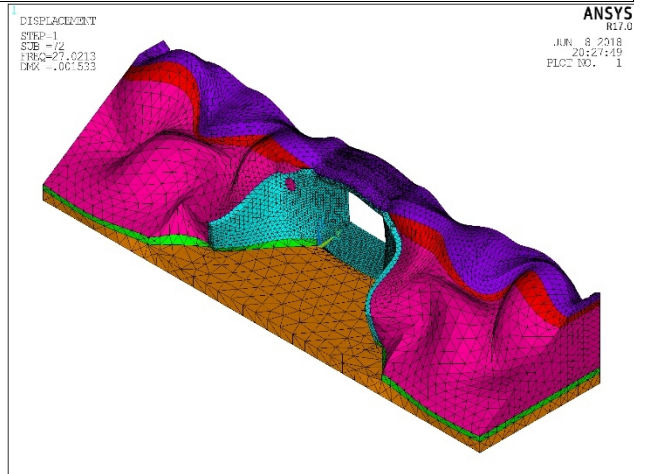
Thirteenth vertical mode shape: 25.66 Hz



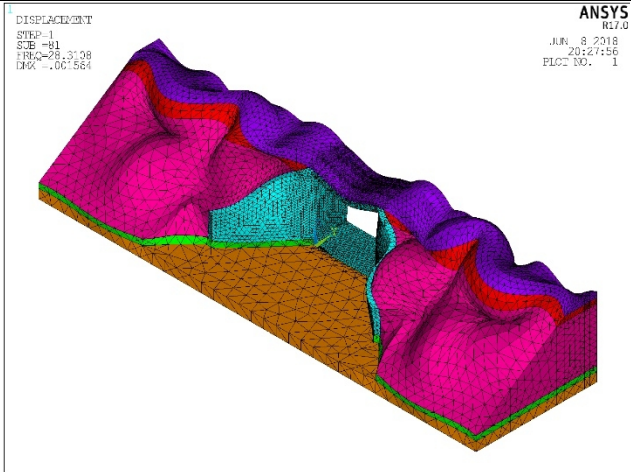
Fourteenth vertical mode shape: 26.39 Hz



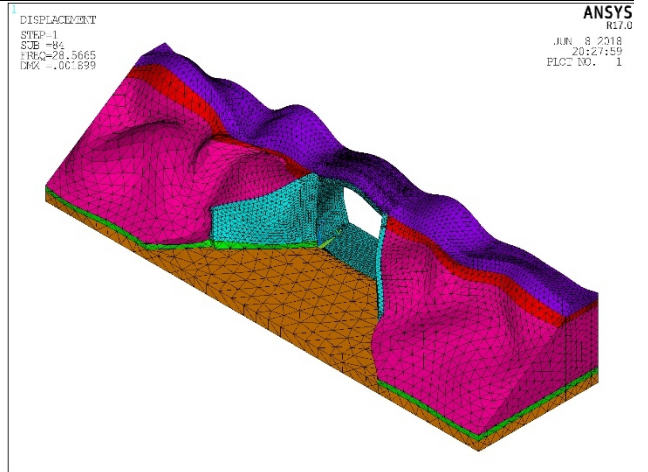
Fifteenth vertical mode shape: 26.64 Hz



Sixteenth vertical mode shape: 27.02 Hz



Seventeenth vertical mode shape: 28.31 Hz



Eighteenth vertical mode shape: 28.57 Hz

## Annex A9. Input parameters for ANSYS software

! INPUT PARAMETERS

!-----

$l1 = 7.$	! span length of the bridge
$l2 = 5.9$	! height of the abutment
$b1 = 7.1$	! width of the bridge/abutment
$br = 0.072$	! the width of the rail head (UIC 60 / 60E1)
$gt = 1.435$	! the track gauge
$Lsleep = 2.6/2$	! the half of total length of sleeper
$hp = 0.6$	! thickness of the ballast-prism
$sba = 1.5*hp$	! width of the shoulder of ballast-prism for slope 1:1.5
$h1 = 0.55$	! thickness of the bottom slab
$h2 = 0.55$	! thickness of the abutment
$h3 = 0.55$	! thickness of the bridge deck
$h4 = 1.0$	! thickness of the subsoil layer (ground layer)
$Lem = 24.$ from the center of the bridge	! length of the embankment in longitudinal direction(X)
$ssb = 1.5*h3$ 1:1.5	! width of the shoulder of sub-ballast-prism for slope 1:1.5
$Lb = 1.5*l2$ (X)	! length of the backfill material in longitudinal direction
$Lf = Lem-(l1/2)$	! the end of filling material of LEFT side of the bridge
$Lfr = Lem+(l1/2)$	! the end of filling material of RIGHT side of the bridge
$Ls = 1.5*l2$	! the width of slope's base in Y direction
$bhalf = b1/2$	! half of the total width of abutment
$ba1 = (gt/2)+(br/2)$ profile	! the distance between axis of line track and axis of rail profile
$b = bhalf-ba1$	! width between rail and end of ballast
$ba = Lsleep-ba1$	! width of sleeper external to the rail
$bc = bhalf-Lsleep$	! width of ballast external to the sleeper
$NUMMODOS = 100$	

! THE GEOMETRY AND COORDINATES OF WINGS AND SLOPES

!-----



$\sin a = 0.495$	! sin. of angle
$\cos a = 0.869$	! cos. of angle
$\tan a = 1.093$	! tan. of angle
$Lw = 6.2$	! length of wing
$x_{89} = ssb/\tan a$	! point 89's coordinate of X axis
$x_{90} = x_{89}$	! point 90's coordinate of X axis
$x_{92} = Lw \cdot \cos a$	! point 92's coordinate of X axis
$y_{92} = \tan a \cdot x_{92}$	! point 92's coordinate of Y axis
$z_{92} = l2 - ((y_{92} - ssb)/1.5) + h1$	! point 92's coordinate of Z axis
$x_{99} = x_{89}$	! point 99's coordinate of X axis

## Annex A10. Determination of dynamic factor according to Annex C from EN 1991-2

For the bridge design, considering all the effects of vertical traffic loads, the most unfavorable value between the followings has to be used.

$$(1 + \varphi'_{dyn} + \varphi''/2) \times \begin{pmatrix} HSLM \\ \text{or} \\ RT \end{pmatrix}$$

or

$$\Phi \times (LM71 + "SW/0)$$

### Case with 7 meters span length

STEP=1  
SUB =3  
FREQ=18.2737  
DMX =.005795

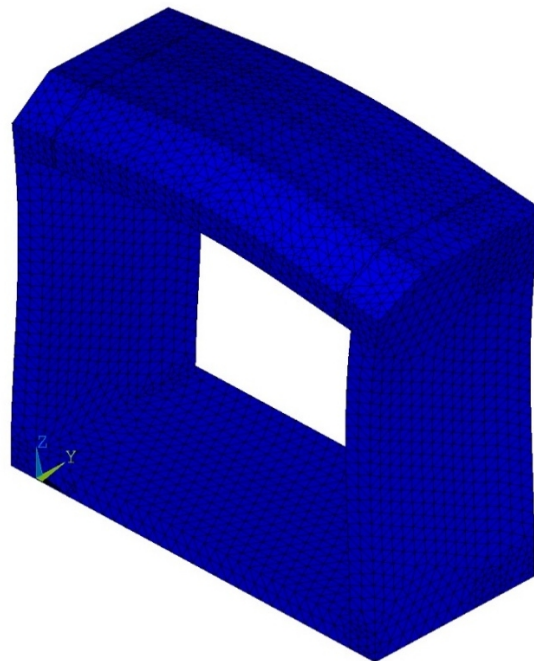


Figure A10.1 – The mode shape and the first natural bending frequency of the bridge loaded by permanent actions (7 meters span length)

$L_{\Phi} := 8.8\epsilon$  the determinant length (m) in accordance with 6.4.5.3 from EN 1991-2

$\alpha := 1$  coefficient for speed

$n_0 := 18.2737$  first natural bending frequency of the bridge loaded by permanent loads

$$\varphi'' := \frac{\alpha}{100} \left[ 56 \cdot e^{-\left(\frac{L_{\Phi}}{10}\right)^2} + 50 \cdot \left(\frac{L_{\Phi} \cdot n_0}{80} - 1\right) \cdot e^{-\left(\frac{L_{\Phi}}{20}\right)^2} \right] = 0.676$$

$\varphi'_{dyn} := 0.3544$  dynamic increment which corresponds to train A6

$\delta_{dyn} := 0.31\text{mm}$  vertical displacement determined for dynamic analysis



$$D_{\text{dynamic}} := \left( 1 + \varphi'_{\text{dyn}} + \frac{\varphi''}{2} \right) \cdot \delta_{\text{dyn}} = 0.525 \cdot \text{mm}$$

$$\alpha_f := 1$$

$$\delta_{\text{LM}} := 0.686 \text{mm} \quad \text{vertical displacements due to LM 71 from static analysis}$$

$$\Phi := 1.34 \quad \text{dynamic factor in accordance with 6.4.4 from EN 1991-2}$$

$$D_{\text{static}} := \Phi \cdot \delta_{\text{LM}} = 0.919 \cdot \text{mm}$$

$$D_{\text{static}} \geq D_{\text{dynamic}} = 1$$

Thus, in order to obtain the design value of the internal forces, the dynamic factor obtained from static analysis will be used further.

### Case with 10 meters span length

STEP=1  
SUB =2  
FREQ=13.8415  
DMX =.004653

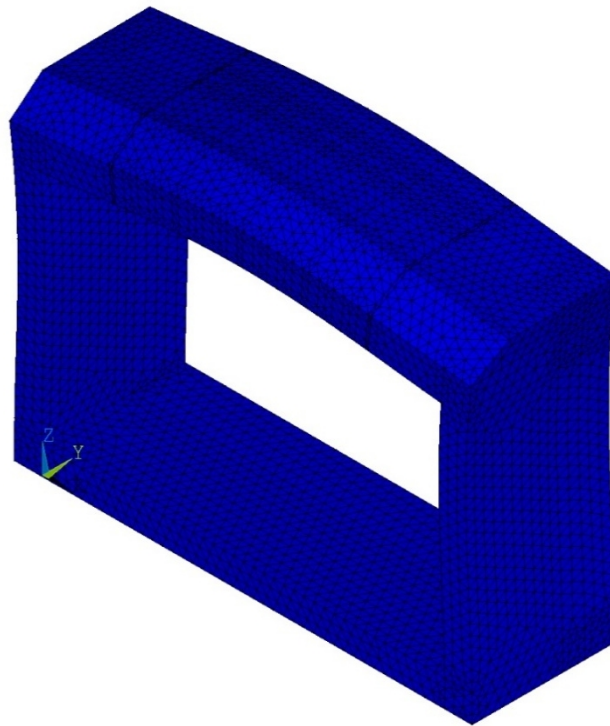


Figure A10.2 – The mode shape and the first natural bending frequency of the bridge loaded by permanent actions (10 meters span length)

$$L_{\Phi} := 10.37 \quad \text{the determinant length (m) in accordance with 6.4.5.3 from EN 1991-2}$$

$$\alpha := 1 \quad \text{coefficient for speed}$$

$$n_0 := 13.8415 \quad \text{the first natural bending frequency of the bridge loaded by permanent actions (Hz)}$$

$$\varphi'' := \frac{\alpha}{100} \cdot \left[ 56 \cdot e^{-\left(\frac{L_{\Phi}}{10}\right)^2} + 50 \cdot \left(\frac{L_{\Phi} \cdot n_0}{80} - 1\right) \cdot e^{-\left(\frac{L_{\Phi}}{20}\right)^2} \right] = 0.495$$

$$\begin{aligned} \varphi'_{\text{dyn}} &:= 0.6720 && \text{dynamic increment which corresponds to train A6} \\ \delta_{\text{dyn}} &:= 0.11\text{mm} && \text{vertical displacement determined for dynamic analysis} \\ D_{\text{dynamic}} &:= \left(1 + \varphi'_{\text{dyn}} + \frac{\varphi''}{2}\right) \cdot \delta_{\text{dyn}} = 0.211\text{mm} \\ \alpha_f &:= 1 \\ \delta_{\text{LM}} &:= 0.898\text{mm} && \text{vertical displacements due to LM 71 from static analysis} \\ \Phi &:= 1.30 && \text{dynamic factor in accordance with 6.4.4 from EN 1991-2} \\ D_{\text{staic}} &:= \Phi \cdot \delta_{\text{LM}} = 1.167\text{mm} \\ D_{\text{staic}} &\geq D_{\text{dynamic}} = 1 \\ L_b &:= 10.75 \end{aligned}$$

The upper limit is:

$$n_o := 94.76 L_b^{-0.748} = 15.993$$

Thus, in order to obtain the design value of the internal forces, the dynamic factor obtained from static analysis will be used further.

### Case with 13 meters span length

```
STEP=1
SUB =2
FREQ=11.0901
DMX =.003609
```

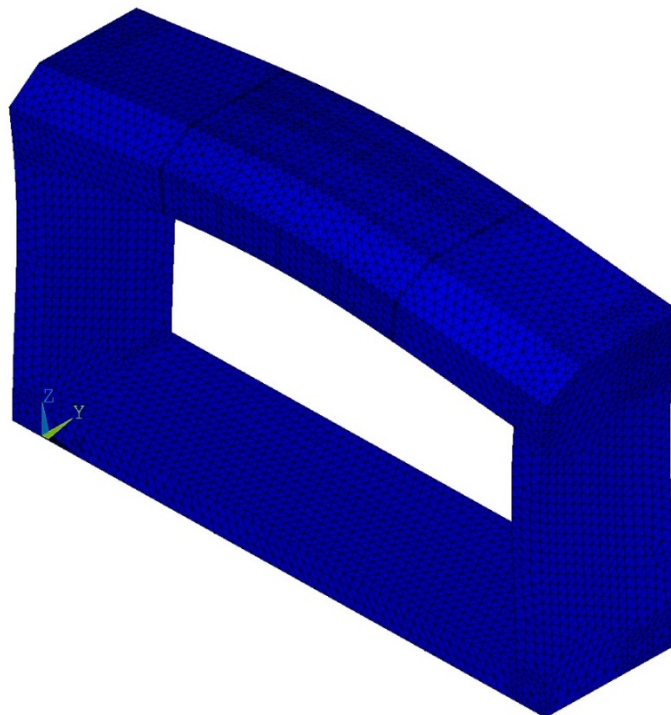


Figure A10.3 – The mode shape and the first natural bending frequency of the bridge loaded by permanent actions (13 meters span length)



$L_{\Phi} := 11.8\text{€}$  the determinant length (m) in accordance with 6.4.5.3 from EN 1991-2

$\alpha := 1$  coefficient for speed

$n_0 := 11.090\text{€}$  the first natural bending frequency of the bridge loaded by permanent actions (Hz)

$$\varphi'' := \frac{\alpha}{100} \cdot \left[ 56 \cdot e^{-\left(\frac{L_{\Phi}}{10}\right)^2} + 50 \cdot \left(\frac{L_{\Phi} \cdot n_0}{80} - 1\right) \cdot e^{-\left(\frac{L_{\Phi}}{20}\right)^2} \right] = 0.364$$

$\varphi'_{\text{dyn}} := 0.341\text{€}$  dynamic increment which corresponds to train A1

$\delta_{\text{dyn}} := 0.39\text{mm}$  vertical displacement determined for dynamic analysis

$$D_{\text{dynamic}} := \left( 1 + \varphi'_{\text{dyn}} + \frac{\varphi''}{2} \right) \cdot \delta_{\text{dyn}} = 0.594\text{mm}$$

$\alpha_f := 1$

$\delta_{\text{LM}} := 1.084\text{mm}$  vertical displacements due to LM 71 from static analysis

$\Phi := 1.26$  dynamic factor in accordance with 6.4.4 from EN 1991-2

$$D_{\text{staic}} := \Phi \cdot \delta_{\text{LM}} = 1.366\text{mm}$$

$$D_{\text{staic}} \geq D_{\text{dynamic}} = 1$$

$L_b := 11.0\text{€}$

The upper limit is:

$$n_0 := 94.76 L_b^{-0.748} = 15.742$$

Thus, in order to obtain the design value of the internal forces, the dynamic factor obtained from static analysis will be used further.



## Annex A11. Drawings of slab reinforcement details

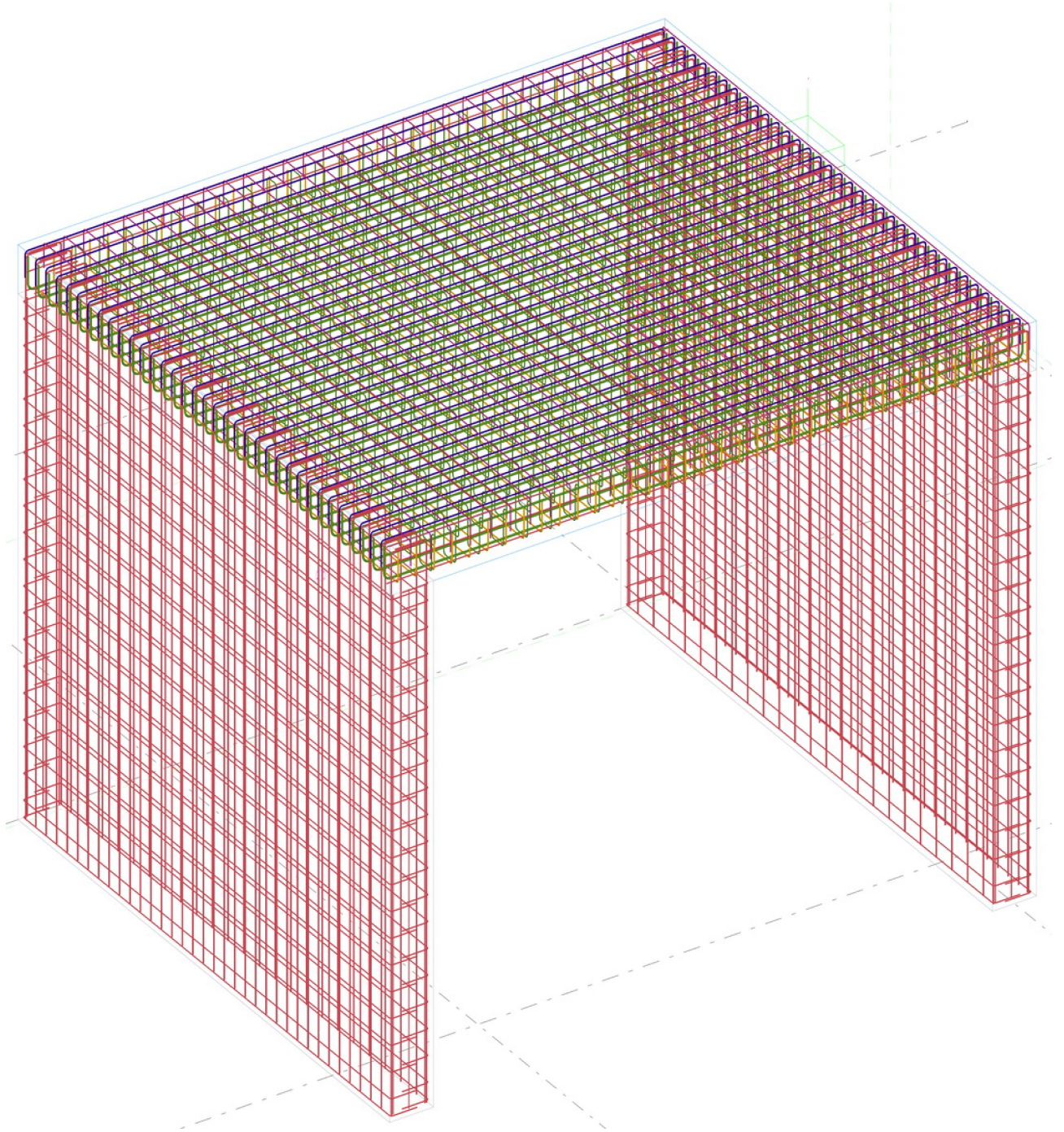
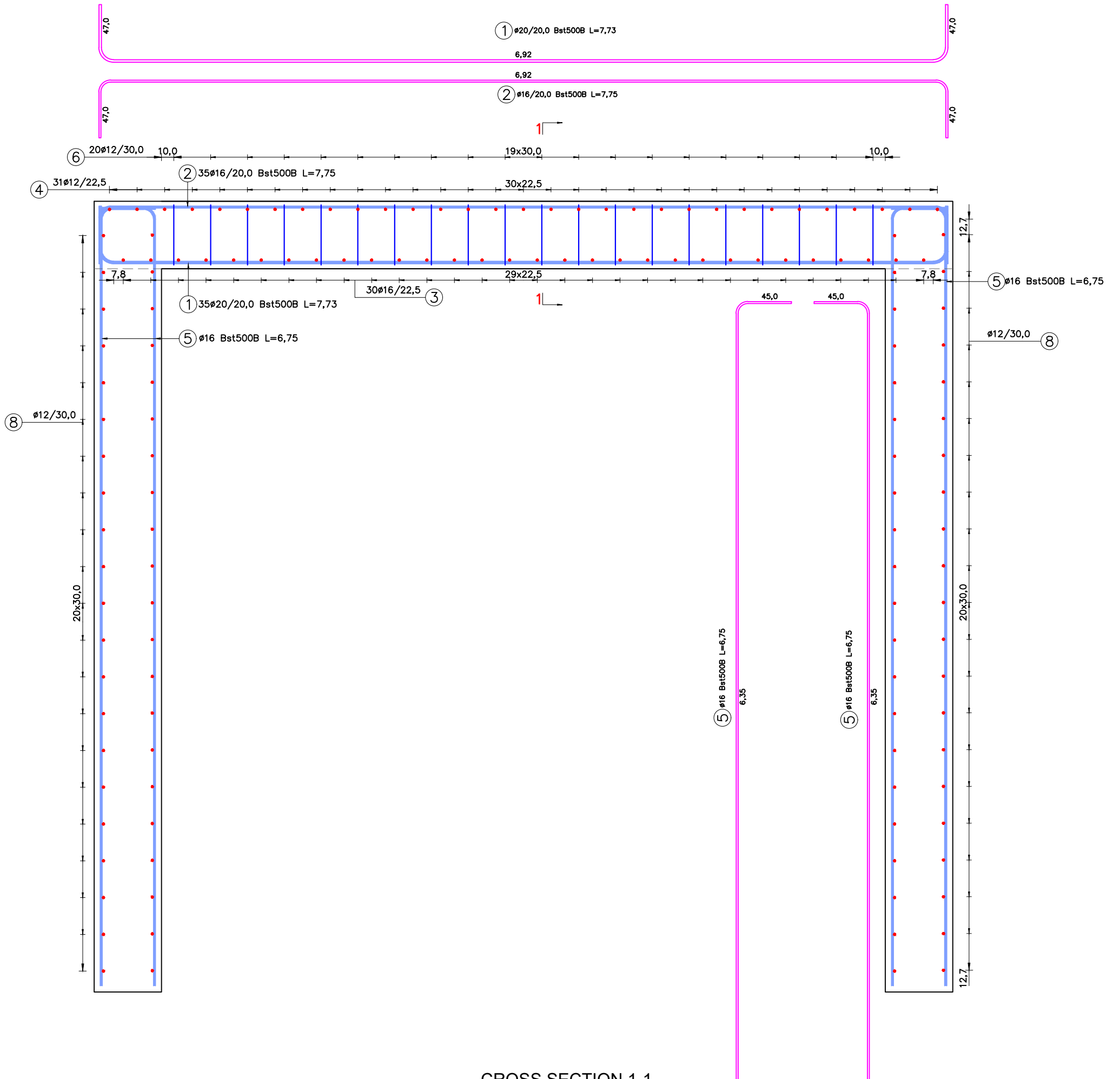


Figure A11.1 - The 3D reinforcement of the bridge



# LONGITUDINAL SECTION



# CROSS SECTION 1-1

